



Kennisprogramma Natte Kunstwerken  
*Kennisplan 2019*

## Technische levensduur

Probabilistische tools: gebruik data in  
updaten levensduur kunstwerken  
*(case gecorrodeerde stalen damwand)*

Hans Brinkman (Deltares)  
Mark Post (Deltares)  
Renger van de Kamp (Rijkswaterstaat)

Kenmerk : KpNK-2019-BKW-03b003  
Versie : 2.0  
Datum publicatie : 31 mei 2021



In het **Kennisprogramma Natte Kunstwerken** (KpNK) werken Deltares, MARIN, Rijkswaterstaat en TNO samen aan de kennisontwikkeling om de vervangings- en renovatieopgave bij natte kunstwerken (stuwen, sluisen, gemalen en stormvloedkeringen) efficiënt en kostenbesparend aan te pakken.

**Deltares**

**MARIN**



Rijkswaterstaat  
Ministerie van Infrastructuur en Waterstaat

**TNO**

Voor het kennisprogramma wordt er jaarlijks een inhoudelijk **Kennisplan** inclusief bijbehorend financieringsplan opgesteld. Andere partijen (zoals waterschappen en marktpartijen) worden nadrukkelijk uitgenodigd om deel te nemen.

Meer informatie over het Kennisprogramma Natte Kunstwerken vindt op [www.nattekunstwerkenvandetoekomst.nl](http://www.nattekunstwerkenvandetoekomst.nl) waar ook de onderzoeksresultaten ter beschikking worden gesteld.

**NKWK**

De samenwerking binnen het Kennisprogramma Natte Kunstwerken vormt de uitwerking van de onderzoekslijn “Toekomstbestendige Natte Kunstwerken” binnen het **Nationaal Kennisplatform voor Water en Klimaat** (NKWK). Dit kennisplatform brengt Nederlandse overheden, kennisinstellingen en bedrijven bij elkaar om samen te werken aan pilots, actuele vraagstukken en lange termijnontwikkelingen op gebied van water- en klimaatvraagstukken.

Meer informatie staat op [www.waterenklimaat.nl](http://www.waterenklimaat.nl).

Voor vragen met betrekking tot het rapport kunt u terecht bij de auteurs:

Hans Brinkman - [hans.brinkman@deltares.nl](mailto:hans.brinkman@deltares.nl)

Mark Post - [mark.post@deltares.nl](mailto:mark.post@deltares.nl)

Voor vragen over Kennisprogramma Natte Kunstwerken en Kennisplan 2019 kunt u terecht bij:

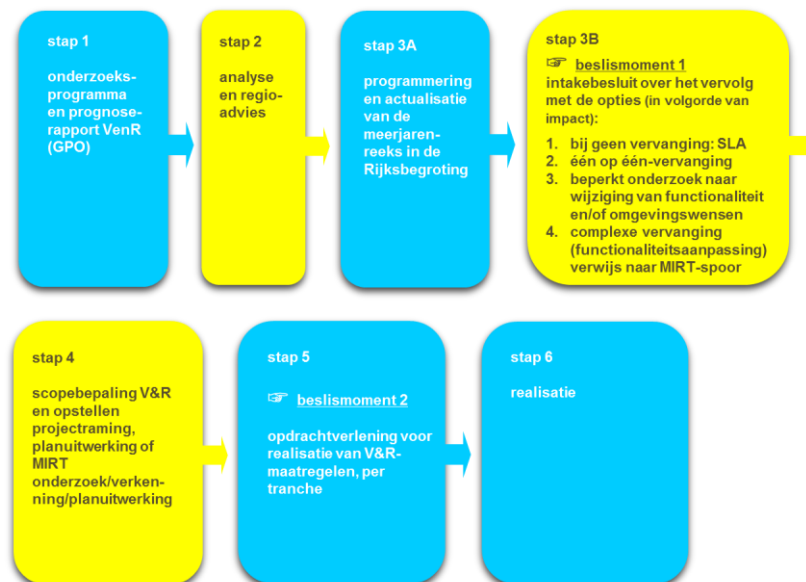
Daan Dunsbergen - [daan.dunsbergen@rws.nl](mailto:daan.dunsbergen@rws.nl)



## Voorwoord

Sluizen, stuwen, gemalen en stormvloedkeringen zijn belangrijke assets van beheerders zoals Rijkswaterstaat en de waterschappen. Een groot deel van deze natte kunstwerken bereikt komende decennia het einde van de (technische) levensduur waarvoor het is ontworpen. Er dient zich dan ook een aanzienlijke vervangings- en renovatieopgave van deze kunstwerken aan.

De laatste jaren wordt steeds meer gezocht naar mogelijkheden om levensduur van kunstwerken te verlengen, en om bij einde levensduur (noodzakelijke) ingrepen aan gebiedsontwikkelingen en/of functionele/netwerk ontwikkelingen te koppelen. Rijkswaterstaat heeft daartoe als asset manager een vernieuwde werkwijze voor het Vervanging en Renovatie (VenR) proces opgesteld, welke de basis vormt voor de inrichting van het Kennisprogramma Natte Kunstwerken (zie Figuur 1).



Figuur 1. Vernieuwde RWS-werkwijze Vervanging en Renovatie.

In het Kennisprogramma Natte Kunstwerken wordt kennis ontwikkeld die bijdraagt aan de verschillende stappen binnen deze vernieuwde VenR-werkwijze, met als focuspunten stap 1 (prognoserapport) en stap 2 (regio-analyse en -advies). Het prognoserapport richt zich op de (einde) technische levensduur, het regio-advies brengt met name de relatie object-netwerk-gebied in kaart.

Het onderzoek in het Kennisprogramma Natte Kunstwerken vindt plaats langs de onderstaande 3 onderzoekssporen en heeft tot doel om een effectieve en efficiënte aanpak van de vervanging- en renovatie-opgave en nieuwbouw van natte kunstwerken mogelijk te maken:

- bestaand object
  - inzicht in (einde) technische levensduur
  - levensduurverlenging
- object-systeem
  - inzicht in (einde) functionele levensduur en object-systeemrelaties
- nieuw(e) object/objectonderdelen
  - toepassen innovaties
  - inspelen op toekomstige ontwikkelingen.



## Kennisprogramma Natte Kunstwerken *Kennisplan 2019*

Sinds enkele jaren is er het Nationaal Kennisplatform voor Water en Klimaat (NKWK). Hieronder lopen diverse onderzoeklijnen. Eén van de onderzoeklijnen is “Toekomstbestendige Natte Kunstwerken”. Voor het praktisch laten functioneren van deze onderzoeklijn is er een Samenwerkingsovereenkomst Natte Kunstwerken en een Kennisprogramma Natte Kunstwerken opgesteld:

- Samenwerkingsovereenkomst Natte Kunstwerken. De partijen die momenteel binnen deze overeenkomst samenwerken aan onderwerpen rondom de vervangings- en renovatieopgave bij natte kunstwerken zijn Deltares, MARIN, Rijkswaterstaat en TNO.
- In het kader van de bovengenoemde Samenwerkingsovereenkomst Natte Kunstwerken en de 3 onderzoekssporen van het Kennisprogramma Natte Kunstwerken wordt er jaarlijks een inhoudelijk Kennisplan inclusief bijbehorend financieringsplan opgesteld.

Naast de genoemde partijen zijn en worden andere partijen nadrukkelijk uitgenodigd om deel te nemen aan de Samenwerkingsovereenkomst Natte Kunstwerken en/of het Kennisplan. Inzet kan zowel in kind en/of financieel zijn. In het Kennisplan 2019 is er binnen het kader van het Kennisprogramma Natte Kunstwerken op verschillende onderwerpen met Acotec BV, Arcadis, ArcelorMittal, DIANA FEA en Boskalis samengewerkt.

Resultaten uit het Kennisprogramma Natte Kunstwerken worden gedeeld met de gehele sector, onder andere via de website [www.nattekunstwerkenvandetoekomst.nl](http://www.nattekunstwerkenvandetoekomst.nl).

De hierop volgende samenvatting heeft betrekking op het onderliggende onderzoeksrapport “Probabilistic Tools: Reliability-based soil-structure analysis using FE - Application on degrading steel sheet pile retaining wall”. Dit onderzoek is geleid door Deltares in het kader van het Kennisplan 2019 van Kennisprogramma Natte Kunstwerken. In verband met de Algemene Verordening Gegevensbescherming is het originele Deltares rapport ten behoeve van het publiceren op de website alleen qua persoonsgegevens, maar niet qua inhoud aangepast.



## Samenvatting

# Technische levensduur – Probabilistische tools: gebruik data in updaten levensduur kunstwerken (case gecorrodeerde stalen damwand)

## Aanleiding

The objective of the Research programme on Hydraulic Infrastructure (KpNK) is to develop knowledge and tools allowing for an efficient and cost-effective replacement of hydraulic structures in the Netherlands in the coming decades. To reach this objective, a transition is needed in engineering practice: from robust design of new structures to optimised assessment of existing structures.

The reliability of the concrete and steel foundations (the “chassis”) of the hydraulic structures determine to a large extent the end of technical service life of the complete hydraulic structure. Since the “chassis” is embedded in soil, the analysis of the soil-structure interaction is relevant. Nowadays, FEM is the preferred tool to analyse soil-structure analysis, as it allows to gain a deep insight into the (soil) mechanics involved.

However, as typical in geotechnical engineering, the uncertainties in the properties influencing the soil-structural performance are large. When dealing with large uncertainties, probabilistic methods offer a rational framework to quantify reliability and end of service life in a better way than the existing deterministic (design) approaches. Coupling of these probabilistic methods with the FEM model is therefore a logical next step; the FEM model allows for an optimal reliability analysis, as it combines most (if not all) relevant failure mechanisms. In 2016 the first exploratory phase of the KpNK research into coupling of probabilistic methods with FEM was reported.

## Onderzoeksvraag en -opzet (WAT)

The second phase of the KpNK research into coupling of probabilistic methods with FEM, focusing on the development and testing of a practical approach, is documented in this report. The objective is twofold:

- To make probabilistic methods practically applicable to FEM based analysis of soil-structure interaction, allowing for a more rational assessment.
- To come to a more realistic and balanced physical model for steel sheet pile structures, by including two aspects known to be lacking: a more realistic corrosion model and softening of the steel sheet pile. A more realistic and balanced physical model will allow for less conservative assessment of existing hydraulic structures.



### Onderzoeksaanpak en -methode (HOE)

In the research recorded in this report first a generic and “easy to use” coupling between the FEM program PLAXIS and the Deltares software Probabilistic Toolkit has been developed and described.

Secondly, by means of a case study on a steel sheet pile wall experience has been gained with:

- The potential of the developed ‘probabilistic approach’ for assessing a realistic case.
- The impact of modelling thickness reduction (corrosion) as a stochastic variable using data collected and analysed within the context of KpNK.
- The impact of modelling the yield stress of the steel sheet pile as a stochastic variable.
- The impact of using a more realistic mechanical model, by incorporating plastic hinges and rotation capacity (including softening), on the reliability of the steel sheet pile retaining wall.
- The impact of an improved Class 4 strength formulation for the sheet pile on the reliability of the structure.
- The impact of using different reference periods on the transition in time between dominant soil influence and dominant structural influence on the reliability.
- The impact of using the plane strain soil strength instead of the non-plane strain soil strength as obtained from e.g. triaxial tests.

The gained experiences have been recorded in the research report.

### Onderzoeksresultaten en synthese

The next conclusions are made based on the experiences with the case study:

- Using the probabilistic approach, the effects of (a priori) uncertainties on the reliability can be quantified, including the benefit of incorporating inspection results of corrosion.
- A-priori there is a high uncertainty in the degree of degradation (corrosion) and this is likely one of the dominant uncertainties at the end of the technical service life of (unprotected) steel sheet piles. The a-priori uncertainty associated with corrosion may have a large negative influence on the (calculated) reliability and thus the remaining technical service life.
- Incorporating the results of inspection of corrosion, in general, leads to a significant reduction of the uncertainty compared with the a-priori uncertainty. This reduction has a significant positive influence on (calculated) reliability and, thus, the residual technical service life (i.e. updated reliability).
- Incorporating more realistic mechanical behaviour (i.e. plastic hinges, rotation capacity and softening) into the assessment of a steel sheet pile structure is likely to have a large positive influence on reliability.
- Incorporating the yield stress as a stochastic variable into the assessment of a steel sheet pile structure is likely to have a positive influence on reliability. However, the positive influence will become less for slender (corroded) sheet piles profiles and potentially it may become insignificant as for slender class 4 geometrical instability of steel sections becomes decisive.
- The impact of the improved (less conservative) Class 4 strength formulation for the sheet pile appears to be small for this case study as the design point is located near the transition of the Class 3 to Class 4 area. For other situations the impact may however be more significant.



- For this case study the analyses of different reference periods showed that the transition in time, in dominance by soil uncertainty to a dominance by structure uncertainty, largely depends on the used variation coefficient for the corrosion. The larger the variation coefficient the sooner the structure uncertainty becomes dominant on reliability.
- Using the higher plane-strain soil strength results in an increased reliability compared to the triaxial strength as expected. Interesting to note is that the relative impact of plane-strain soil strength on reliability seems larger in case the sheet pile has significant rotation capacity (which happens for relative low corrosion rates). The latter seems plausible as in this case the structure can mobilize the available extra soil strength.
- At present, the created probabilistic approach is (due to calculation times in the order of weeks) more of a research approach with which first test runs have been made as a proof of concept. The approach is currently fit for use in a pilot project, such as a calibration study for the next generation Eurocode 7.

### Evaluatie en vooruitblik

Main recommendation for the next phase of the research is to continue the development of the probabilistic approach/method and use it amongst others to:

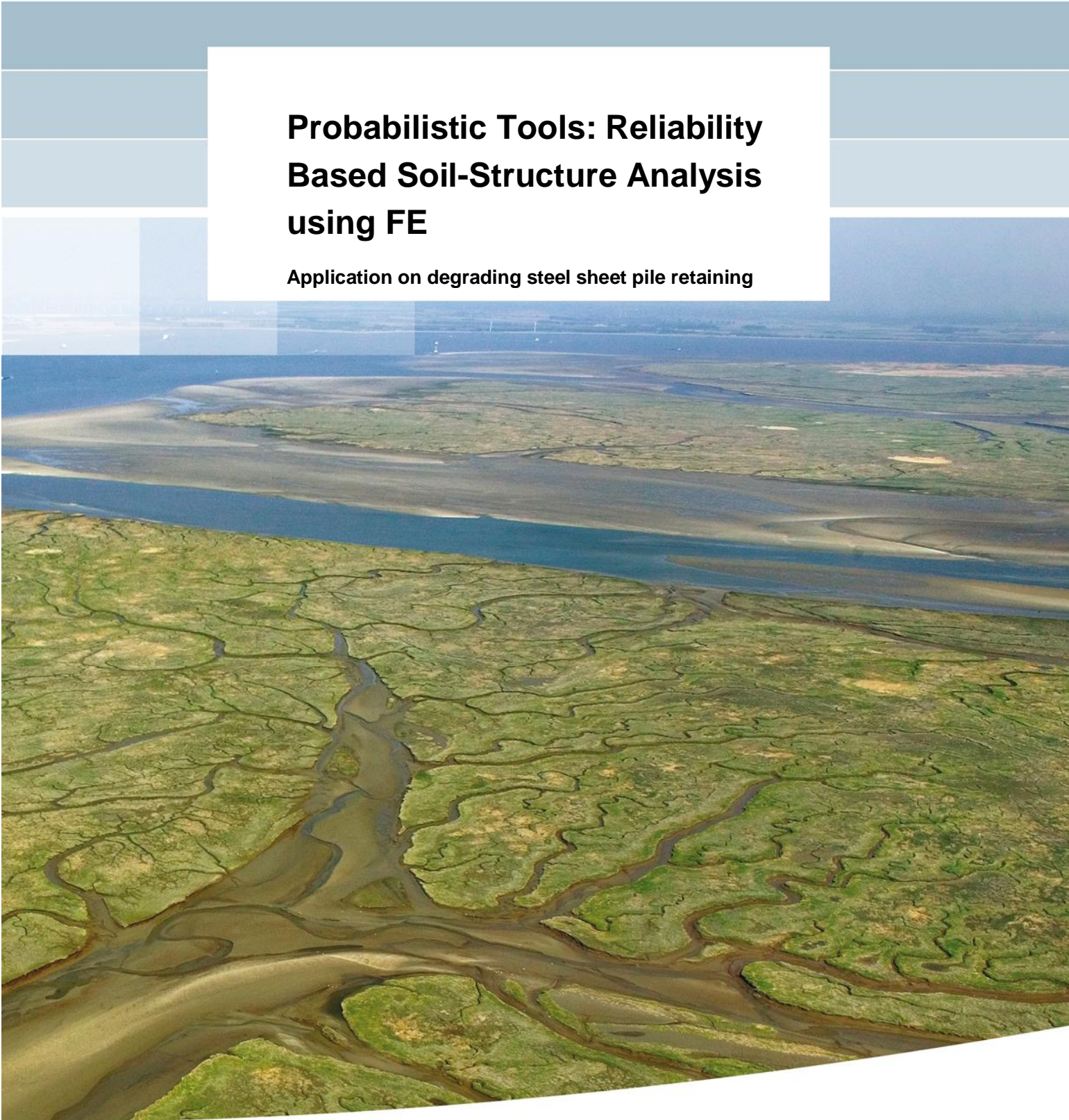
- To investigate the potential of recently developed reliability analysis methods using surrogate (or response surface) modelling, allowing for a significant reduction of calculation times.
- To investigate the potential of using other (open-source) FE programs, such as the Kratos.GEO software developed by Deltares, allowing for large numbers of calculations at the same time instead of one by one calculations, reducing calculation times.
- To investigate the potential to derive annual reliability taking in account past performance of a degrading structure from a limited set of calculations with the reliability approach.
- To investigate the potential for reliability updating by incorporating survived loads and other performance or monitoring data.





# **Probabilistic Tools: Reliability Based Soil-Structure Analysis using FE**

**Application on degrading steel sheet pile retaining**



# **Probabilistic Tools: Reliability Based Soil-Structure Analysis using FE**

**Application on degrading steel sheet pile retaining wall**

ir. M. Post  
ir. J. Brinkman

## Contents

<b>1 Introduction</b>	<b>1</b>
1.1 Context	1
1.2 Previous studies on the subject	1
1.3 Objectives and scope of this report	3
1.4 Outline	5
<b>2 Coupling probabilistic library with FEM</b>	<b>7</b>
2.1 Introduction	7
2.2 Coupling the Probabilistic Toolkit and PLAXIS	7
2.3 Coupling: features	8
2.4 Coupling: version control	10
<b>3 Case study: retaining wall</b>	<b>12</b>
3.1 Introduction	12
3.2 Geometry, water levels and loads	13
3.3 Soil characterisation	14
3.4 Structure characterisation	15
3.5 Corrosion characterisation	16
3.6 Corrosion effect	18
3.7 Sheet pile parameters as function of corrosion	21
3.8 Plastic rotation capacity (softening)	24
<b>4 Random variables and correlations</b>	<b>27</b>
4.1 Introduction	27
4.2 Soil parameters	27
4.3 Water levels	28
4.4 Surcharge loads	29
4.5 Water bottom level	30
4.6 Corrosion	31
4.7 Yield stress	33
4.8 Summary of all stochastic variables	34
4.9 Correlations	35
<b>5 Limit state Functions</b>	<b>37</b>
5.1 Introduction	37
5.2 Subset A LSF for the sheet pile	38
5.3 Subset B LSF for the anchorage	42
5.4 Subset C LSF for the soil	42
5.5 Implementation in PTK	45
<b>6 Calculation results (2<sup>nd</sup> series)</b>	<b>48</b>
6.1 Introduction	48
6.2 Summary of results	48
6.3 Analyses of results	51
6.4 Additional runs	54
6.5 Verification of results	55

<b>7 Calculation results (3<sup>rd</sup> series)</b>	<b>56</b>
7.1 Introduction	56
7.2 Summary of results	56
7.3 Analyses of results	57
<b>8 Conclusions and recommendations</b>	<b>62</b>
8.1 Objective and scope	62
8.2 Results and conclusions	62
8.3 Recommendations	65
<b>9 References</b>	<b>66</b>
<b>Appendices</b>	
<b>A Background on soil properties</b>	<b>A-1</b>
A.1 Non associative soil properties	A-1
A.2 Model	A-1
A.2.1 Drained	A-1
A.2.2 Best Guess Equivalent model	A-2
A.2.3 Materiaal model	A-3
<b>B Corrosion</b>	<b>B-1</b>
B.1 Definition of corrosion zones [NEN-EN 1993-5 ]	B-1
B.2 Thickness reduction due to corrosion [RWS 2013]	B-2
B.3 Thickness reduction due to corrosion of soil embedded steel sheet pile sections [Deltares 2014]	B-2
<b>C The Probabilistic Toolkit</b>	<b>C-1</b>
C.1 Introduction	C-1
C.2 Theoretical background of reliability methods	C-1
C.3 Coupling the Probabilistic Toolkit and PLAXIS	C-3
C.4 Experiences using Directional sampling in the PTK	C-6
<b>D PLAXIS model</b>	<b>D-11</b>
D.1 PLAXIS base model	D-11
D.2 InputCommand file (i.e. change file)	D-12
D.3 PLAXIS settings	D-14
<b>E Plastic rotation capacity</b>	<b>E-16</b>
E.1 Classification of cross sections	E-16
E.2 Rotation capacity according to annex C of [EC3-5:2008]	E-18
E.3 Principles of softening: moment capacity vs rotation capacity	E-21
E.4 Implementation of Softening module	E-22
E.5 Calculation of rotation angle ( $\Phi_{max}$ ) from PLAXIS	E-24
<b>F Summary of results of [Deltares, 2018] (1<sup>st</sup> series)</b>	<b>F-25</b>
<b>G Results of calculations (2<sup>nd</sup> series)</b>	<b>G-26</b>
<b>H Verification of results</b>	<b>H-27</b>

H.1	Check on Input values	H-27
H.2	Check on output / softening values	H-30
H.3	Check on calculated rotations ( $\Phi_{max}$ )	H-35
H.4	Check on LSF values	H-38
H.5	Check on influence yield stress	H-40
<b>I</b>	<b>Improved Class 4 strength in 3<sup>rd</sup> series of calculations</b>	<b>I-43</b>
<b>J</b>	<b>Results of calculations (3<sup>rd</sup> series)</b>	<b>J-45</b>

# 1 Introduction

## 1.1 Context

This report is part of the research programme on Hydraulic Structures (*Dutch: -Kennis programma Natte Kunstwerken (KpNK)-*). Objective of this research programme is to develop knowledge and tools allowing for an efficient and cost-effective replacement of over 200 Hydraulic Structures in the Netherlands in the coming decades. To reach this objective a transition is needed in engineering practice: from robust design of new structures to optimised assessment of existing structures.

The reliability of the concrete and steel foundations (the “chassis”) of the hydraulic structures determines to a large extent the end of technical service life of the complete hydraulic structure. Since the “chassis” is embedded in soil the analysis of the soil-structure interaction is relevant. Now-a-days FEM is the preferred tool to analyse soil-structure analysis as it allows to gain a deep insight into the (soil) mechanics involved. However, as typical in geotechnical engineering, the uncertainties in the properties influencing the soil-structural performance are large. In the past, the partial (safety) factors for the design of hydraulic structures [CUR 166, 2012], [CUR 211, 2013] were derived based on simple models, limited probabilistic calculations (e.g. [Calle, 1991]) and several conservative assumptions. The developments that link advanced FEM and probabilistic calculations started a number of years ago, e.g. [Schweckendiek, 2007] and [Wolters, 2012], and seem an ideal solution to quantify the implicit safety margins in the semi-probabilistic assessments.

Probabilistic methods are the basis to develop proper assessment tools to explicitly handle the different types of uncertainties. These techniques can be used for various types of engineering structures. This report is a continuation of previous work performed on coupling FEM and reliability libraries in the KpNK context and has been performed and reported in the period 2019 – 2021. ArcelorMittal was the partner from industry that participated in the research project<sup>1</sup>.

## 1.2 Previous studies on the subject

In [Deltares, 2016a] firstly a summary is presented of previous research, outside the KpNK context, about coupling probabilistic libraries with FEM. Studies mentioned are [Waarts et al., 2000], [Schweckendiek, 2007a en 2007b], [Wolters, 2012] and [Rippi, 2015]. In short, the following conclusions are drawn from these studies:

- All studies conclude that further research on the topic will contribute to design and optimization concepts and hopefully to a better understanding of the system behavior.
- Some studies point out the limitation (and conservatism) of the classical (mechanical) models and the higher efficiency of FEM.
- The main gaps detected so far are robust and efficient analysis for real-life problems and modelling of the structural elements closer to reality (plastic behaviour).

[Deltares, 2016a] furthermore indicates that the aim of the study is to make a step towards a “FEM – probabilistic library” connection in an “easy to use” way and applicable to general soil-structure interaction problems. In the study a connection was made between geotechnical

<sup>1</sup> ArcelorMittal provided the Class 4 strength for an AZ26 profile according to a critical stress calculation for several situations [ArcelorMittal, 2019]. Furthermore, AM provided feedback on the concept version of this document.

software *PLAXIS* and the open source probabilistic software *OpenTurns*. As case study a reliability analysis of an anchored sheet pile wall was carried out. Following conclusions are made:

- Instability of the structure could not robustly be analysed with First Order Reliability Methods (FORM). Directional Sampling (DS) was used and found to be more robust.
- Future research efforts should address:
  - Structural modelling closer to design practice.
  - Increasing robustness of the reliability analysis while decreasing computation times.
- A first exploration is made of including corrosion of the sheet pile wall as a stochastic variable. It is concluded that there is insufficient insight in the uncertainty for corrosion in fresh water conditions. A data gathering campaign is needed to provide further insight.
- It was recommended to improve and generalize the coupling, including testing other reliability libraries and more detailed post processing of the results of DS.
- It was recommended to extend the models used to match the degree of detail commonly used in practice, this includes a.o.: constitutive soil models used, structural modelling (e.g. plastic deformations), spatial variability of soil parameters and corrosion, influence of reliability as a function of time.

In [Deltares, 2018] the work of [Deltares, 2016a] was continued. In this study a first simplistic implementation of plastic hinges was added to the existing coupling between *PLAXIS* and *OpenTurns* allowing for plasticity and/or plastic hinges in the model. And an additional limit state function was added for deformations. Furthermore, a variation was made in strength parameters of the soil (between triaxial and plane strain parameters). Conclusions made:

- The dominant aspect of any assessment is the definition of the Limit State Function used. The calculated reliability for the case study with triaxial parameters and elastic section modulus capacity was Beta = 0.88 and ranged up to Beta = 3.95 using plain strain parameters and plastic hinges.
- Calculated reliability for the case study, with triaxial parameters, no softening, but with plastic section modulus capacity is Beta = 2.02; and with plastic hinges, triaxial parameters and fixed value of softening Beta = 2.97.

The results of the previous study [Deltares, 2018] are summarised in appendix F and referred to hereafter as the 1<sup>st</sup> series of calculations.

In [Deltares, 2019a and b] sheet pile degradation measurements were collected and analysed to obtain a first indication of the uncertainty involved. Main conclusions made:

- For sheet pile walls the average value of the degradation in a horizontal plane<sup>2</sup> over the width  $L_B$  of a failure mechanism,  $\Delta \bar{t}$  is the key degradation parameter. The length  $L_B$  represents the width of a failure mechanism for the sheet pile structure and this always concerns a significant width. The length  $L_B$  is furthermore not a fixed number but is case dependent. Also see Figure 1.1.

<sup>2</sup> The mechanism washout (soil transport through a hole) is an exception, for that mechanism the maximum corrosion in a specific point/small area is of relevance.

- The observed coefficient of variation of this average degradation over the width  $L_B$  was on regional scale  $V_{\Delta\bar{\epsilon};reg} = \sim 0.5 - 0.65$  and at local scale  $V_{\Delta\bar{\epsilon};loc} = \sim 0.2 - 0.3$ .
- There is a vast potential for inspection by reducing the high a-priori  $V_{\bar{\epsilon};reg}$  to the lower local values as for most of the cases the a-priori conditions based on regional data sets will be conservative.

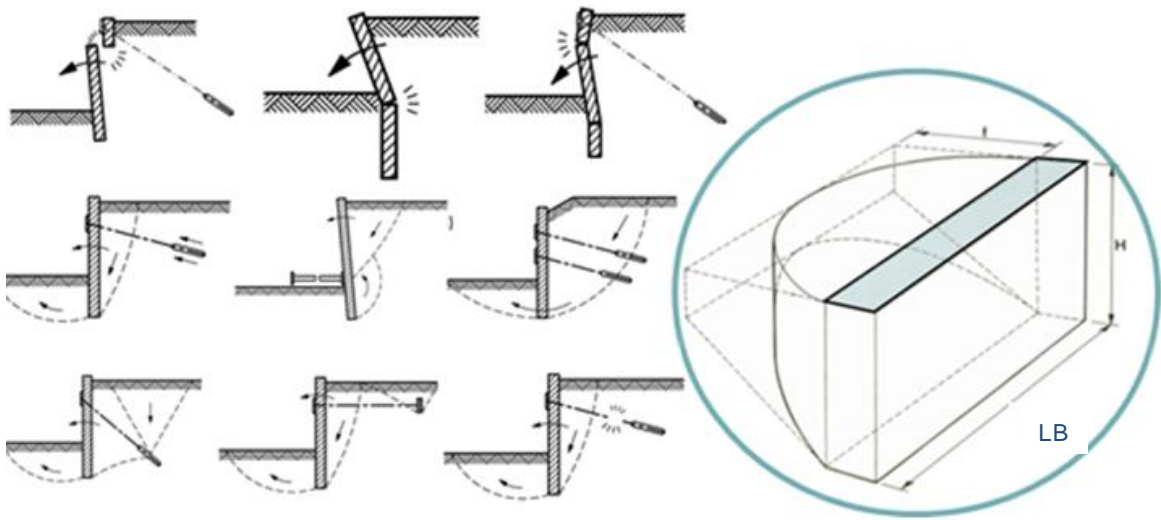


Figure 1.1. The length  $L_B$  represents the width of a failure mechanism for the sheet pile structure and this always concerns a significant width

### 1.3 Objectives and scope of this report

The ultimate research objective is:

*To enable probabilistic analyses with the Finite Element Method (FEM) using a probabilistic library/toolkit in an 'easy to use' way, and applicable to realistic soil-structure interaction problems.*

It is believed that by integrating mechanical (deterministic) understanding of the problem on one hand, and a probabilistic approach for dealing with (and quantifying) the uncertainties on the other hand, an overall better insight is obtained in the (safety of) the structure, see Figure 1.2.



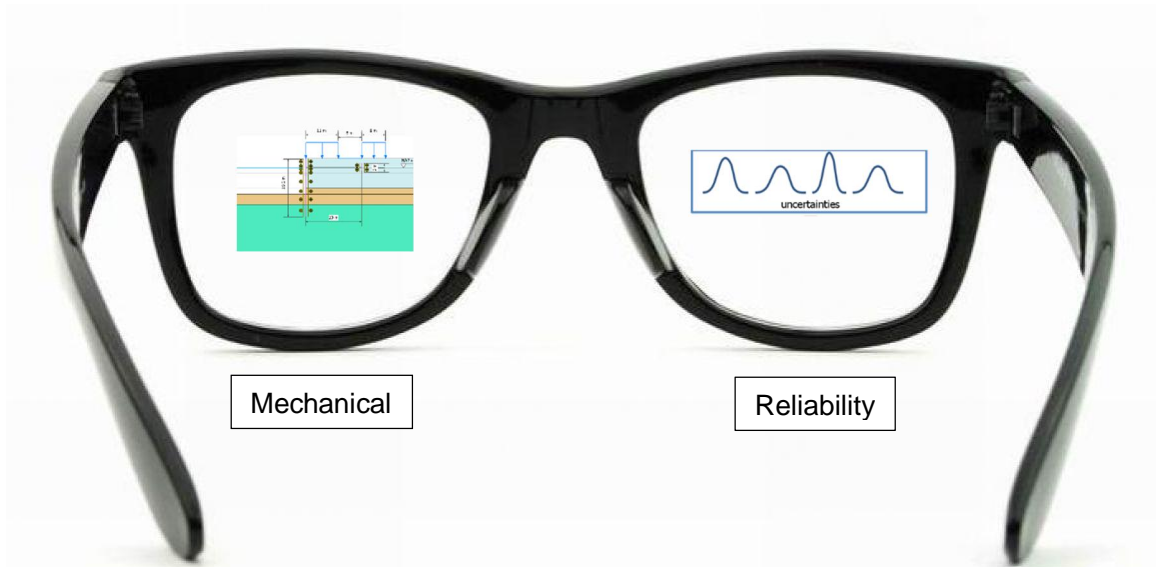


Figure 1.2 Integration of mechanics and reliability theory for designing or assessing (geotechnical) structures

The scope of this study is:

To keep focus on anchored sheet piles by means of the case study as presented in [Deltares, 2016a] and to continue and extend the work done in [Deltares, 2018]. Effectively the following scope is foreseen:

- To set-up and gain experience with a more generic and “easy to use” coupling between the program PLAXIS and the Deltares software Probabilistic Toolkit<sup>3</sup>. This approach enables the coupling to the PLAXIS model and application of advanced probabilistic techniques. The principle of the coupling is explained in Figure 1.3.
- To make use of the Directional Sampling method (DS) due to its robustness.
- To gain experience with the impact of modelling corrosion as a stochastic variable and to incorporate the results of a first analysis of corrosion data gathered from sheet pile structures on fresh water in the Netherlands [Deltares, 2019b].
- To improve the mechanical modelling by including plastic hinges and rotation capacity (i.e. softening), which is expected to positively influence reliability of existing structures.
- To gain experience with the impact of modelling the yield stress as a stochastic variable.
- To gain insight in the development of reliability over the lifespan of the structure as a function of different reference periods for the time-dependent variables.
- To report the experiences such that these can be of benefit to the geotechnical practice.

<sup>3</sup> In this study it is proposed to use the Deltares software Probabilistic Toolkit instead of the open source software OpenTurns previously used. The arguments for this choice have been further elaborated in Chapter 2.

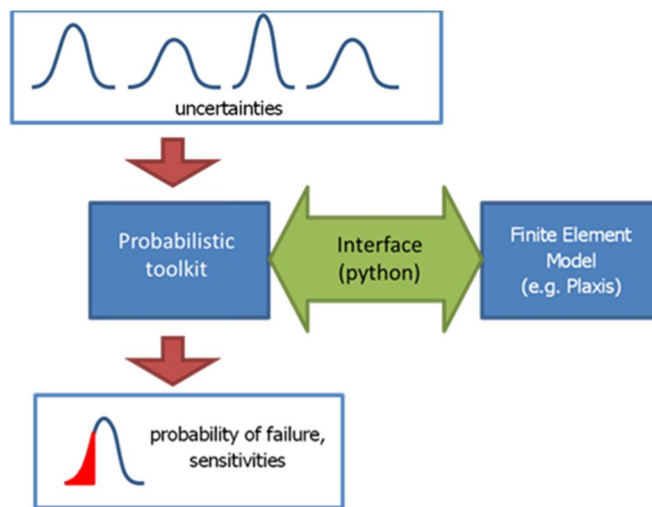


Figure 1.3 Principle of the coupling between PTK and PLAXIS

The case study as presented in [Deltares, 2016a] refers to an anchored retaining wall, as encountered frequently in hydraulic structures such as quay walls or locks. This case study is still considered suitable here because:

- In the coming years, several retaining walls must be re-assessed in the Netherlands.
- For several hydraulic structures additional measures are required (e.g. a more detailed assessment) due to insufficient safety of the steel sheet piles.
- The behaviour of a sheet pile structure is strongly influenced by soil-structure interaction and is therefore a good example to study the class of soil-structure interaction problems.
- More specifically, the case study presented in this research, is the wall of a lock chamber in fresh water. Specific for this application is the high fluctuation of water levels, causing significant corrosion during the service life.

#### 1.4 Outline

Subsequent to this introduction, this report is structured as follows:

- **Chapter 2** describes the setup of the coupling between PLAXIS and the Probabilistic Toolkit
- **Chapter 3** presents the case study and corresponding data and assumptions
- **Chapter 4** presents the stochastic variables, as used in the case study, and their mutual correlations
- **Chapter 5** presents the limit state functions used in the case study
- **Chapter 6** presents the calculation results of the 2<sup>nd</sup> series of calculations performed in 2019 and the analyses of these results
- **Chapter 7** presents the calculation results of the 3<sup>rd</sup> series of calculations performed in 2020 and the analyses of these results
- finally, **Chapter 8** summarizes the most important findings and recommendations.

Furthermore note:

- 1<sup>st</sup> series of calculations: these are the calculations separately reported in [Deltares, 2018] and for which results are summarised here in appendix F. These are calculations made in which corrosion is a deterministic value, using rotation capacity in a simplified form and for the final year of a fixed reference period of 50 years;

- 2<sup>nd</sup> series of calculations: these are the calculations reported in this document and for which corrosion is a stochastic variable, using rotation capacity in a more realistic general form and for the final year of a fixed reference period of 50 years;
- 3<sup>rd</sup> series of calculations: these are the calculations reported in this document and for which corrosion is a stochastic variable, using rotation capacity in a more realistic general form, using a more realistic Class 4 strength formulation and for the final year of different reference periods.

This report is mainly written for the research and development community, i.e. reporting technical details and findings in order to reproduce and incrementally improve the accomplished work. Readers interested in the main results and impact of this research should refer to the summary and conclusions and recommendations.

## 2 Coupling probabilistic library with FEM

### 2.1 Introduction

When considering the reliability of an element or structure (reliability analysis), the determination of the probability of failure is the central issue, as well as the determination of the influence coefficients. The limit between failure and non-failure is defined as a “limit state” and the reliability is given by the probability that this limit state is not exceeded.

In the case of hydraulic structures, as studied in this report, the limit state evaluations are carried out with the commercial software *PLAXIS 2D*, which is a two-dimensional finite element method (FEM) software used to perform deformations and stability analysis for various types of geotechnical applications (e.g. plane strain and axi-symmetric modelling of soil and rock behaviour).

The reliability analysis is carried out through a probabilistic and reliability analysis library, called the Probabilistic Toolkit or PTK. The PTK is developed by Deltares. The PTK has a library with all common reliability distributions (i.e. normal or Gumbel) and reliability integration methods (e.g. Monte Carlo, directional sampling). Important advantage of the PTK is that it is used for implementing novel developments regarding reliability analysis. One such development is a reliability analysis method using surrogate (or response surface) modelling which may allow for a significant reduction of calculation times [Van den Eijnden, 2019]. Some (theoretical) background information on the PTK is presented in Appendix C. For more detailed information on the PTK the reader is referred to the PTK manual [Deltares, 2016b].

This chapter presents a description of the coupling between the PTK and PLAXIS.

### 2.2 Coupling the Probabilistic Toolkit and PLAXIS

The coupling of the PTK with PLAXIS requires an interface for the communication between both programs. The communication between both programs consists of modifying PLAXIS' inputs and read its outputs for important variables such as material parameters, pore pressures generation and stresses development and corresponding deformations inside the soil body. PLAXIS has to be able to obtain the (new) values that are set (simulated) by the probabilistic library for the variables (inputs) that are treated as stochastic during an iterative process, according to the chosen reliability analysis method.

In Figure 2.1, an illustration of the coupling is shown. In principle a reliability run has to be prepared inside the PTK, the user sets (1) the preferable reliability analysis (RA) method, (2) the stochastic/random input parameters and their probability distributions, (3) the corresponding correlation matrix and finally (4) the limit state function(s) depending on the situation. These required inputs, used for the case study, are further elaborated in chapter 3 and 4.

Based on the prepared reliability run the PTK will prepare a PLAXIS simulation that has to be sent to PLAXIS. For this transmission an “input interpreter” (script in python) is required. The interpreter sends the input to PLAXIS and a new PLAXIS run is started. After the calculation is finished an “output interpreter” (python scripts) extracts the desired output variables and sends them to the PTK. The PTK evaluates the results and prepares a new simulation, which is again send, etcetera. This iterative loop continues until some convergence criteria are met and the loop is stopped. A more detailed step wise explanation is given in appendix C.3.

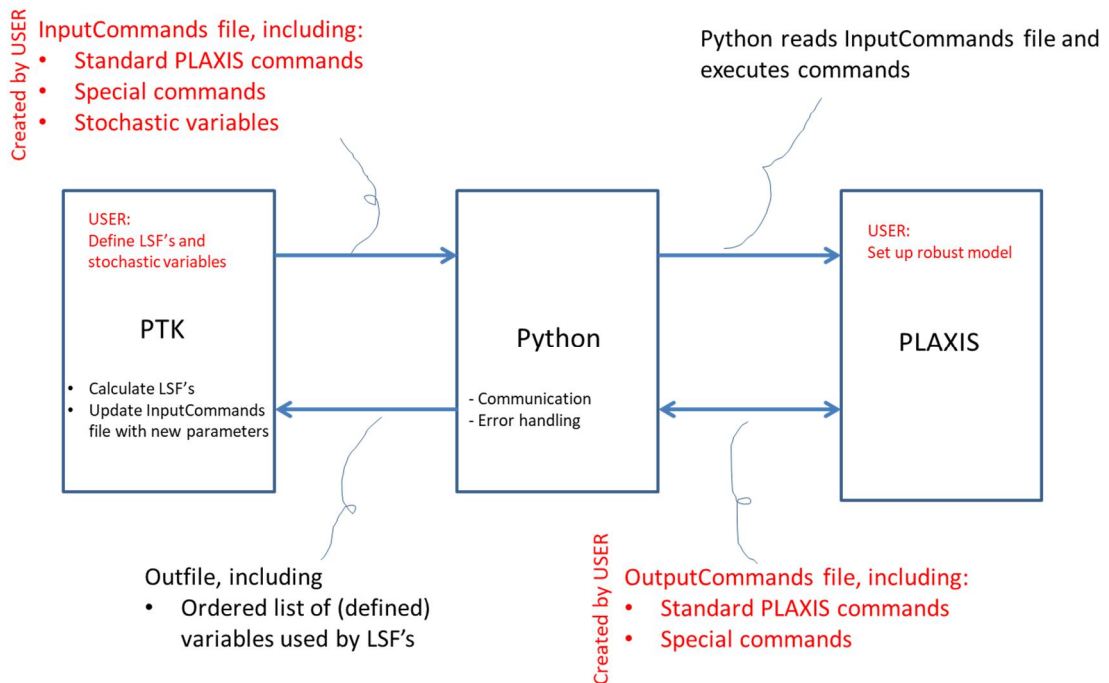


Figure 2.1 Coupling scheme as implemented: Probabilistic Toolkit-PLAXIS. In red all the required user input and in black the automated features. Also see paragraph 2.3 for further explanation on the terms used

### Set up of a robust PLAXIS model

Essential in the preparation of the probabilistic analysis is the preparation of the PLAXIS model. This preparation should include:

- Make the PLAXIS model as robust as possible (i.e. least amount of numerical errors) by entering more extreme parameter combinations to see if any numerical issues are to be expected. If numerical issues occur, they can in general be handled by making changes to for example: tension cut-off, adding small amount of cohesion, simplifying geometry/phases, adjusting numerical settings (e.g. switching off arc length control). Adjustments should be made without compromising the main results.
- Reduce calculation times by removing non-essential phases.
- It should be judged to what extent failure is expected during the “construction phases”.

## 2.3 Coupling: features

To explore the features and limitations of the PLAXIS software reference is made to the PLAXIS manuals, these can be downloaded from the PLAXIS website: [www.PLAXIS.com](http://www.PLAXIS.com).

To explore the features and limitations of PTK reference is made to the PTK manual. An introduction to the PTK as well as experiences gained during this study are presented in Annex C.

The PTK includes the following features which have been developed within this project:

- To be able to read and write general text files allowing for generic coupling with external models, such as PLAXIS.

- Introduced a so-called block function for DS which allows for a more efficient interpolation around  $z = 0$ .
- More robust execution of external models (PLAXIS) by the PTK. Since random errors happen now and then on the PLAXIS side, an efficient way of recalculating the same PLAXIS input is introduced, without having to recalculate all previous results.
- Introduced the option for live update of calculation results, so the user can inspect progress of the calculation.
- A more detailed logging function is introduced, including reference to the failed PLAXIS calculation, allowing for more efficient bug fixing.
- An automatic backup function (every hour) is introduced. In case of a crash of the PTK the maximum loss of data is limited to one hour.

Within the project several generic python files have been developed that deal with the communication between PTK and PLAXIS. The features of the developed generic python files have been explained in Table 2.1.

Python file	Does what?
PLAXISController	Called by PTK. File management system, calls PLAXISInterface, fires commands and handles them.
PLAXISInterface	Called by PLAXISController. Opens PLAXIS, deals with password, deals with arc length control, reads InputCommands file, calls special commands from the Special Commands file
SpecialCommands	<p>Library of special commands to handle more complicated tasks that the PLAXIS command line cannot handle. User can call these commands through the InputCommands file</p> <p>Special commands developed and used for the case study in this report:</p> <ul style="list-style-type: none"> <li>- MaxAngularDestortionSheetPile</li> <li>- MaxBendingMoment</li> <li>- CorrosionReductionSheetPile</li> <li>- CorrosionReductionAnchor</li> <li>- SofteningModule</li> <li>- CorrosionReductionSheetPileElastic</li> <li>- OutputValues</li> </ul> <p>Existing special commands can be adjusted by USER if needed, or new special commands can be added to the library, dependent on the project at hand.</p>
Distortion	Algorithm that generates rotations from the PLAXIS output of plates (x,y,dx,dy). Is called by the special command "MaxAngularDestortionSheetPile".

Table 2.1 Features of the developed generic python coupling files

Next to the python coupling files several other files are used for the communication between PTK and PLAXIS, see Table 2.2. Most importantly there is a file called InputCommands. This is a neutral (text) file and can be filled by the USER with the relevant PLAXIS commands for his/her project at hand just like it may done in the PLAXIS commands line. Special commands can be added in the InputCommands file to allow for more complicated tasks not directly possible with the PLAXIS command line. These special commands have to be created for the specific project at hand. But it is feasible that a database with special commands is created allowing for re-using these commands. The special commands which have been developed for the case study presented in this study have been further elaborated in appendix C.3.

File	Who creates?	Content
InputCommands.in  <i>See appendix D.2 for the file used in the case study</i>	USER	<ul style="list-style-type: none"> <li>This file contains all the relevant PLAXIS commands to make changes to the PLAXIS model (i.e. change file) as well as the commands to extract the relevant output</li> <li>Using flags %..% the PTK recognizes the stochastic variables that can be read/edited by the PTK</li> <li>Using flags * to indicate a special command from Python library follows in order to perform complicated tasks (e.g. determining new properties per sheet pile section based on corrosion value or sorting and finding max values from output)</li> <li>The input file also contains all the initial (deterministic) properties of soil and structure</li> <li>File is read by Python script PLAXISInterface which “fires” the commands to PLAXIS Input or Output.</li> </ul>
PLAXIS.out  <i>See Table 5.2 for the outfile used in the case study</i>	Python	<p>This file contains the output results of the PLAXIS analysis. File is read by the PTK.</p> <p>For the case study in this report per section of the sheet pile frontwall the following output is listed:</p> <ul style="list-style-type: none"> <li>Mmax;i (max calculated in PLAXIS per section)</li> <li>Mpl;max;i (max. allowable Mpl;hinge per section)</li> <li>Mel;corr;i (max allowable Mel per section)</li> <li>Phi;max;i (max calculated in PLAXIS per section)</li> <li>Phi;CD;i (max allowable plastic rotation per section)</li> <li>Rho;max;i (the reached reduction value Rho per section) (not directly used in LSF's, but for information)</li> <li>SUMMstage (of last phase)</li> <li>Mmax;anchorwall</li> <li>Nmax;anchor</li> </ul>
Temporary files	PTK	The PTK generates intermediate temporary files during calculation

Table 2.2 Other files used in the PTK – PLAXIS coupling

### Challenges and limitations to consider

An overview of the challenges and limitations to consider is presented in appendix C.3.

A main challenge identified are the long calculation times when using the numerical integration method Directional Sampling. This method has been chosen here due to its robustness, however calculation times are in de order of weeks. Interesting to note is the ongoing developments relating to reliability analysis methods using surrogate (or response surface) modelling allowing for significant reductions of calculation times. Such a technique is reported in [Van den Eijnden, 2019] and this technique is expected to become available in the PTK soon.

## 2.4 Coupling: version control

In this study use is made of the following versions:

- PLAXIS 2D v2018.00.
- Probabilistic Toolkit v1.9.x.x.

- Python v3.4 (as installed with PLAXIS 2D v2018.00).

Within Python a number of scripts are developed. These scripts have been regularly updated throughout the project in 2018 and 2019. Version control is done by means of a Deltares repository<sup>4</sup>. The version of the scripts used for the case study within the project have been listed in Table 2.3 and Table 2.4.

Python file	Version
PLAXISController	8.1
PLAXISInterface	8.1
SpecialCommands	8.1
Distortion	8.1

Table 2.3 Version control of generic Python coupling scripts developed

File	Version
InputCommands.in	No specific version, created by USER for project at hand
PLAXIS.out	Automatically created per project
Temporary files	Automatically created per project

Table 2.4 Version control of other relevant files used

<sup>4</sup> <https://repos.deltares.nl/repos/ProbPLX>



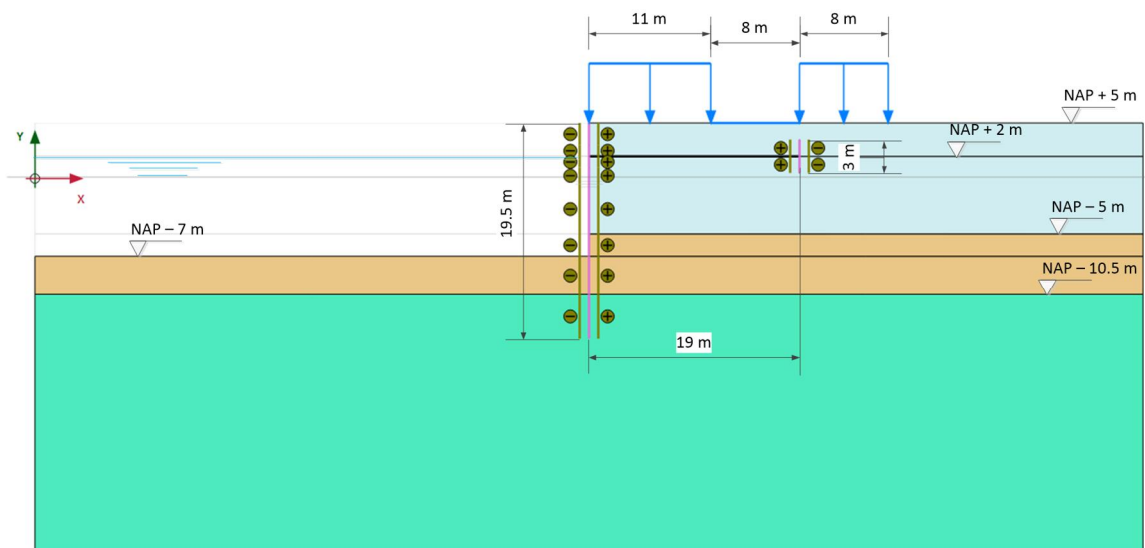
### 3 Case study: retaining wall

#### 3.1 Introduction

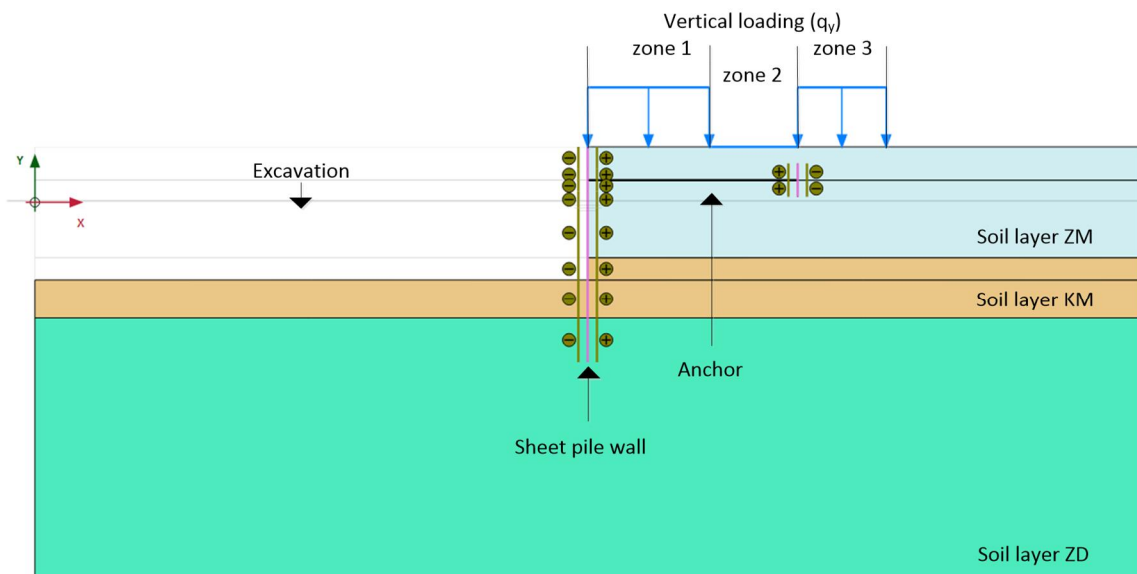
The case study as presented in [Deltares, 2016a] refers to an anchored retaining wall and has also been used in this report based on the following considerations:

- Currently and in the coming years, many sheet pile walls have to be re-assessed in the Netherlands.
- The behaviour of a sheet pile structure is strongly influenced by soil-structure interaction and is therefore a good example to study this problem.
- The case study presented is the wall of a lock chamber in fresh water. Specific for this application is the high fluctuation of water levels, causing significant corrosion during the service life.
- The case study allows for dealing with all relevant failure mechanisms relevant for an anchored sheet pile wall.

A detailed description of the case study is presented in this chapter. The geometry and various elements of the case study are presented in Figure 3.1. It is assumed that the lock is 25 years old and should function for another 50 years, thus until a service life of 75 years. Or in other words the reference period considered is 50 years. This aspect is relevant because reliability is always related to a certain reference period. The reference period is considered in the distributions for the time-dependent variables in load (i.e. waterlevels, surface load) and strength (corrosion) parameters.



a) dimensions



a) elements and names

Figure 3.1 Schematisation of the case study

**Note on Case Study**

It should be recognised that although the Case Study was based on a real situation the sheet pile type used here, an AZ26, is a less strong profile than might be used in reality due to design conservatism 25 years ago. The choice for a less strong profile was made to achieve lower reliability values and thus reduce calculation times and as such better allowing to highlight effects of different assumptions. As a result, no absolute conclusions can be drawn for this situation. Focus should be on relative effects.

**3.2 Geometry, water levels and loads**

The soil is built up of three horizontal layers, with the ground surface level at NAP +5 m. The soil layering is presented in Table 3.1.

Layer	Top	Code	Soil
[#]	[m NAP]	[-]	[-]
1	+5,0	ZM	Medium dense sand
2	-5,0	KM	Medium stiff / Firm clay
3	-10,5	ZD	Dense/very dense sand

Table 3.1 Soil layering used in case study

Concerning the water levels the following assumptions are made:

- The original water level, at the time of installation of the sheet pile was at NAP +1.0 m.
- The ground water level and the ground water potential of the sand layer ZD were in the past at NAP -1.0 m.
- The expected value of the ground water potential (layer ZD) is NAP 0.0 m.
- The expected value of the average water level is NAP +1.0 m.

- the expected value of the lowest water level, which is reached once in 50 years, is NAP – 1.0 m and the *decimeringshoogte*<sup>5</sup> is 0.3 m, these characteristics are necessary to define the distribution of the water level of the problem with extreme minima.
- There is a vertical linear gradient between the (ground) water pressures directly above and directly below the clay layer KM.

Concerning the surcharge loads on the ground surface, 3 zones are defined (as shown in Figure 3.1). The maximum expected value of the load is 30 kPa, which can be integrally present in the 3 zones or only locally. We consider zone 1 the one closest to the sheet pile (11 m length). Zones 2 and 3 are next to zone 1 and have a length of 8 m each. Each load/zone is characterized by its maximum value (30 kPa) and the fact that it can be present 10% of the time (in each zone). The loads are assumed to be uncorrelated.

### 3.3 Soil characterisation

The material model used in this study is the so-called ‘Mohr-Coulomb’ soil model. Here only one stiffness parameter is necessary. Nevertheless, the characteristics of the three soil layers (taken as in [Wolters, 2012]), considering the non-associative parameter-set ( $\phi \neq \psi$ ) for the ‘Hardening soil’, model for non-plain strain conditions (as found in triaxial tests) are summarised in Table 3.2 while in Table 3.3 the associative set is presented.

The transformation from non-associative to associative is done using the so-called best-guess equivalent model. More information on non-associative, associative and best-guess equivalent model is given in Appendix A. The sheet pile wall is a plain strain situation. In case of plain strain conditions in FEM calculations the best estimate angle of internal friction derived from triaxial test results has to be increased by a factor 9/8 to get the correct best estimate value. The by the factor 9/8 increased values of  $\phi$  and  $\psi$  for the Hardening Soil model in plain strain condition are presented in Table 3.4.

	Soil type	$\gamma$	$\gamma_{\text{sat}}$	$c'$	$\phi'$	$\psi'$	$E_{50;\text{ref}}$	$E_{\text{Oed};\text{ref}}$	$E_{\text{Ur};\text{ref}}$	$R_{\text{int}}$	$m$
[#]	[-]	[kN/m <sup>3</sup> ]	[kN/m <sup>3</sup> ]	[kN/m <sup>2</sup> ]	[°]	[°]	[MN/m <sup>2</sup> ]	[MN/m <sup>2</sup> ]	[MN/m <sup>3</sup> ]	[-]	[-]
1	SM	18.5	20.7	0.0	38.9	8.9	69.2	69.2	207.7	0.90	0.5
2	CM	-	17.4	14.8	26.9	-	7.69	5.27	15.38	0.67	1.0
3	SD	-	21.8	0.0	41.9	11.9	115.4	115.4	346.2	0.90	0.5

Table 3.2 *Non-associative soil parameters for non-plain strain conditions, average values of each layer, for Hardening soil*

	Soil type	$\gamma$	$\gamma_{\text{sat}}$	$c_a^*$	$\phi_a^*$	$\psi_a^*$	$E_{50;\text{ref}}$	$E_{\text{Oed};\text{ref}}$	$E_{\text{Ur};\text{ref}}$	$R_{\text{int}}$	$m$
[#]	[-]	[kN/m <sup>3</sup> ]	[kN/m <sup>3</sup> ]	[kN/m <sup>2</sup> ]	[°]	[°]	[MN/m <sup>2</sup> ]	[MN/m <sup>2</sup> ]	[MN/m <sup>3</sup> ]	[-]	[-]
1	SM	18.5	20.7	1.0	37.0	37.0	69.2	69.2	207.7	0.90	0.5
2	CM	-	17.4	14.1	25.8	25.8	7.69	5.27	15.38	0.67	1.0
3	SD	-	21.8	1.0	39.8	39.8	115.4	115.4	346.2	0.90	0.5

Table 3.3 *Associative soil parameters for non-plain strain conditions, average values of each layer, for Hardening soil*

<sup>5</sup> A measure of the increase or decrease of the height of the water level as a result of the respective increase or decrease of the frequency of occurrence of this water level with an increment factor of 10

	Soil type	$\gamma$	$\gamma_{\text{sat}}$	$c_a^*$	$\phi_{\alpha}^*$	$\psi_{\alpha}^*$	$E_{50;\text{ref}}$	$E_{\text{oed};\text{ref}}$	$E_{\text{ur};\text{ref}}$	$R_{\text{int}}$	$m$
[#]	[-]	[kN/m <sup>3</sup> ]	[kN/m <sup>3</sup> ]	[kN/m <sup>2</sup> ]	[°]	[°]	[MN/m <sup>2</sup> ]	[MN/m <sup>2</sup> ]	[MN/m <sup>3</sup> ]	[-]	[-]
1	SM	18.5	20.7	1.0	41.6	41.6	69.2	69.2	207.7	0.90	0.5
2	CM	-	17.4	14.1	29.1	29.1	7.69	5.27	15.38	0.67	1.0
3	SD	-	21.8	1.0	44.7	44.7	115.4	115.4	346.2	0.90	0.5

Table 3.4 Associative soil parameters for plain strain conditions, average values of each layer, for Hardening soil

The non-associative parameter-set ( $\phi=\psi$ ) in non-plain strain conditions for 'Mohr-Coulomb' soil model is given in Table 3.5 and the associative parameter-set is given in Table 3.6.

	Soil type	$\gamma$	$\gamma_{\text{sat}}$	$c_a^*$	$\phi_{\alpha}^*$	$\psi_{\alpha}^*$	$E'$	$R_{\text{int}}$
[#]	[-]	[kN/m <sup>3</sup> ]	[kN/m <sup>3</sup> ]	[kN/m <sup>2</sup> ]	[°]	[°]	[MN/m <sup>2</sup> ]	[-]
1	SM	18.5	20.7	1.0	37.0	37.0	50	0.90
2	CM	-	17.4	14.1	25.8	25.8	6.5	0.67
3	SD	-	21.8	1.0	39.8	39.8	125	0.90

Table 3.5 Associative soil parameters for non-plain strain conditions, average values of each layer, for Mohr-Coulomb. This parameter set is used in this study

	Soil type	$\gamma$	$\gamma_{\text{sat}}$	$c_a^*$	$\phi_{\alpha}^*$	$\psi_{\alpha}^*$	$E'$	$R_{\text{int}}$
[#]	[-]	[kN/m <sup>3</sup> ]	[kN/m <sup>3</sup> ]	[kN/m <sup>2</sup> ]	[°]	[°]	[MN/m <sup>2</sup> ]	[-]
1	SM	18.5	20.7	1.0	41.6	41.6	50	0.90
2	CM	-	17.4	14.1	29.1	29.1	6.5	0.67
3	SD	-	21.8	1.0	44.7	44.7	125	0.90

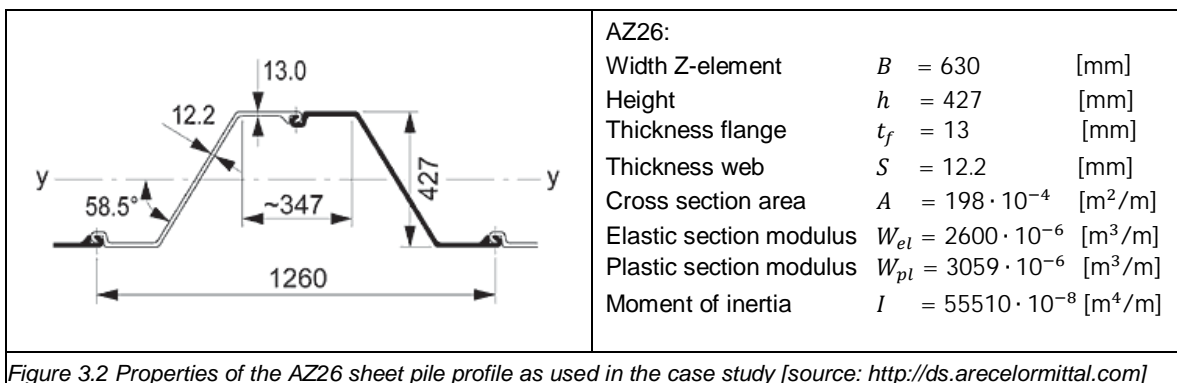
Table 3.6 Associative soil parameters for plain strain conditions, average values of each layer, for Mohr-Coulomb

For this case study a drained analysis is carried out with the associative non-plain strain parameter-set just like [Deltares, 2016a] and [Deltares, 2018], see Table 3.5.

The main argument in this research phase for choosing the lower non-plain strain values was calculation time of the runs. Another argument for not using the high plain strain values (compared with non-plane strain values) is that the (potential) softening of the soil also needs to be taken into account when allowing for softening in the sheet pile structure (as described in paragraph 3.8). Basically, a strain analysis needs to be made to see if using peak strength parameters of the soil is allowed in combination with large deformations/strains due to softening of the front wall. If this is not allowed lower strength parameters must be used. These types of analyses are however considered to be outside the scope of this research. Generically speaking an engineer needs always to assess per situation which parameters are applicable.

### 3.4 Structure characterisation

For both the sheet pile front wall and the anchor sheet pile wall, an AZ26 profile is chosen. The dimensions of the AZ26 profile are presented in Figure 3.2). For the steel quality S240 GP is chosen with a yield stress of  $f_y = 240 \cdot 10^3 \text{ kN/m}^2$



For the anchor rod connecting the front wall and the anchor wall an initial diameter of  $63.4 \cdot 10^{-3}$  m (area  $3156 \cdot 10^{-6}$  m<sup>2</sup>) is chosen with a yield stress of  $f_y = 355 \cdot 10^3$  [kN/m<sup>2</sup>]. For the spacing between the anchors a distance of 1.6 m is chosen.

Note that relevant for the Class definition according to Eurocode 3-5 is the value 'b', this value is a measure of the width of the flange. In this width part of the curvature from flange to web is included. According to [ArcelorMittal, 2017] this value is 356 mm. Also see appendix E.1 for more information on the principle of Class definitions.

### 3.5 Corrosion characterisation

#### Sheet pile vertical zone discretization

In practice, the effect of corrosion on the sheet pile and anchor reliability is incorporated in the analysis by applying a deterministic value of the corrosion, leading to a reduced cross section. Various thickness reduction(s) can be assigned to different sections of the retaining structure, depending on the 'zone' (i.e. contact with air, soil and/or water). In this study it was chosen to use the degree of discretisation (i.e. the nr. of zones) in accordance with the proposal in EN 1993-5:2008, also see appendix B.1.

As the zone D between NAP -0,5 m and NAP -7.0 m is the zone that is expected to be the governing one with the highest moment and high reduction of wall thickness reduction due to corrosion for the probabilistic analysis this zone will be split in 3 sections:

- Zone D1 between NAP -0,5 m and NAP -1.5 m.
- Zone D2 between NAP -1,5 m and NAP -5.0 m.
- Zone D3 between NAP -5 m and NAP -7.0 m.

In zone A, B, C and E no additional discretisation is to be applied.

#### Thickness reduction due to corrosion

In appendix B.2 and B.3 the recommend (deterministic) values for corrosion as currently used in geotechnical practice are presented. This includes recommended values for thickness-reduction on the side of the soil by Deltares [ENW, 2104], while thickness-reduction on the side without soil are recommended by [RWS, 2013]. In this study it has been chosen to consider the presented values as mean corrosion values to be expected. Based on the analyses of the collected degradation data [Deltares, 2019b] this seems a reasonable assumption as in 50 % of the about 80-year-old cases these deterministic corrosion values were exceeded.

In Table 3.7 and Table 3.8 the mean thickness reduction of the various vertical sections or zones of the sheet pile are presented at  $T = 75$  years, these values will be the basis for the

calculations in line with EN 1993-5:2008, for a specific design service life (i.e. to include the degradation effect at the end of the service life).

Zone	Level		Mean thickness reduction due to corrosion		
	Top [m NAP]	Bottom [m NAP]	Left [mm]	Right [mm]	Total [mm]
<b>A:</b> Above upper lockage level	+5.0	+3.0	0.75	1.70	2.45
<b>B:</b> Upper lockage level-GWL	+3.0	+1.0	1.50	1.70	3.20
<b>C:</b> GWL- lower lockage level	+1.0	-0.5	1.50	0.90	2.40
<b>D:</b> Lower lockage level-bottom	-0.5	-7.0	3.75	0.90	4.65
<b>E:</b> Below bottom	-7.0	-14.5	0.90	0.90	1.80

Table 3.7 Mean thickness reduction of sheet pile after 75 years (mean values per zone)

Zone	Level		Mean thickness reduction due to corrosion		
	Top [m NAP]	Bottom [m NAP]	Left [mm]	Right [mm]	Total [mm]
<b>F:</b> Top -GWL	+3.5	+1.0	1.7	1.7	3.4
<b>G:</b> GWL- tip (*)	+1.0	-0.5	0.9	0.9	1.8

Table 3.8 Mean thickness reduction of the anchor wall after 75 years (mean values per zone)

(\*) note: the anchor wall is positioned from NAP +3.5 m to NAP +0.5 m. The part of the anchor wall between NAP +1 m and NAP +0.5 m will have a smaller thickness reduction according to the above definition. This is ignored in this study. Thickness reduction values according to zone F are also used in zone G.

In this study also, some additional calculations are made taking the time depending effect of the corrosion in account. As such two alternative sets for the corrosion are presented:

- At the beginning of the chosen reference period  $T = 25$  years, Table 3.9 and Table 3.10.
- In the middle of the chosen reference period at  $T = 50$  years, Table 3.11 and Table 3.12.

Zone	Level		Mean thickness reduction due to corrosion		
	Top [m NAP]	Bottom [m NAP]	Left [mm]	Right [mm]	Total [mm]
<b>A:</b> Above upper lockage level	+5.0	+3.0	0.5	1.2	1.7
<b>B:</b> Upper lockage level-GWL	+3.0	+1.0	1	1.2	2.2
<b>C:</b> GWL- lower lockage level	+1.0	-0.5	1	0.6	1.6
<b>D:</b> Lower lockage level-bottom	-0.5	-7.0	2.5	0.6	3.1
<b>E:</b> Below bottom	-7.0	-14.5	0.6	0.6	1.2

Table 3.9 Mean thickness reduction of sheet pile after 50 years (mean values per zone)

Zone	Level		Mean thickness reduction due to corrosion		
	Top [m NAP]	Bottom [m NAP]	Left [mm]	Right [mm]	Total [mm]
<b>F:</b> Top -GWL	+3.5	+1.0	1.2	1.2	2.4

<b>G:</b> GWL- tip	+1.0	-0.5	0.6	0.6	1.2
--------------------	------	------	-----	-----	-----

Table 3.10 Mean thickness reduction of the anchor wall after 50 years (mean values per zone)

Zone	Level		Mean thickness reduction due to corrosion		
	Top [m NAP]	Bottom [m NAP]	Left [mm]	Right [mm]	Total [mm]
<b>A:</b> Above upper lockage level	+5.0	+3.0	0.25	0.6	0.85
<b>B:</b> Upper lockage level-GWL	+3.0	+1.0	0.5	0.6	1.1
<b>C:</b> GWL- lower lockage level	+1.0	-0.5	0.5	0.3	0.8
<b>D:</b> Lower lockage level-bottom	-0.5	-7.0	1.25	0.3	1.55
<b>E:</b> Below bottom	-7.0	-14.5	0.3	0.3	0.6

Table 3.11 Mean thickness reduction of sheet pile after 25 years (mean values per zone)

Zone	Level		Mean thickness reduction due to corrosion		
	Top [m NAP]	Bottom [m NAP]	Left [mm]	Right [mm]	Total [mm]
<b>F:</b> Top -GWL	+3.5	+1.0	0.6	0.6	1.2
<b>G:</b> GWL- tip	+1.0	-0.5	0.3	0.3	0.6

Table 3.12 Mean thickness reduction of the anchor wall after 25 years (mean values per zone)

In the calculations for this case study, a uniform (i.e. not differentiating within a vertical zone) corrosion rate  $\Delta t_i$  is assumed along a vertical section of the sheet pile, as a random variable. The thickness loss due to corrosion is considered truncated normally distributed, with a mean value as presented in Table 3.7 to Table 3.12. Truncation is done on a minimum value of 0 mm (logically) and a maximum value of 13 mm (thickness of flange AZ26). The coefficient of variation of the thickness loss is a variable. The approach how to deal with corrosion as a stochastic variable in relation to the different zones is further elaborated in chapter 4.6.

### 3.6 Corrosion effect

The effect of a thickness reduction on the mechanical behaviour of the sheet pile is non-linear with respect to the moment and plastic rotation capacity.

In Figure 3.3 the linear part of the effect of a thickness reduction on the plastic and elastic section moduli are presented. Effectively the program presents 5.09 mm corrosion as the upper limit of Class 2. In this study for the end of Class 2 a value of 45 is used. Also see appendix E.1 for more background information on the principle of Classes of sheet pile cross-sections.

$$\frac{b/t_f}{\epsilon} \leq \sim 45 \quad [-] \quad (1)$$

with

$$\epsilon = \sqrt{\frac{235}{f_y}} \quad [-] \quad (2)$$

Furthermore, the program presents 7.59 mm as the upper limit of Class 3. For the end of Class 3 a value of 66 is used in this study.

$$\frac{b/t_f}{\epsilon} \leq \sim 66 \quad [-] \quad (3)$$

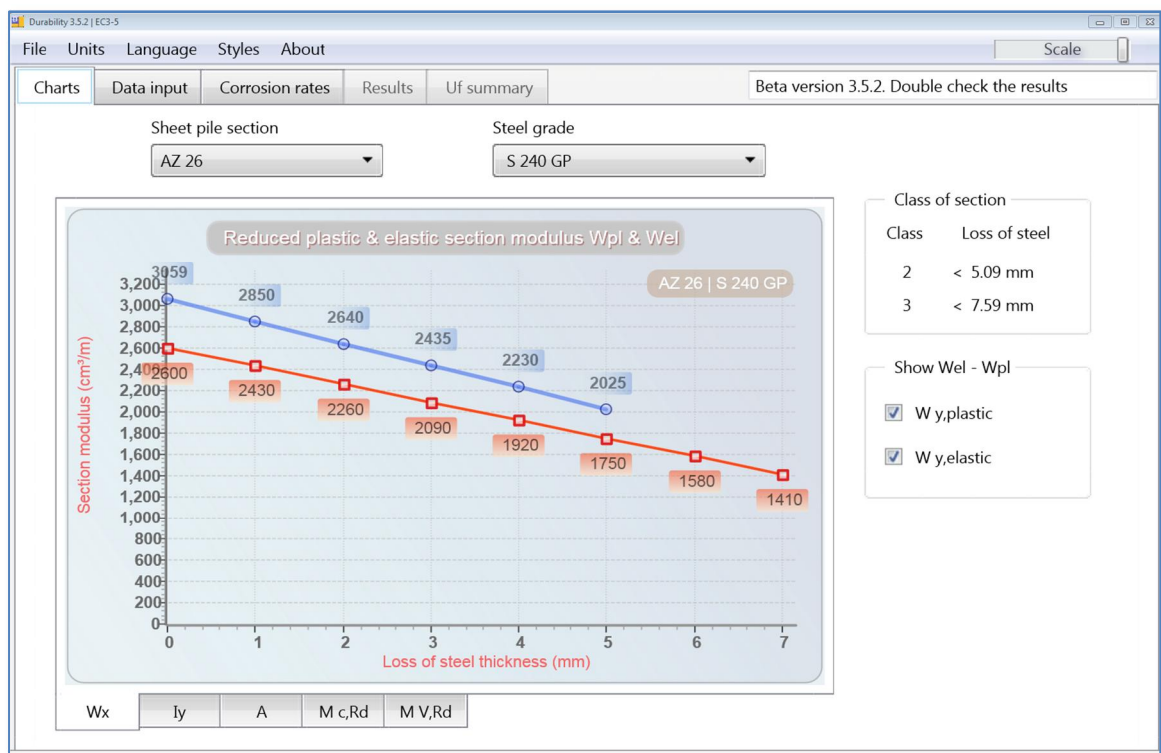


Figure 3.3 For loss of steel thickness reduced plastic and elastic section moduli of a AZ26 S240GP by [ArcelorMittal, 2017]

In this research the nonlinear effect on the plastic section modulus for wall thickness reduction beyond 5 mm is taken in account as well as the nonlinear effect on Plastic rotation angle capacity by using [EN1993-5:2008] Figure C-1b, see Figure 3.4. In this research a linear interpolation will be applied in between the lines in Figure 3.4.

EN1993-5:2008 allows for taking plastic rotation capacity into account. Even for a Class 3 sections some plastic rotation capacity is allowed albeit that the allowed stress level in the section should be lowered such that basically a Class 1 or 2 is found. Or in other words EN 1993-5:2008 allows that some strength (bending moment capacity) is exchanged with some rotation capacity (within certain limits).



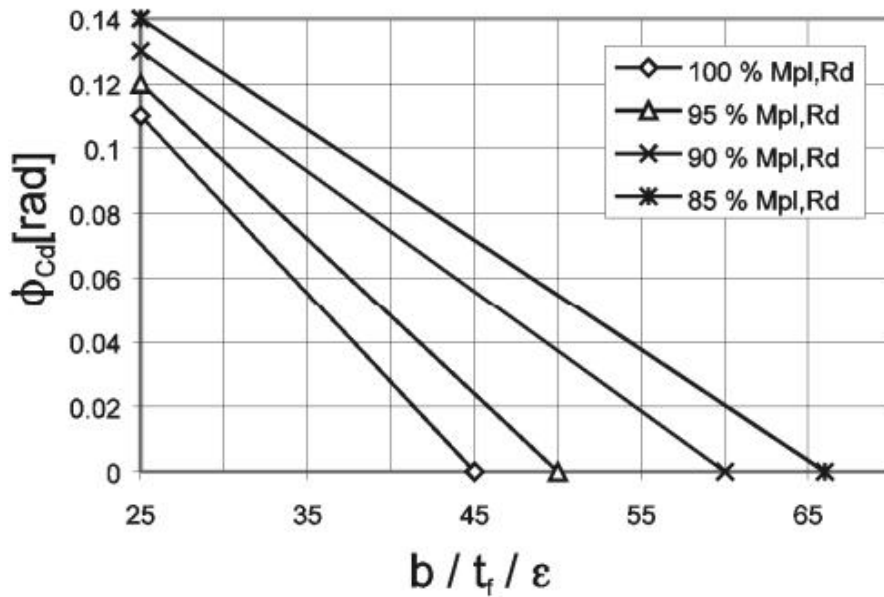


Figure 3.4 Plastic rotation angle of a z-section  $\phi_{Cd}$  provided by the cross-section at different levels of reduced plastic moment capacity  $M_{pl,Rd}$  [EN 1993-5:2008] Figure C-1b

When combining the information in Figure 3.3 and Figure 3.4 it is possible to create Figure 3.5. Figure 3.5 presents for an AZ26 with steel grade S240GP (as used in this case study) the (nonlinear) relation between bending moment capacity and plastic rotation capacity vs the wall thickness reduction of the flange. To create this figure use has to be made of the principles explained in the paragraphs 3.7 and 3.8. More background information can also be found in appendix E.

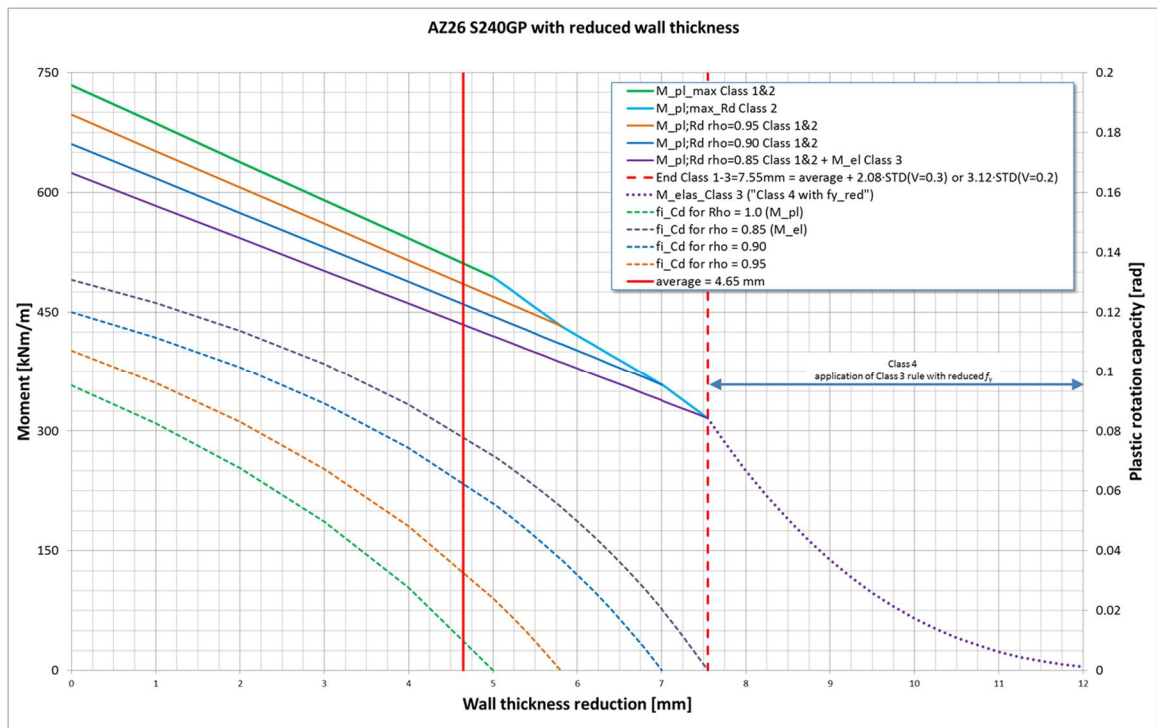


Figure 3.5 Effect of thickness reduction on moment capacity and plastic rotation capacity of an AZ26 S240GP. Note that due to switching from the  $b/t_f / \epsilon$  -axis to a wall thickness reduction axis a non-linear trend is found for  $\phi_{cd}$

### 3.7 Sheet pile parameters as function of corrosion

In this paragraph for the AZ26 the relations as function of thickness reduction  $\Delta t_i$  for the cross-sectional area, section moduli and moment of inertia are presented. Some of the relations use the reduced thickness of the flange of the sheet pile section,  $t_{f_i}$ :

$$t_{f_i} = t_f - \Delta t_i \quad (4)$$

Where:

$t_f$	[mm]	initial thickness of flange of the sheet pile (see Figure 3.2)
$\Delta t_i$	[mm]	thickness reduction due to corrosion of sheet pile section, i
$t_{f_i}$	[mm]	corroded thickness of flange of sheet pile section, i

#### Cross sectional area

The Cross sectional area given the thickness reduction,  $\Delta t_i$ , is:

$$A_{\Delta t_i} = (198 - 14 \cdot \Delta t_i) \cdot 10^{-4} \quad [m^2/m] \quad (5)$$

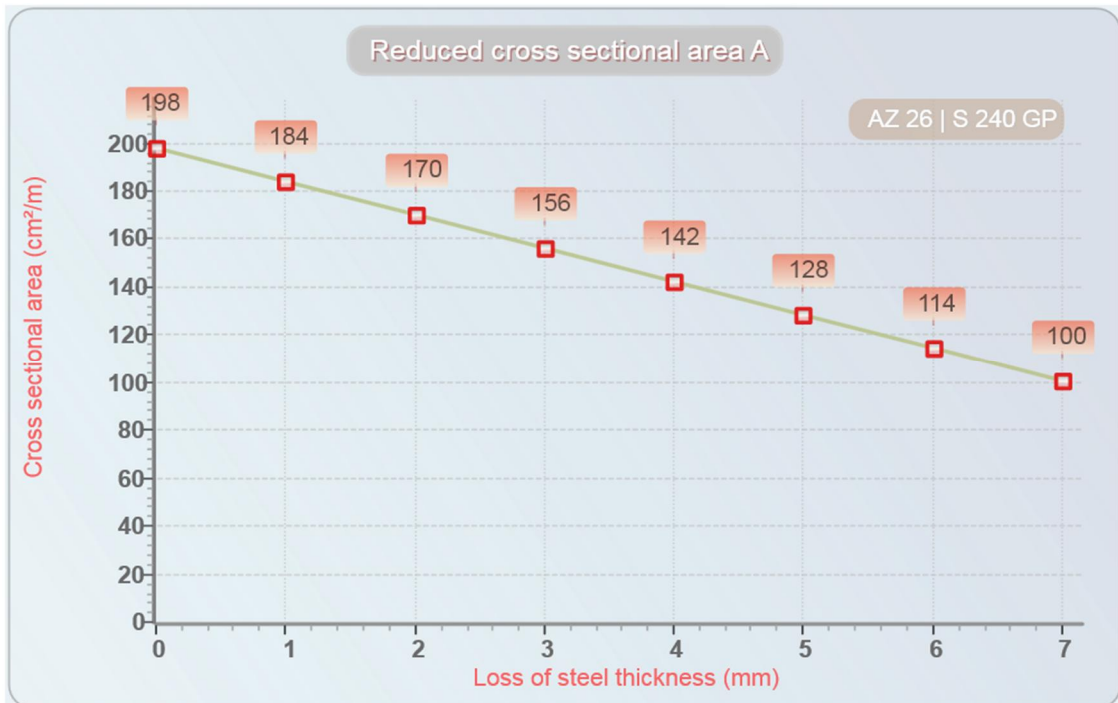


Figure 3.6 For loss of steel thickness reduced cross sectional area of a AZ26 S240GP by [ArcelorMittal, 2017]

#### Moment of inertia

The Moment of inertia given the thickness reduction,  $\Delta t_i$ , is:

$$I_{\Delta t_i} = (55510 - 3680 \cdot \Delta t_i) \cdot 10^{-8} \quad [m^4/m] \quad (6)$$

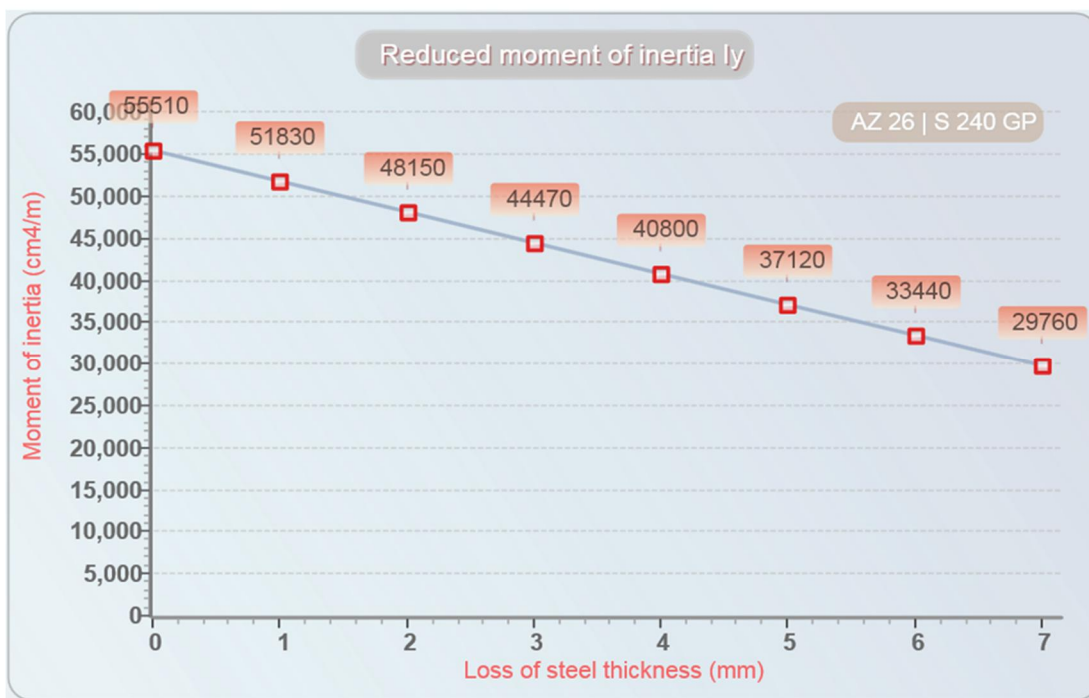


Figure 3.7 For loss of steel thickness reduced moment of inertia of a AZ26 S240GP by [ArcelorMittal, 2017]

### Elastic and full plastic section modulus

The elastic section modulus given the thickness reduction,  $\Delta t_i$ , is:

$$W_{el:\Delta t_i} = (2600 - 170 \cdot \Delta t_i) \cdot 10^{-6} \quad [m^3/m] \quad (7)$$

The full plastic section modulus is:

$$W_{pl:i} = \left( \frac{W_{el:\Delta t_i}}{0.85} \right) \quad [m^3/m] \quad (8)$$

Note that formula (8) is an approximation of the  $W_{pl}$  as presented in Figure 3.8. The value 0.85 is based on the initial ratio between  $W_{el}$  and  $W_{pl}$  for no thickness reduction, i.e. loss of steel is 0 mm.

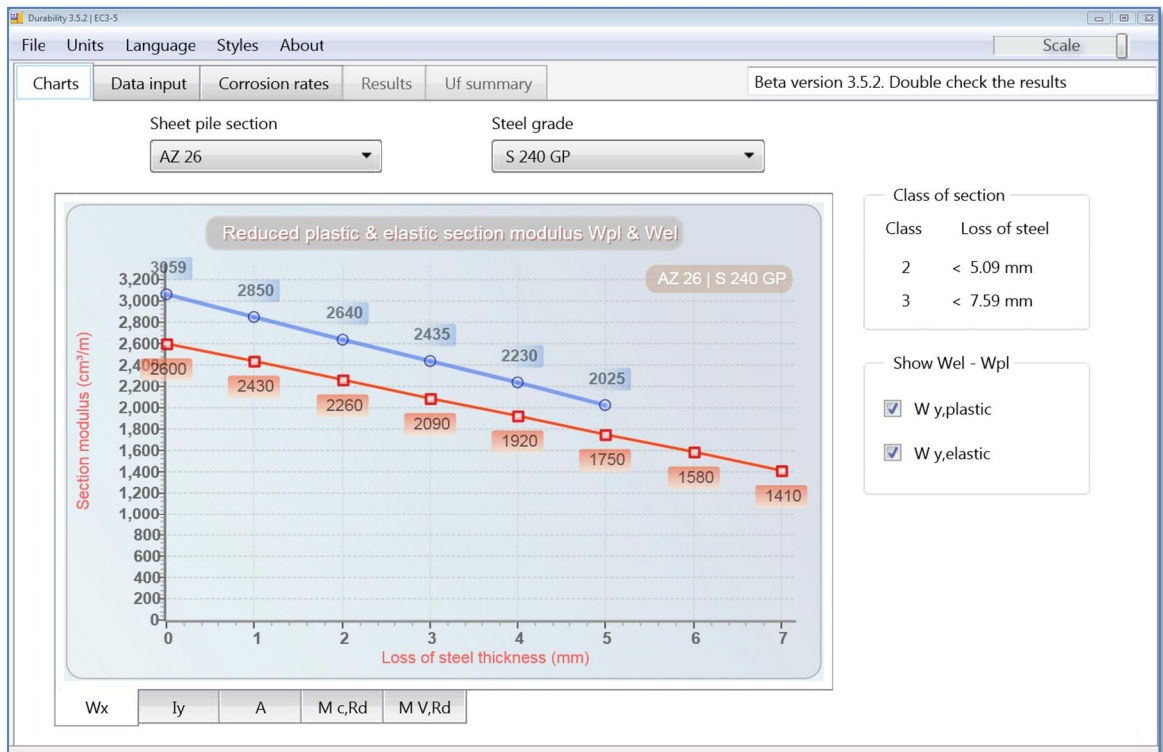


Figure 3.8 For loss of steel thickness reduced plastic and elastic section moduli of a AZ26 S240GP by [ArcelorMittal, 2017]

### Plastic section moduli, $(b/t_{f_i}/\epsilon) \leq 66$

For sheet pile sections with a thickness reduction  $(b/t_{f_i}/\epsilon) \leq 66$  the maximum reduced plastic section modulus, given the thickness reduction,  $\Delta t_i$  is based on a linear interpolation for  $(b/t_{f_i}/\epsilon)$  in between the maximum value of plastic section modulus at 45, 50, 60 and 66. with a  $\rho_c = 1; 0.95; 0.9$  and  $0.85$  for no plastic rotation capacity (Class 2) based on  $\phi_{Cd,i} = 0$  in EN 1993-5:2008 fig C-1, see Figure 3.4.

$$W_{pl,max;i} = \rho_{C,max;i} \cdot W_{pl,i} \quad [m^3/m] \quad (9)$$

For  $(b/t_{f_i}/\epsilon) \leq 45$  the maximum reduction factor is  $\rho_{C,max;\leq 45;i}$ :

$$\rho_{C,max;\leq 45;i} = 1 \quad [-] \quad (10)$$

For  $45 \leq (b/t_{f_i}/\epsilon) \leq 50$  the maximum reduction factor is  $\rho_{C,max;45-50;i}$ :

$$\rho_{C,max;45-50;i} = 1 + \left( \frac{\left( \frac{b}{\epsilon \cdot t_{f_i}} - 45 \right) \cdot (0.95 - 1)}{(50 - 45)} \right) [-] \quad (11)$$

For  $50 \leq (b/t_{f_i}/\epsilon) \leq 60$  the maximum reduction factor is  $\rho_{C,max;50-60;i}$ :

$$\rho_{C;max;50-60;i} = 0.95 + \left( \frac{\left( \frac{b}{\epsilon \cdot t_{fi}} - 50 \right) \cdot (0.9 - 0.95)}{(60 - 50)} \right) [m^3] \quad (12)$$

For  $60 \leq (b/t_{fi}/\epsilon) \leq 66$  the maximum reduction factor is  $\rho_{C;max;60-66;i}$  :

$$\rho_{C;max;60-66;i} = 0.90 + \left( \frac{\left( \frac{b}{\epsilon \cdot t_{fi}} - 60 \right) \cdot (0.85 - 0.9)}{(66 - 60)} \right) [m^3] \quad (13)$$

### 3.8 Plastic rotation capacity (softening)

Annex C from [EC3-5:2008] gives guidelines for incorporating plastic hinges and rotation capacity in the design and/or assessment of steel sheet pile structures. It also allows to make use of a reduced yield strength (resulting in a reduced  $M_{pl,Rd}$ ) effectively shifting the boundaries of the Class 1 and 2 area. As such also within Class 3 (according to the definition of EN 1993-5:2008 Table 5-1) use can be made of rotation capacity. Basically EN 1993-5:2008 allows to exchange bending moment capacity and rotation capacity.

#### Principle of softening

The principle of softening is explained in Figure 3.9. The figure shows that the sheet pile has a certain maximum (peak) capacity. After reaching this maximum capacity the capacity will start to decrease (softening), however the decrease of the capacity happens in a trustworthy manner. Based on tests it is shown that the sheet pile has a certain minimum bending moment capacity ( $M_{pl,Rd}$ ) in combination with a certain minimum rotation capacity ( $\phi_{Cd}$ ).

Note that softening of the sheet pile is only possible in case  $(b/t_{fi}/\epsilon) < 66$ . When this condition is not met this basically means the sheet pile is a Class 4 section profile without any rotation capacity. In appendix E more background information can be found on plastic rotation capacity.

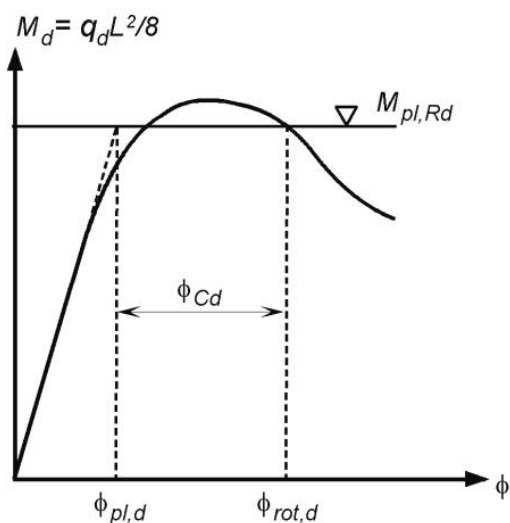


Figure 3.9 Interaction between bending moment capacity (vertical axis) and rotation capacity (horizontal axis).  $\phi_{Cd}$  is the available rotation capacity of the sheet pile section at a certain bending moment capacity ( $M_{pl,Rd}$ )

It should be noted that the rotation capacity of the sheet pile profile ( $\phi_{Cd}$ ) is defined as the rotation attributed to the plastic (non-reversible) deformations. In the current implementation of

the python SofteningModule (see Table C.1) however all rotations (elastic + plastic) are extracted from PLAXIS and used in the LSF. This is a conservative approach. In general, however the elastic rotations are relatively small compared with the plastic rotations.

#### Illustration of softening

The above described Softening process has been illustrated in Figure 3.10 and Figure 3.11. Figure 3.10 may be seen as a 3D plot. The third axis in this case is then perpendicular to the figure and displays the bending moment capacity  $M_{pl,Rd}$ . If 4 cross-sections were made of this 3D figure (i.e. the 4 coloured lines in the figure) these would look like the lines in Figure 3.11. In Figure 3.11 use has been made of “softening steps” of 1% just like the way it has been implemented into the python script SofteningModule (see Table C.1).

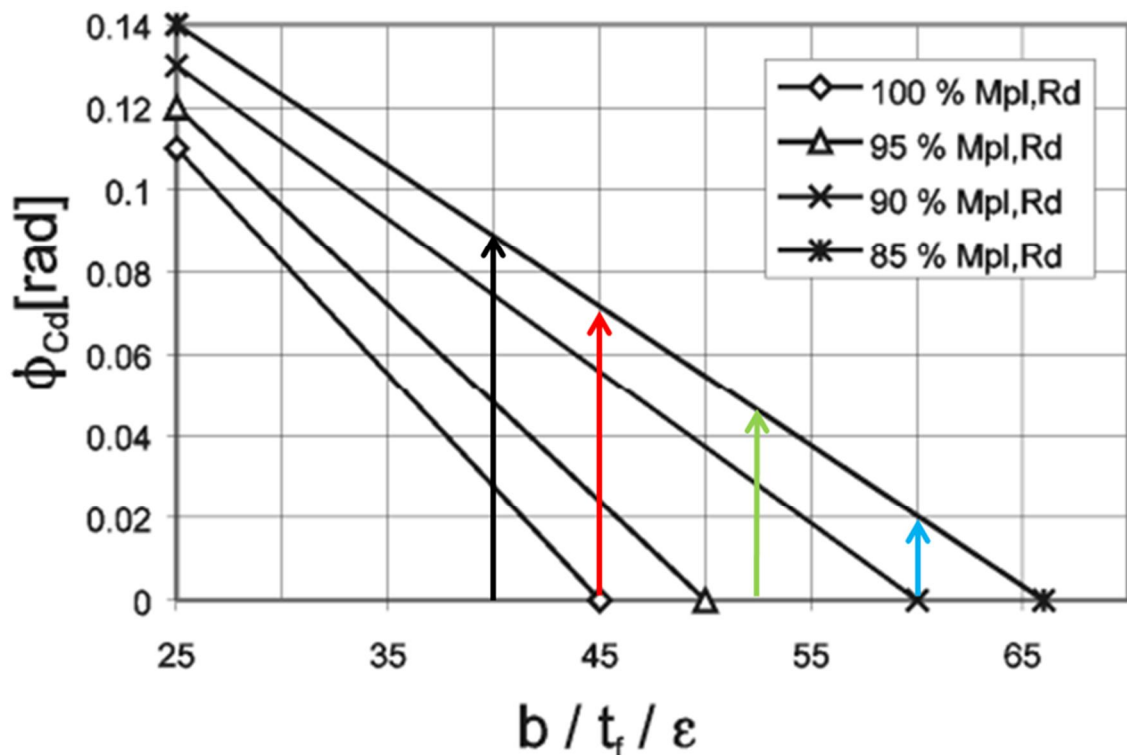


Figure 3.10 This figure is a copy of Figure 3.4. showing the plastic rotation angle of a z-section  $\phi_{cd}$  provided by the cross-section at different levels of reduced plastic moment capacity  $M_{pl,Rd}$  [EC3-5:2008] Figure C-1b. Indicated are four coloured lines which are cross-sections of the 3D figure that can be imagined

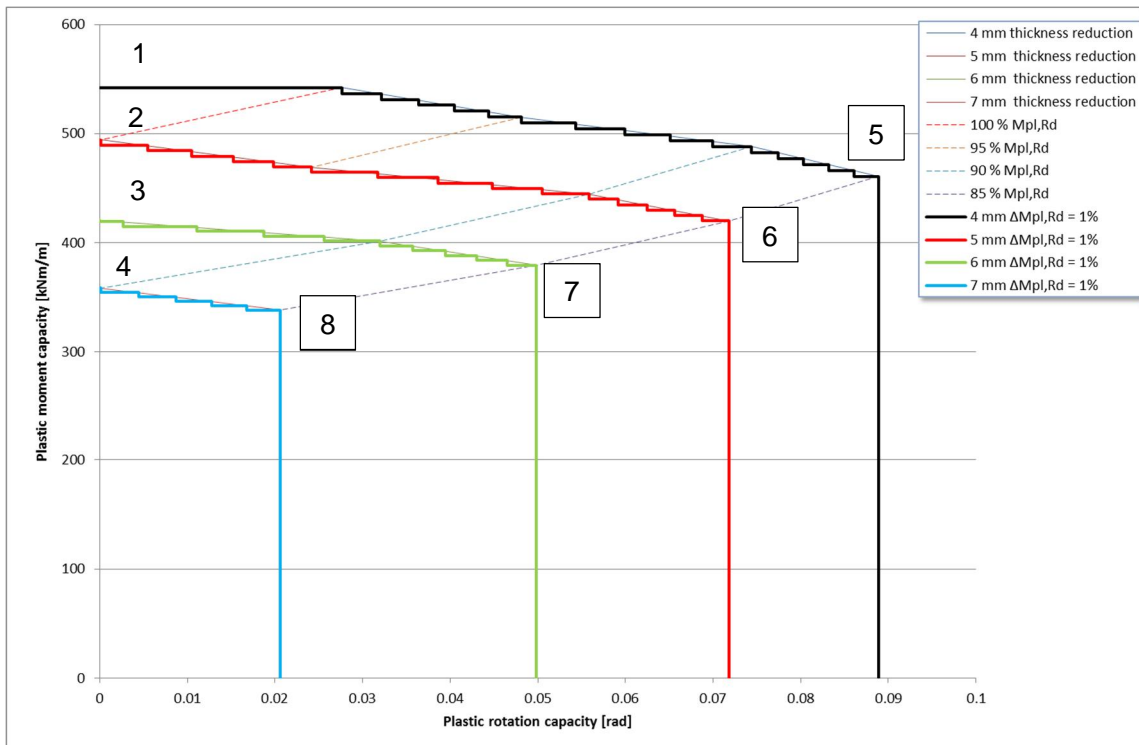


Figure 3.11 The relationship between plastic rotation capacity and plastic bending moment capacity, using softening steps of 1%, for the four cross-sections shown in Figure 3.10

The values of the bending moment capacity indicated within the graph with the numbers 1 - 8 are quantified in Table 3.13. The values of the numbers 1 – 4 can be calculated using the formulas in paragraph 3.7. The values for numbers 5 – 8 follow from numbers 1 – 4 using a factor of 0.85.

Nr	Bending moment [kNm/m]	Nr	Bending moment [kNm/m]
1	542	5	$542 * 0.85 = 461$
2	494	6	$494 * 0.85 = 420$
3	$446 * 0.943 = 421$	7	$446 * 0.85 = 379$
4	$398 * 0.90 = 358$	8	$398 * 0.85 = 338$

Table 3.13 Quantification of the bending moment capacities at numbers 1 – 8 in Figure 3.11

## 4 Random variables and correlations

### 4.1 Introduction

Although all parameters have a stochastic nature, a high number of stochastic variables leads to less robust probabilistic calculation and a significant increase in necessary computation time. Furthermore, it is also unnecessary to consider uncertainties that do not have significant influence in the probability of failure, although it may not always be directly clear whether a parameter is relevant or not. For this case study the choice made regarding the stochastic variables and their correlations is partly based on [Deltares, 2016a]. Different assumptions are made regarding the surcharge loads, corrosion and yield stress.

### 4.2 Soil parameters

For this case study the soil parameters that are expected to have the most influence have been selected as stochastic variables and are presented in Table 4.1. The relevant soil layering has been repeated in Figure 4.1. The soil parameters are assumed to be time independent.

Stochastic variable	symbol	Unit	25-75 year period			distribution
			$\mu$	$\sigma$	var	
sand medium (SM), unsaturated weight	$\gamma_{\text{unsat\_SM}}$	[kN/m <sup>3</sup> ]	18.7	1.04	0.06	normal
sand medium (SM), saturated weight	$\gamma_{\text{sat\_SM}}$	[kN/m <sup>3</sup> ]	20.7	1.04	0.05	normal
sand medium (SM), friction angle	$\varphi_a^*_{\text{SM}}$	[°]	37.0	3.70	0.1	truncated normal [0;60]
sand medium (SM), effective stiffness	$E'_{\text{SM}}$	[MN/m <sup>2</sup> ]	50.0	15.00	0.3	lognormal
clay medium (CM), friction angle	$\varphi_a^*_{\text{CM}}$	[°]	25.8	2.58	0.1	truncated normal [0;60]
clay medium (CM), stiffness	$E'_{\text{CM}}$	[MN/m <sup>2</sup> ]	6.5	1.95	0.3	lognormal
clay medium (CM), cohesion	$c_a^*_{\text{CM}}$	[kN/m <sup>2</sup> ]	14.8	2.96	0.2	lognormal
sand dense (SD), friction angle	$\varphi_a^*_{\text{SD}}$	[°]	39.8	3.98	0.1	truncated normal [0;60]

Table 4.1 The selected soil parameters for this case study with their mean values, standard deviations and reliability distribution

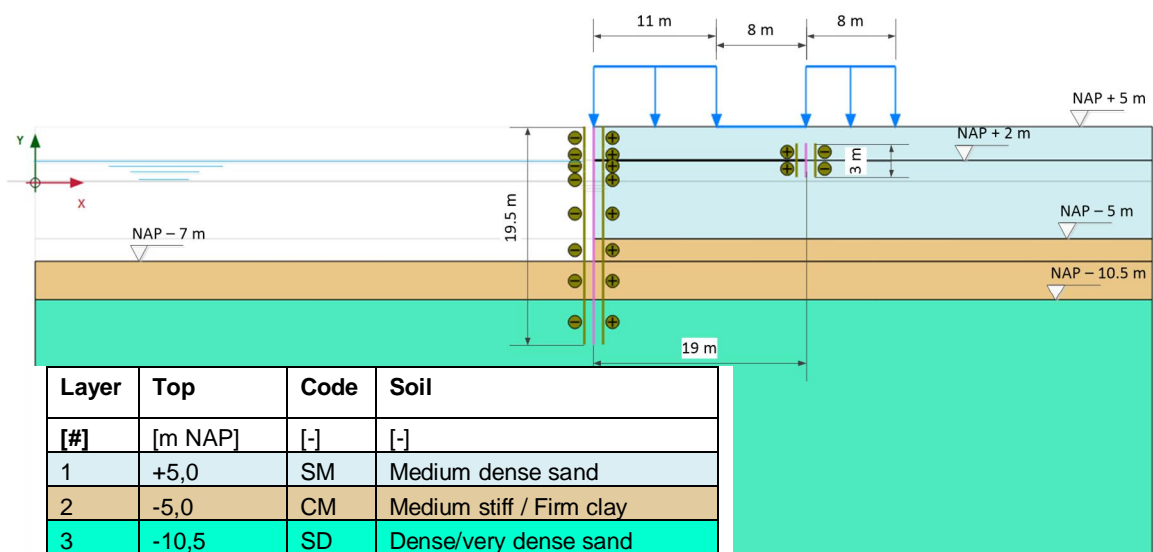


Figure 4.1 Geometry and soil layering used in the case study



### 4.3 Water levels

For the water level it is known that the value which is exceeded once in 50 years is NAP –1.0 m and once in 500 years is NAP -1.3 m. From this knowledge we can find a ‘decimeringshoogte’ of 0.3 m. In Figure 4.2 one can see the resulting extreme value fit and the parameters corresponding to this extreme minima (Gumbel) distribution.

Water level:

- 1/50y = NAP -1 m
- 1/500y = NAP -1.3 m
- extreme value fit
  - Mean - 0.5685**
  - Std dev 0.1664**
  - a (loc) = - 0.4936
  - b (disp) = 0.1298

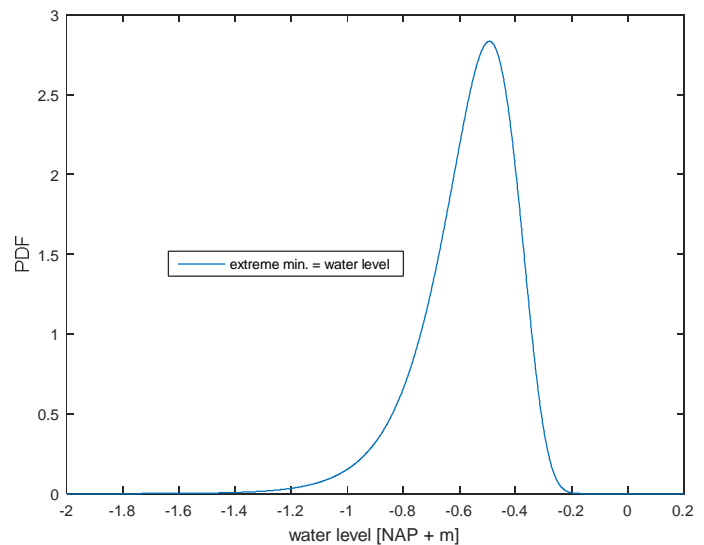


Figure 4.2 Characterisation of the water level uncertainty (per year). PDF on the vertical axis stand for Probability Density Function

It should be noted that the distribution in Figure 4.2 provides a resulting probability of failure **per year**. However, in the design codes (norms) like the Eurocode and CUR, requirements are specified per lifetime of the structure. Then, if one needs to have a resulting probability of failure per e.g. 50 years (reference period used in the case study), one should build a PDF/CDF such that the expected value in 50 years corresponds to the 1/50 frequency water level, i.e.:

- 1/1 lifetime (50y) = NAP –1.0 m.
- 1/10 lifetime (500y) = NAP –1.3 m.
- Keeping the ‘decimeringshoogte’ of 0.3 m.

In this case the probability that the water level is lower than NAP –1.0 m within the lifetime is given by:

$$P_{50yr} = 1 - (1 - P_{1yr})^{50} \quad (14)$$

Then:

$$P[h < -1.0] = 1 - \left(1 - \frac{1}{50}\right)^{50} = 0.636 \quad (15)$$

Contrarily to what one might think,  $P[h < -1.0]$  is not given as  $P[h < -1.0] = 1.0$ . Likewise:

$$P[h < -1.3] = 1 - \left(1 - \frac{1}{500}\right)^{50} = 0.095 \sim 1/10 \quad (16)$$

Note that the ‘decimeringshoogte’ is not always a constant, regardless the level of (small) probabilities of exceedance. Also, it does not necessarily remain unchanged if one transfers from a 1 year distribution to an N year distribution. However, for the Gumbel type distribution the ‘decimeringshoogte’ is a constant, and the transition from 1 year to N year distribution involves a shift of the location parameter of  $d \cdot \log(N)$ , where  $d$  is the ‘decimeringshoogte’ (positive shift for extreme max and negative shift for extreme min). As such, roughly, one needs to fit a PDF of the maximum water level in the lifetime on the annual water level PDF. Based on this, the following uncertainties are defined to achieve a probability of failure for  $N = 50$  years:

Water level (h):

- $P[h < -1.0] = 0.636$
- $P[h < -1.3] = 0.1$
- $d \cdot \log(N) = 0.3 \cdot \log(50) = 0.51$
- extreme value fit
  - Mean -1.0782**
  - Std dev 0.1664**
  - a (loc) = -1.0033
  - b (disp) = 0.1298

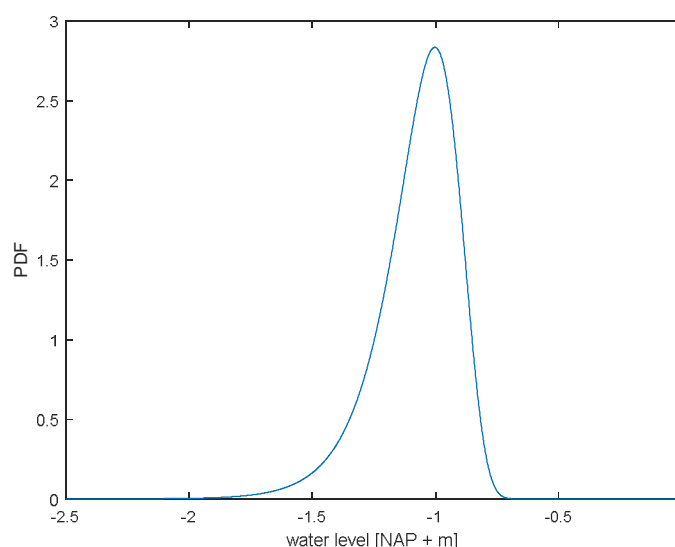


Figure 4.3 characterisation of the water level uncertainty (per 50 years)

The method elaborated in this paragraph to scale the water level uncertainty for a certain reference period can also be used to come to values for other reference periods. In Table 4.2 values are shown for other reference periods.

Reference period from T=25 y to	Mean [m NAP]	Standard deviation [m NAP]
Tc = 75 (Tref = 50 y)	-1.078	0.1664
Tc = 50 (Tref = 25 y)	-0.988	0.1664
Tc = 26 (Tref = 1 y)	-0.569	0.1664

Table 4.2 Characterisation of the water level uncertainty using a Gumbel distribution for different reference periods

The groundwater level and the water pressures in the deeper layers are considered to be deterministic values and hence are not varied in the case study.

#### 4.4 Surcharge loads

In previous analyses [Deltares, 2016a] the surcharge loads were modelled using a Gumbel (extreme maxima) distribution. In effect this caused a large load to be present in all three zones all of the time. During this study it was decided this does not reflect the intended behaviour of the surface loads, namely a load that is only present in 10% of the time and the three zones being uncorrelated (meaning in one zone there can be a large load while the other two zones have no loading). This behaviour is for example relevant for failure of the passive wedge in

front of the sheet pile anchor wall. In case there is a constant high surcharge load in front of the anchor wall this creates a more stable situation for this specific failure mechanism.

To be able to model the intended behaviour of the surcharge loads ideally an “on/off” switch would be implemented in the code that would allow for the surface load per zone to be switched on or off during the analysis. Although this would seem feasible to implement it was believed to be outside the scope of this project and hence a different (simpler) approach was chosen.

The approach chosen here was to use a truncated normal distribution. Relevant parameters chosen are mean = 0 kPa and standard deviation = 10 kPa on a truncated range of [0,100]. An example of the corresponding PDF and CDF is shown in Figure 4.4. This approach results in a behaviour where with a large probability a small surface load (~0 to 10 kPa) is present and with a small probability a large value (~20 to 40 kPa). The distribution was tuned such that the probability of exceeding a surface load of 20 kPa during a reference period of 50 years is 5%. Assumed is then that the surcharge loading per year is independent.

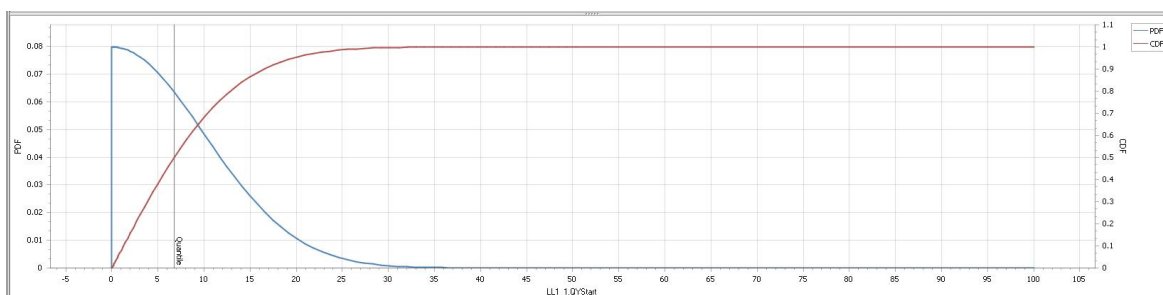


Figure 4.4 Probability Density Function (PDF) and Cumulative Density Function (CDF) of truncated normal distribution assumed for surface load (per 50 years)

With the mentioned assumptions rough fits were made for other reference periods for the PDF and CDF of the surcharge loads, leading to characterisation of the surcharge load uncertainty for different reference periods in Table 4.3.

Reference period from $T=25y$ to	Mean [kPa]	Standard deviation [kPa]
$T_c = 75$ ( $T_{ref} = 50$ y)	0	10.0
$T_c = 50$ ( $T_{ref} = 25$ y)	0	9.0
$T_c = 26$ ( $T_{ref} = 1$ y)	0	6.0

Table 4.3 Characterisation of the water level uncertainty using a truncated normal distribution for different reference periods

#### 4.5 Water bottom level

Concerning the bottom of the lock it is assumed its uncertainty follows a normal distribution with a mean value of NAP  $-7$  m and a standard deviation of 0.15 m. Since it is assumed that the water bottom level is independent of time the characteristics are independent of the reference period. The resulting distribution has been shown in Figure 4.5. The water bottom level is assumed to be time independent in this case study<sup>6</sup>.

<sup>6</sup> It may however be argued that the water bottom level is not a deterministic value throughout the service life of a sheet pile structure. If the water bottom is unprotected, then currents or propeller jets of passing ships may have significant erosion effects.

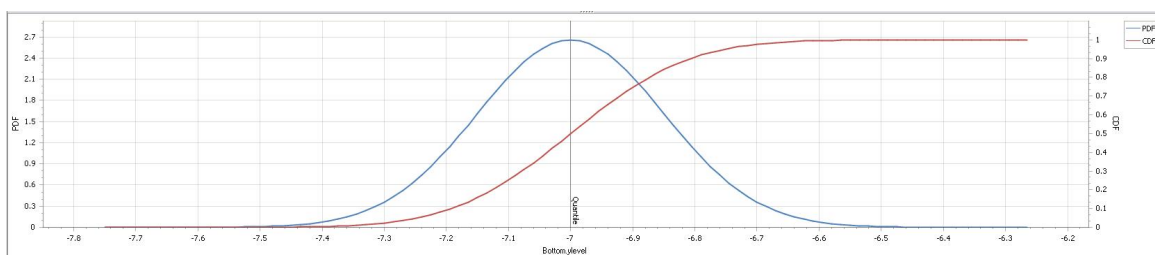


Figure 4.5 PDF and CDF for the normally distributed water bottom level as used in the case study

## 4.6 Corrosion

In paragraph 3.5 the distinguished corrosion zones for the sheet pile structure have been elaborated. Furthermore, mean values for the corrosion are presented for the specified zones of the sheet pile structure: zones A, B, C, D1, D2, D3, E and F. The mean values for the corrosion per zone are repeated here in Table 4.4 and Table 4.5.

Zone	Level		Mean corrosion value $\Delta t_{\text{mean}_i}$ [mm]
	Top [m NAP]	Bottom [m NAP]	
A: Above upper lockage level	+5.0	+3.0	2.45
B: Upper lockage level-GWL	+3.0	+1.0	3.20
C: GWL- lower lockage level	+1.0	-0.5	2.40
D1: Lower lockage level-bottom	-0.5	-1.5	4.65
D2: Lower lockage level-bottom	-1.5	-5.0	4.65
D3: Lower lockage level-bottom	-5.0	-7.0	4.65
E: Below bottom	-7.0	-14.5	1.80

Table 4.4 Mean thickness reduction of sheet pile after 75 years (mean values per zone)

Zone	Level		Mean corrosion value $\Delta t_{\text{mean}_i}$ [mm]
	Top [m NAP]	Bottom [m NAP]	
F: Top -GWL	+3.5	+1.0	3.4
G: GWL-tip (*)	+1.0	-0.5	1.8

Table 4.5 Mean thickness reduction of the anchor wall after 75 years (mean values per zone)

(\*) as explained in paragraph 3.5 section G is not further used here for reasons of simplicity.

Here it is assumed that two corrosion stochastic variables exist, i.e.  $\Delta t_{D1}$  belonging to section D1 and  $\Delta t_{D2}$  belonging to section D2. So, both stochastic variables have a mean value of 4.65 mm. It is assumed that these two corrosion variables are largely correlated (but not fully) by using a correlation value of 0.75<sup>7</sup>. It is furthermore assumed that sections A, B, C, D3, E and F are fully correlated with section D1. The corrosion in these zones is scaled in the same relative manner as in zone D1.

So, for sheet pile section  $i$  the (stochastic) thickness reduction is calculated as:

<sup>7</sup> Since it is not considered realistic that the corrosion is fully correlated over the full height of the sheet pile, in this exploratory study it was assumed that two (strongly correlated) stochastic variables exist simulating the thickness reduction in the critical part of the sheet pile.

$$\Delta t_i = \Delta t_{\text{mean}_i} \left[ \frac{\Delta t_{D1}}{\Delta t_{\text{mean}_{D1}}} \right] \quad [m] \quad (17)$$

The variation coefficient ( $V$ ) used for the corrosion is based on results obtained by [Deltares, 2019b]. The a-priori uncertainty results in a large  $V = 0.5$ . Due to inspection it is expected that the uncertainty can be reduced to a value of  $V = 0.2$  a  $0.3$ .

Furthermore, the results obtained by [Deltares, 2019] suggest that a normal distribution seems to reasonably match the gathered data. It should be noted that further research based on significant more field observations is needed to determine the “actual” distribution. In order to prevent unrealistic stochastic values (i.e. negative values or values larger than the initial thickness of the sheet pile) a truncated normal is used with limits  $[0, 13]$ . The resulting distributions have been shown for the different variation coefficients in Figure 4.6 to Figure 4.8.

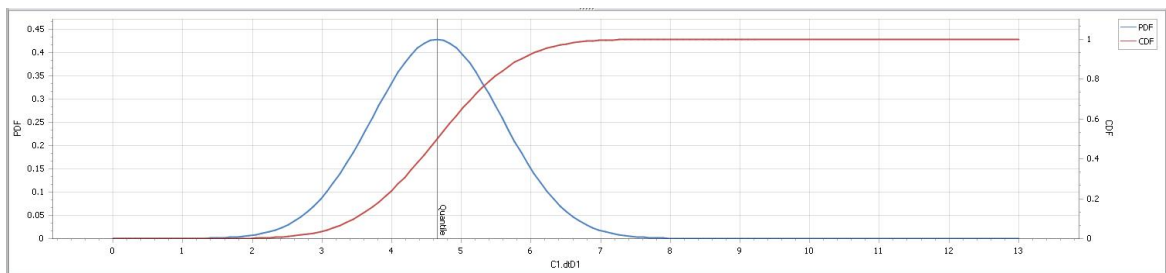


Figure 4.6 PDF and CDF of stochastic variable  $dt_{D1}$  and  $dt_{D2}$ , truncated normal distribution with a mean value of 4.65 mm and a variation coefficient ( $V$ ) of 0.2

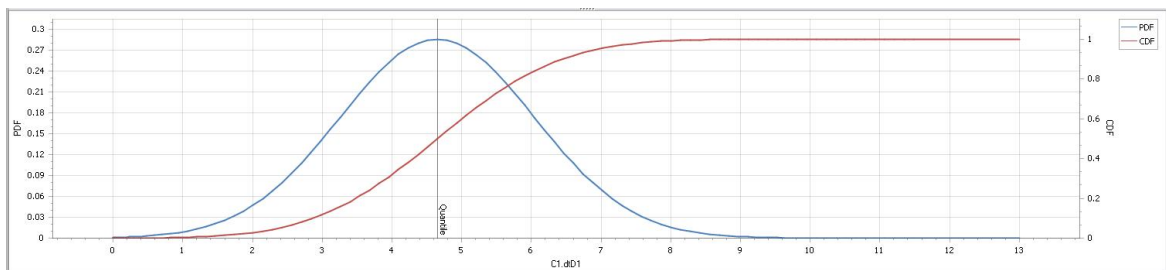


Figure 4.7 PDF and CDF of stochastic variable  $dt_{D1}$  and  $dt_{D2}$ , truncated normal distribution with a mean value of 4.65 mm and a variation coefficient ( $V$ ) of 0.3

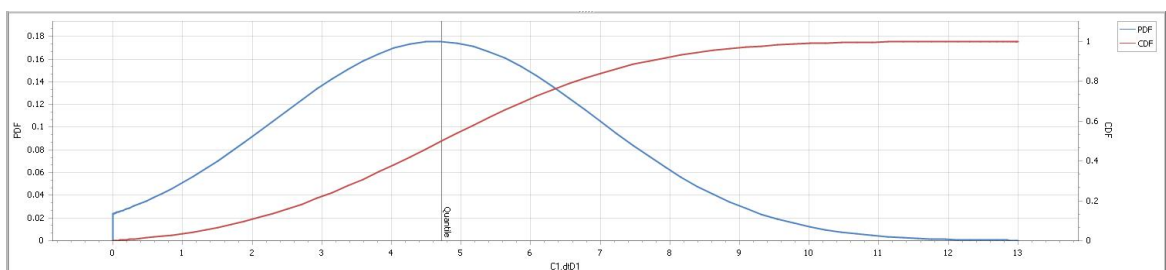


Figure 4.8 PDF and CDF of stochastic variable  $dt_{D1}$  and  $dt_{D2}$ , truncated normal distribution with a mean value of 4.65 mm and a variation coefficient ( $V$ ) of 0.5

In Table 4.7 corrosion values are presented for zone D1, 2 and 3 for different reference periods. The standard deviation is not shown but can be calculated based on the chosen variation coefficient of  $V = 0.2, 0.3$  or  $0.5$ .

Reference period from $T=25$ y to	Mean [mm] at end of reference period
$T = 75$	4.65
$T = 50$	3.10
$T = 26$	1.61

Table 4.6 Characterisation of the mean corrosion in zone D1, 2 and 3 using a truncated normal distribution for different reference periods

#### 4.7 Yield stress

Throughout all the calculations the yield stress for the anchor rod ( $f_y = 355 \text{ N/mm}^2$ ) and the anchor wall ( $f_y = 240 \text{ N/mm}^2$ ) is set as a deterministic value.

The yield stress for the sheet pile wall is taken as deterministic (with  $f_y$  is  $240 \text{ N/mm}^2$ ) throughout the first calculations and in following calculations the yield stress was set as a stochastic variable. This has been explicitly indicated for each calculation in the presentation of results in chapter 6. The yield stress is assumed to be time independent.

To obtain a realistic distribution of the yield stress use was made of the information on page 104 in [Houyoux, C, 2004]. For this S320 steel grade a distribution is presented, also see Figure 4.9. A curve fit was made of this data (and also plotted in Figure 4.9). The curve fit resulted in the next stochastic parameters for a S320 steel grade:

- Lognormal distribution with
  - Mean =  $383 \text{ N/mm}^2$
  - Variation coefficient =  $0.08$  ( $\sigma = 30.64 \text{ N/mm}^2$ )
  - Shift =  $319.6 \text{ N/mm}^2$

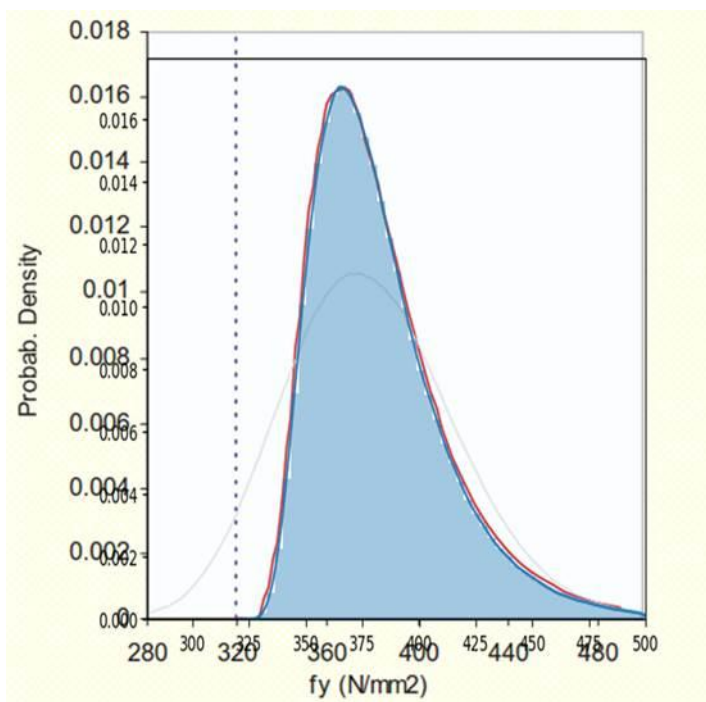


Figure 4.9 PDF plot of yield stress distribution for a S320 steel grade. This figure is taken from [Houyoux, C, 2004]. Plotted on top of this figure is the curve fit made for the case study

To obtain the parameters for a S240 steel grade the mean, standard deviation and shift were multiplied with a factor 240/320. This resulted in the following parameters for the calculation:

- Mean =  $(240/320) * 3.83E5 = 2.87E5$  kN/m<sup>2</sup>
- Deviation =  $(240/320) * 0.08 * 3.83E5 = 2.3E4$  kN/m<sup>2</sup>
- Shift =  $(240/320) * 3.196E5 = 2.4E5$  kN/m<sup>2</sup>

The resulting distribution is presented in orange (S240GP) in Figure 4.10.

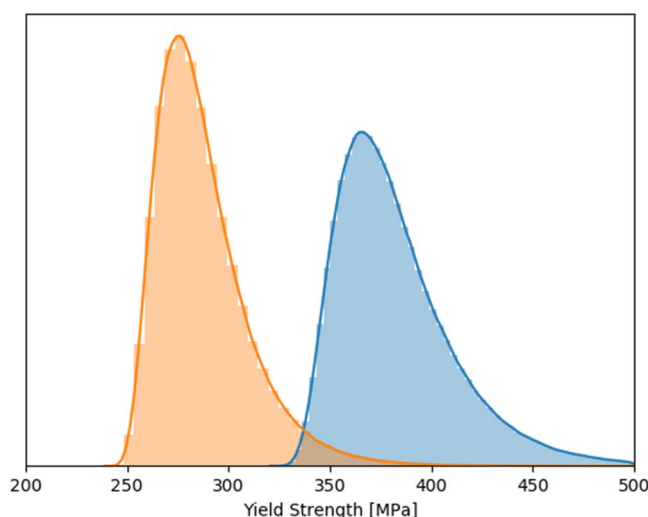


Figure 4.10 PDF distributions of the S320 steel grade presented in [Houyoux, C, 2004] (in blue) and the derived distribution for a S240 as used in this case study (in orange)

#### 4.8 Summary of all stochastic variables

For the probabilistic calculations a resume of the stochastic parameters and their chosen properties are presented in Table 4.7. These are the ones assumed for the case study and are mainly chosen based on expert judgment and might not be generalized.

#	Stochastic variable	symbol	Unit	25-75 year period			distribution
				$\mu$	$\sigma$	var	
1	sand medium (SM), unsaturated weight	$\gamma_{unsat\_SM}$	[kN/m <sup>3</sup> ]	18.7	1.04	0.06	normal
2	sand medium (SM), saturated weight	$\gamma_{sat\_SM}$	[kN/m <sup>3</sup> ]	20.7	1.04	0.05	normal
3	sand medium (SM), friction angle	$\varphi_a^*_{SM}$	[°]	37.0	3.70	0.1	truncated normal [0:60]
4	sand medium (SM), effective stiffness	$E'_{SM}$	[MN/m <sup>2</sup> ]	50.0	15.00	0.3	lognormal
5	clay medium (CM), friction angle	$\varphi_a^*_{CM}$	[°]	25.8	2.58	0.1	truncated normal [0:60]
6	clay medium (CM), stiffness	$E'_{CM}$	[MN/m <sup>2</sup> ]	6.5	1.95	0.3	lognormal
7	clay medium (CM), cohesion	$c_a^*_{CM}$	[kN/m <sup>2</sup> ]	14.8	2.96	0.2	lognormal
8	sand dense (SD), friction angle	$\varphi_a^*_{SD}$	[°]	39.8	3.98	0.1	truncated normal [0:60]
9	lock bottom	z	[NAP m]	-7.00	0.15	-0.02	normal

10	outside waterlevel	$h$	[NAP m]	-1.078	0.1664	-0.15	gumbel (ext min)
11	load zone 1	$q1$	[kN/m <sup>2</sup> ]	0.00	10		truncated normal [0;100]
12	load zone 2	$q2$	[kN/m <sup>2</sup> ]	0.00	10		truncated normal [0;100]
13	load zone 3	$q3$	[kN/m <sup>2</sup> ]	0.00	10		truncated normal [0;100]
14	thickness reduction D1	$\Delta t_{D1}$	[mm]	4.65	1.395	0.3	truncated normal [0;13]
15	thickness reduction D2	$\Delta t_{D2}$	[mm]	4.65	1.395	0.3	truncated normal [0;13]
16	steel yield stress	$f_y$	[kN/m <sup>2</sup> ]	2.87E+05	2.30E+04	0.08	lognormal
17	time	$T$	[yr]	5.00E+01	2.50E+01		uniform

Table 4.7 Assumed distribution type, mean value, standard deviation and coefficient of variation for the defined stochastic variables at  $T = 75$  years

Note 1: the variation coefficient for loss of thickness due to corrosion will be varied over values of 0.2, 0.3 and 0.5.

Note 2: stochastic variable nr. 17 is time and has not been discussed before in this chapter. Time is added as a stochastic variable to allow for a calculation in which time is also a "stochastic variable". This approach and the results of the calculation made are discussed in paragraph 6.4.

#### 4.9 Correlations

The correlation matrix for the chosen stochastic parameters is presented in Table 4.8. As one can see correlations are assumed in between soil parameters of the same soil layer. Furthermore, a correlation is assumed between the two corrosion values. In between different soil layers, geometry, water level, loads and corrosion parameters no correlations are used (they are considered independent from each other).



#	symbol	#1	#2	#3	#4	#5	#6	#7	#8	#9	#10	#11	#12	#13	#14	#15	#16	#17
1	$\gamma_{\text{unsat\_SM}}$	1																
2	$\gamma_{\text{sat\_SM}}$	1	1															
3	$\varphi_a^*_{\text{SM}}$	0	0.5	1														
4	$E'_{\text{SM}}$	0	0.5	0.25	1													
5	$\varphi_a^*_{\text{CM}}$	0	0	0	0	1												
6	$E'_{\text{CM}}$	0	0	0	0	0.25	1											
7	$c_a^*_{\text{CM}}$	0	0	0	0	-0.65	0.12	1										
8	$\varphi_a^*_{\text{SD}}$	0	0	0	0	0	0	0	1									
9	$z$	0	0	0	0	0	0	0	0	1								
10	$h$	0	0	0	0	0	0	0	0	0	1							
11	$q1$	0	0	0	0	0	0	0	0	0	0	1						
12	$q2$	0	0	0	0	0	0	0	0	0	0	0	1					
13	$q3$	0	0	0	0	0	0	0	0	0	0	0	0	1				
14	$\Delta t_{\text{D1}}$	0	0	0	0	0	0	0	0	0	0	0	0	0	1			
15	$\Delta t_{\text{D2}}$	0	0	0	0	0	0	0	0	0	0	0	0	0	0.75	1		
16	$f_y$	0	0	0	0	0	0	0	0	0	0	0	0	0	0	0	1	
17	$T$	0	0	0	0	0	0	0	0	0	0	0	0	0	0	0	0	1

Table 4.8 Defined stochastic variables and their correlations

## 5 Limit state Functions

### 5.1 Introduction

The Limit State Functions (LSF) describe the situation wherein the acting (extreme) loads are just balanced by the (extreme) strength of the construction. If the limit state is exceeded it is assumed the construction will lose its functionality and thus collapse or fail. The LSF is a mathematical function generally represented in a form of  $Z = R - S$ . Here  $Z$  is the LSF value,  $R$  is a measure for the resistance or strength and  $S$  is a measure for the load in the structure.

The fault-tree as presented in Figure 5.1 is relevant for retaining structures and indicates the relevant failure mechanisms:

- A. The sheet pile front wall.
- B. The anchorage, i.e. the anchor rod and/or the anchor sheet pile wall.
- C. The soil.

In this study it was decided to proceed with the reliability analysis that considers the three mechanisms simultaneously (i.e. system reliability analysis), i.e. if one of the failure mechanisms occurs it is assumed the system fails.

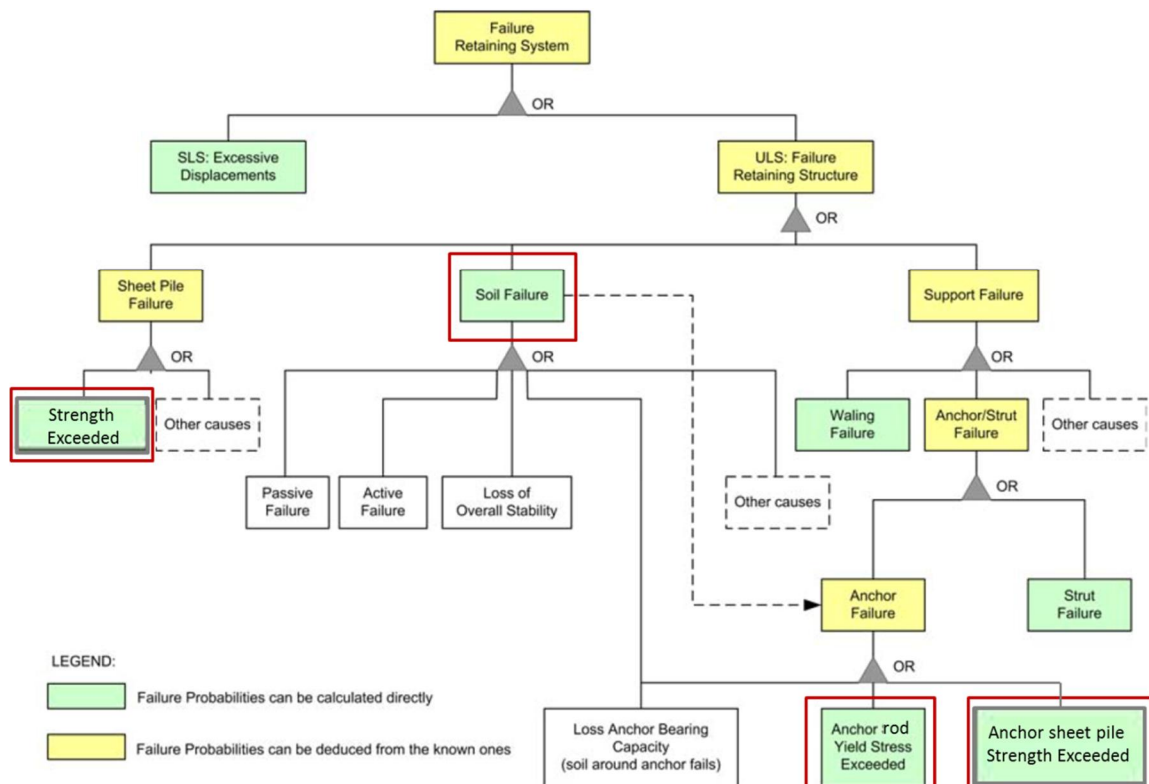


Figure 5.1 Fault-tree for retaining structures using sheet piles, after [Schweckendiek, 2007a]

When modelling the LSF it is important to keep in mind:

- Ideally the LSF is a continuous mathematical function.

- When analysing the separate LSF functions preference is given to a formulation in a dimensional manner as the resulting numbers have an actual physical and are therefore a “measure” for how safe/unsafe the construction is. This is relevant since the outcome of the LSF is used by the reliability integration method in finding  $z = 0$ . The outcome of the LSF functions plays a role in the efficiency of the calculation process.
- When dealing with system analysis (i.e. the minimum of the separate LSF functions) the different LSF are ideally formulated in a non-dimensional manner, this way normalising the different  $z$  functions and thus preventing that one LSF function could become dominant (by generating much larger values than the other formulas).

## 5.2 Subset A LSF for the sheet pile

In the calculations there will be in total eight sheet pile sections (A, B, C, D1, D2, D3, E and F) with each an individual  $LSF_i$ . Depending on the amount of thickness reduction due to corrosion the Sheet pile section can have a Moment capacity with and without plastic rotation capacity.

### 5.2.1 LSF A1 Moment capacity with NO plastic rotation capacity, $(b/t_{f_i}/\epsilon) \leq 66$

This LSF (A1) applies to the sheet pile sections where the thickness reduction is such that [EC3-5:2008] terms Class 1, 2 or 3 applies but for this LSF it is chosen NOT to make use of the available plastic rotation capacity. These sections have been modelled in PLAXIS with an elastic capacity (or actually an elastic-plastic beam with the plastic capacity set to an “infinite” high value)). The LSF for these sections is based on the maximum available plastic capacity. Based on corrosion reduction of a section, this section  $i$  has a certain plastic moment capacity  $M_{pl,max;corr;i}$ .

$$M_{pl,max;corr;i} = \rho_{C,max;i} \cdot W_{pl,corr;i} \cdot f_y \quad [-] \quad (18)$$

The actual bending moment is variable over the depth and that is why it is expressed as  $M(z)_i$  a function of  $z$ -depth over the  $z$ -range of section  $i$ . The python special command determines the maximum absolute value per section and transfers the value to the PTK.

Taking this into account, the LSF (a1) can be formulated as the difference between the maximum developed bending moment and the plastic moment capacity  $M_{pl,max;corr;i}$  of the section:

$$Z_{pl\ sheet\ pile;i} = 1 - \frac{\max|M(z)_i|}{M_{pl,max;corr;i}} \quad (19)$$

*Note that the most relevant failure mode for the sheet pile wall is the exceedance of the yield strength which corresponds to the yield stress of the steel. The response of the structure is mainly due to bending moments and the axial forces (shear forces are considered to be negligible for this case). For the situation were the contribution of the normal force to the maximum stress is less than 10% EC3 states that the normal force can be neglected as there is sufficient steel area in the sheet pile web available to accommodate this normal force. For this case study this is the case since the normal force is relatively small due to the use of a horizontal anchor rod + anchor wall.*

### 5.2.2 LSF A2 Moment capacity with NO plastic rotation capacity, $(b/t_{f_i}/\epsilon) \geq 66$

This LSF (A2) applies to the sheet pile sections where the thickness reduction is such EN 1993-5:2008 terms Class 4 applies. These sections have been modelled in PLAXIS with an elastic beam (or actually an elastic-plastic beam with the plastic capacity set to a “infinite” high value). In line with [ArcelorMittal, 2017] it was chosen to apply a conservative simplification in modelling the sheet pile strength for Class 4. This simplification is not using the actual yield stress but a lower reduced limit stress,  $f_{y:red,class 3}$  such that the ratio  $(b/t_{f_i}/\epsilon) = 66$  is maintained all the time, complying to the application limit of EN1993-5:2008 Class 3 rules.

EN 1993-5:2008 table 5-1 states that the limit of for the Class 3 rules is:

$$\frac{b/t_f}{\epsilon} \leq 66 \quad [-] \quad (20)$$

where

$$\epsilon = \sqrt{\frac{235 \cdot 10^3}{f_y}} \quad [-] \quad (21)$$

For this LSF not the yield strength,  $f_y$  but the lower, reduced limit stress  $f_{y:red,class 3}$  is used:

$$f_{y:red,class 3} = \frac{235 \cdot 10^3}{\left[\frac{b/(t_f)}{66}\right]^2} \quad \left[\frac{kN}{m^2}\right] \quad (22)$$

and  $b = 356 \text{ mm}$  and  $\Delta t_i$  the limit stress in compliance with the Class 3 rule of EC3 for section  $i$  is:

$$f_{y:red,class 3_i} = \frac{235 \cdot 10^3}{\left[\frac{356/(t_f - \Delta t_i)}{66}\right]^2} \quad \left[\frac{kN}{m^2}\right] \quad (23)$$

And combined with the reduced, section modulus,  $W_{el,corr_i}$  the reduced elastic moment capacity,  $M_{el,corr_i}$  is:

$$M_{el,corr_i} = f_{y:red,class 3_i} \cdot W_{el,corr_i} \quad [kNm/m^1] \quad (24)$$

The actual bending moment can be variable over the depth and that is why it is expressed as a function of z-depth over the z-range of section,  $i$ . Taking this into account, the LSF (a1) can be formulated as the difference between the maximum developed bending moment and the reduced elastic moment capacity,  $M_{el,corr_i}$ :

$$Z_{el \text{ sheet pile } i} = 1 - \frac{\max|M(z)_i|}{M_{el,corr_i}} \quad (25)$$

*Note that the normal force is not included in the LSF. This is allowed since the normal force is relatively small for this case (using a horizontal anchor rod + anchor wall).*

**Note on Class 4 strength**

The method proposed in this paragraph is a relatively simple but conservative approach of the strength of thin walled sheet piles. This approach is used in the 2<sup>nd</sup> series of calculations as presented in this report.

In the 3<sup>rd</sup> series of calculations as presented in this report use is made of a more realistic Class 4 strength definition based on [ArcelorMittal, 2019]. In this approach use has been made of the open source software CUFSM - constrained and unconstrained finite strip method: <https://www.ce.jhu.edu/bschafer/cufsm/>

5.2.3 LSF A3 Moment AND plastic rotation capacity,  $(b/t_{fi}/\epsilon) < 66$ 

This LSF (A3) applies to the sheet pile sections where the thickness reduction is such EN 1993-5 Appendix C terms Class 1, 2 or 3 applies. These sections have been modelled in PLAXIS with a plastic hinge option. The LSF for these sections is based on the plastic rotation capacity. Based on corrosion reduction of a section and the in the calculation applied softening of the sheet pile section, this section has a certain plastic hinge capacity  $M_{hinge;i}$ . The in the calculation applied  $M_{hinge;i}$ :

$$M_{hinge;i} = \rho_{C,max;i} \cdot W_{pl;i} \cdot f_y \quad [-] \quad (26)$$

For an applied reduction factor  $1 \geq \rho_i \geq 0.85$  the plastic rotation capacity,  $\phi_{Cd;i}$  can be described by the formulas below. Please also refer to paragraph 3.8 where the relation between the applied reduction factor and rotation capacity has been explained. The formulas below are simply interpolation formulas between the different lines (i.e. the  $\rho = 100, 95, 90$  and  $85\%$  lines) of Figure 3.10.

Note the interaction between the Plastic hinge capacity and the rotation capacity. For a decreasing applied reduction factor  $\rho_{C,max;i}$  the hinge capacity will decrease but the rotation capacity  $\phi_{Cd}$  will increase.

$$\begin{aligned} \phi_{Cd;1-0.95} = & \left[ 0.11 + (0.12 - 0.11) \cdot \left( \frac{1 - \rho_i}{1 - 0.95} \right) \right] \\ & \left\{ 0 - \left[ 0.11 + (0.12 - 0.11) \cdot \left( \frac{1 - \rho_i}{1 - 0.95} \right) \right] \right\} \cdot \left( \frac{b}{\epsilon t_{fi}} - 25 \right) \\ & + \frac{\phantom{\left\{ 0 - \left[ 0.11 + (0.12 - 0.11) \cdot \left( \frac{1 - \rho_i}{1 - 0.95} \right) \right] \right\}} \cdot \left( \frac{b}{\epsilon t_{fi}} - 25 \right)}{\left[ 45 + (50 - 45) \left( \frac{1 - \rho_i}{1 - 0.95} \right) \right] - 25} \quad [rad] \end{aligned} \quad (27)$$

Presenting equation (28) in a simplified format gives:

$$\begin{aligned} \phi_{Cd;1-0.95} = & \left[ 0.11 + 0.01 \cdot \left( \frac{1 - \rho_i}{1 - 0.95} \right) \right] \\ & \left\{ 0 - \left[ 0.11 + 0.01 \cdot \left( \frac{1 - \rho_i}{1 - 0.95} \right) \right] \right\} \cdot \left( \frac{b}{\epsilon t_{fi}} - 25 \right) \\ & + \frac{\phantom{\left\{ 0 - \left[ 0.11 + 0.01 \cdot \left( \frac{1 - \rho_i}{1 - 0.95} \right) \right] \right\}} \cdot \left( \frac{b}{\epsilon t_{fi}} - 25 \right)}{\left[ 20 + 5 \cdot \left( \frac{1 - \rho_i}{1 - 0.95} \right) \right]} \quad [rad] \end{aligned} \quad (28)$$

For an applied reduction factor  $0.95 \geq \rho_i \geq 0.9$  the plastic rotation capacity,  $\phi_{cd,i}$  is:

$$\phi_{cd:0.95-0.9} = \left[ 0.12 + (0.13 - 0.12) \cdot \left( \frac{0.95 - \rho_i}{0.95 - 0.9} \right) \right] \left\{ 0 - \left[ 0.12 + (0.13 - 0.12) \cdot \left( \frac{0.95 - \rho_i}{0.95 - 0.9} \right) \right] \right\} \cdot \left( \frac{b}{\epsilon t_{fi}} - 25 \right) + \frac{\left[ 50 + (60 - 50) \left( \frac{0.95 - \rho_i}{0.95 - 0.9} \right) \right] - 25}{\left[ 50 + (60 - 50) \left( \frac{0.95 - \rho_i}{0.95 - 0.9} \right) \right] - 25} \text{ [rad]} \quad (29)$$

Presenting equation (29) in a simplified format gives:

$$\phi_{cd:0.95-0.9} = \left[ 0.12 + 0.01 \cdot \left( \frac{0.95 - \rho_i}{0.95 - 0.9} \right) \right] \left\{ 0 - \left[ 0.12 + 0.01 \cdot \left( \frac{0.95 - \rho_i}{0.95 - 0.9} \right) \right] \right\} \cdot \left( \frac{b}{\epsilon t_{fi}} - 25 \right) + \frac{\left[ 25 + 10 \cdot \left( \frac{0.95 - \rho_i}{0.95 - 0.9} \right) \right] - 25}{\left[ 25 + 10 \cdot \left( \frac{0.95 - \rho_i}{0.95 - 0.9} \right) \right] - 25} \text{ [rad]} \quad (30)$$

For an applied reduction factor  $0.9 \geq \rho_i \geq 0.85$  the plastic rotation capacity,  $\phi_{cd,i}$  is:

$$\phi_{cd:0.9-0.85} = \left[ 0.13 + (0.14 - 0.13) \cdot \left( \frac{0.9 - \rho_i}{0.9 - 0.85} \right) \right] \left\{ 0 - \left[ 0.13 + (0.14 - 0.13) \cdot \left( \frac{0.9 - \rho_i}{0.9 - 0.85} \right) \right] \right\} \cdot \left( \frac{b}{\epsilon t_{fi}} - 25 \right) + \frac{\left[ 60 + (66 - 60) \left( \frac{0.9 - \rho_i}{0.9 - 0.85} \right) \right] - 25}{\left[ 60 + (66 - 60) \left( \frac{0.9 - \rho_i}{0.9 - 0.85} \right) \right] - 25} \text{ [rad]} \quad (31)$$

Presenting equation (31) in a simplified format gives:

$$\phi_{cd:0.9-0.85} = \left[ 0.13 + 0.01 \cdot \left( \frac{0.9 - \rho_i}{0.9 - 0.85} \right) \right] \left\{ 0 - \left[ 0.13 + 0.01 \cdot \left( \frac{0.9 - \rho_i}{0.9 - 0.85} \right) \right] \right\} \cdot \left( \frac{b}{\epsilon t_{fi}} - 25 \right) + \frac{\left[ 35 + 6 \cdot \left( \frac{0.9 - \rho_i}{0.9 - 0.85} \right) \right] - 25}{\left[ 35 + 6 \cdot \left( \frac{0.9 - \rho_i}{0.9 - 0.85} \right) \right] - 25} \text{ [rad]} \quad (32)$$

Plastic rotation can be variable over the depth and that is why they it is expressed as a function of z-depth over the z-range of section,  $i$ . Taking this into account, the LSF (A3) can be formulated as the difference between the maximum absolute value of the developed plastic rotation and plastic rotation capacity,  $\phi_{cd,i}$ :

$$Z_{\phi_{pl}:sheet\ pile_i} = 1 - \frac{\max|\phi_{pl}(z)_i|}{\phi_{cd:i}} \quad (33)$$

### 5.3 Subset B LSF for the anchorage

The anchorage consists of an anchor rod and an anchor wall.

#### 5.3.1 LSF B1 Anchor wall

For the anchor wall it was chosen not to consider the plastic rotation capacity of the wall but only to use the full plastic capacity of the corroded section. For bending moments larger than the full plastic capacity the anchor wall is considered to be failing.

$$Z_{anchorwall} = 1 - \frac{M_a}{W_{pl:max:corr} \cdot f_y} \quad (34)$$

Here  $M_a$  is the (absolute) calculated bending moment [kNm/m] in the anchor wall and  $W_{pl:max:corr}$  [m<sup>3</sup>/m] is the corroded full plastic section modulus of the sheet pile. The yield stress  $f_y$  is chosen equal to 240 N/mm<sup>2</sup> (no stochastic variable).

*Note: the current implementation always uses the full plastic section modulus. If the corrosion would become so high that the anchor wall sheet pile would fall into Class 4 this would not be correct anymore. It has been double checked that for this case study the corrosion values for the anchor wall are so low for anchor wall this doesn't happen.*

#### 5.3.2 LSF B2 Anchor rod

Similar to the sheet pile wall, the LSF (B2) of the anchor rod involves the certain yield or ultimate strength of the steel members and the maximum stress that the anchor experiences during its loading. Consequently, the LSF is as following:

$$Z_{anchor} = 1 - \frac{N_a}{A_{a:corr} \cdot f_y} \quad (35)$$

where  $N_a$  [kN] is the calculated anchor force and  $A_{a:corr}$  [m<sup>2</sup>] is the corroded cross-sectional area of the anchor rod. The yield stress  $f_y$  is chosen to a fixed value of 355 N/mm<sup>2</sup> (no stochastic variable), which is a higher steel quality then used for the sheet piles.

*Note: In practice the anchor may also be subjected to bending moments, due to soil deformations or settlements. However, here only the axial forces on the anchor are considered without taking into account the lateral deformations and its reaction with the surrounding soil.*

### 5.4 Subset C LSF for the soil

Soil instability can develop in different patterns, as **Error! Reference source not found.** illustrates. PLAXIS assumes the soil to be a continuous body and thus it can model movements in the scale of soil bodies. Thus, applying FEM, the most critical failure mode is determined automatically. However, this is not always straightforward (e.g.: what triggers the mechanism of failure is not clear).

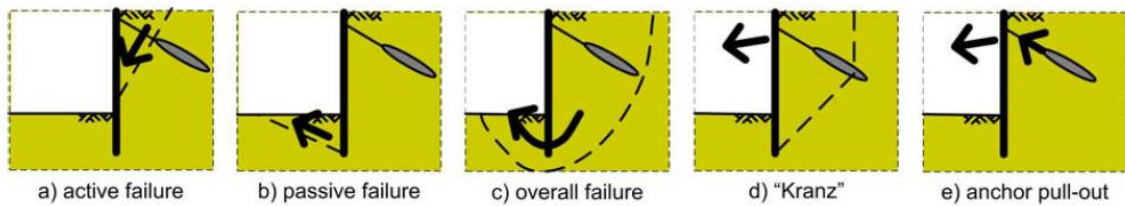


Figure 5.2. Failure mechanism in the soil for anchored retaining walls [4]

Below, a brief description of the available methods to formulate the LSF of the soil failure with FEM is given [Schweckendiek, 2007a], [Rippi, 2015]. After the evaluation of these alternatives, a selection is made regarding the most suitable one (method 4).

### 1. Excessive Deformations

- This method is simple and the same as one would use for a LSF of and serviceability limit state. However, there are some problems. Namely: (1) the fact that sometimes failure mechanisms happen suddenly, and no significant displacements are observed before moving very close to failure (may cause problems for the iterative procedures of some reliability methods), also (2) the determination of suitable maximum admissible deformations is not straightforward and finally (3) the location of the undesirable deformation(s) is also not straightforward and still under investigation, as there can be multiple vulnerable spots in a structure. Concerning the permissible displacements for the ULS, an upper limit for the maximum horizontal displacements of the top of the sheet pile can be set to  $1/50 \cdot L$ , where  $L$  is the vertical length of the sheet pile wall [Deltares, 2013].

### 2. $\phi$ -c Reduction (PLAXIS Safety Calculation)

- This method can provide the probability of failure for a general soil body collapse. However, even if this method seems to be quite simple, there are some issues during its implementation in a reliability analysis: (1) convergence problems for some reliability methods with iterative procedures, i.e. for a  $\phi$ -c reduction, soil strength properties follow a certain path which is independent from the values set for the random variables in each iteration, (2) the safety factor  $M_{sf}$  is a general safety factor regarding the failure of the system. Therefore sometimes, it is not straightforward what the "trigger" factors are that led to a certain type of failure, (3) a safety calculation in PLAXIS is time-consuming and the outcome can be unstable, furthermore, (4) PLAXIS cannot handle safety factors below 1, so a new limit of the safety factor shall be introduced in LSF.

### 3. Relative Shear Resistance

- In this method the basic idea is to define soil failure according to the failure criterion that PLAXIS is set to use for the analysis (in this research, the Mohr Coulomb criteria in combination with a linear-elastic perfectly-plastic stress-strain relationship - the so-called *Mohr-Coulomb model*). However, this requires prior knowledge of the possible relevant failure mechanisms and their potential locations on the soil structure (so that the suitable cluster of integration points). Therefore, the limit state function to be considered is not straightforward and it needs some investigation in advance.



#### 4. PLAXIS definition of soil collapse

- In PLAXIS, the construction stages are analysed by performing a load advancement ultimate level procedure which is controlled by a total multiplier,  $\Sigma Mstage$  (see eq. (18)). The main idea is that PLAXIS applies an incremental load until it reaches the pre-defined one. When  $\Sigma Mstage$  has reached an ultimate level (which by default is 1), the current phase is finished. However, if a staged construction phase calculation did not properly finish, the multiplier  $\Sigma Mstage$  fails to converge to the desired ultimate level at the end of the phase and a warning of ‘**Soil collapses**’ appears in the Log info box. In other words, this means that a collapse load has been reached and the total specified load has not been applied. In physical terms this means that the current value of the stiffness parameter CSP is less than 0.015. CSP is a measure for the amount of plasticity that occurs during the calculation. When the solution is fully elastic, the CSP is equal to unity whereas at failure it approaches zero. Therefore, soil reaches its upper limit of plasticity and it collapses which can be visualized as a settlement of the soil body. **Such a warning is thus assumed to be a possible failure situation.**

$$f_{applied} = f_0 + \Sigma Mstage(f_{defined} - f_0) \quad (36)$$

where  $f_{applied}$  is the load that is applied by PLAXIS,  $f_0$  is the load at the beginning of the calculation phase (i.e. the load that has been reached at the end of the previous calculation phase) and  $f_{defined}$  is the defined load configuration (i.e. water level, soil weight, vertical load, etc.).

For this study approach (4) is selected as it appears to be the most robust LSF.

So, the LSF for the soil is chosen as follows:

$$\begin{aligned} & \text{if } \Sigma Mstage > 0.995; \\ & \quad Z_{soil} = 1; \\ & \text{else:} \\ & \quad Z_{soil} = \Sigma Mstage - 1 \end{aligned} \quad (37)$$

Note that in this formulation:

- It is only a measure for how unstable the structure is (value < 1) and not for how stable the structure is (always 1).
- This set up of the LSF results in a discontinuous function which may result in a less efficient convergence around  $z = 0$ .
- The check value for  $\Sigma Mstage$  is a value a bit smaller than 1 to account for the fact that PLAXIS may return a value a bit smaller than 1 for phases which have converged successfully.

#### Idea

During this project an idea came forward to consider combining methods (2) and (4), i.e. combining the information from  $\Sigma Mstage$  and  $\Sigma Mstage$ . Since the  $\Sigma Mstage$  is a measure for how stable the structure is and the  $\Sigma Mstage$  is a measure for a how unstable the structure is. It has to be further investigated if this is feasible and worthwhile.

## 5.5 Implementation in PTK

In Table 5.1 and Table 5.2 it is shown how the LSF's, as described in the previous paragraphs, are implemented in the PTK. For the implementation some specific adjustments or additions are required to allow the numerical process to work:

- All the LSF related to the front sheet pile wall ( $z_{el}$ ,  $z_{pl}$  and  $z_{phi}$ ) are split up into the 7 different zones defined for the sheet pile front wall (A, B, C, D1, D2, D3 and E).
- An overall LSF is defined (ZStruct) which is the minimum of the separate  $z$  functions. With this LSF the system reliability is evaluated.
- an if/else statement is included in LSF  $z_{phi}$ : this adjustment is made to prevent a division by zero as in some cases a value of  $\Phi_{cd}$  is zero may be returned. This may happen in case the corrosion is so high that a section ends up in Class 4 area with a ratio  $> 66$ . When this section fails then the softening loop directly breaks and may return a  $\Phi_{CD} = 0$  for one of the other sections. Also see more explanation on the softening module in appendix E.4.
- For the LSF ZSoil an if/else statement is included. For the threshold value of SumMstage a value a bit smaller than 1 is selected as it may happen that PLAXIS returns a value a bit smaller than 1 for a successfully converged phase.

```

#z_pl evaluates bending moments in plastic range (Class 1,2,3)
z1_pl = 1 - abs(s1_mm)/s1_mpl
z2_pl = 1 - abs(s2_mm)/s2_mpl
z3_pl = 1 - abs(s3_mm)/s3_mpl
z4_pl = 1 - abs(s4_mm)/s4_mpl
z5_pl = 1 - abs(s5_mm)/s5_mpl
z6_pl = 1 - abs(s6_mm)/s6_mpl
z7_pl = 1 - abs(s7_mm)/s7_mpl
z_pl = min(z1_pl,z2_pl,z3_pl,z4_pl,z5_pl,z6_pl,z7_pl)

#z_el evaluates bending moments in elastic range (Class 4)
z1_el = 1 - abs(s1_mm)/s1_mel
z2_el = 1 - abs(s2_mm)/s2_mel
z3_el = 1 - abs(s3_mm)/s3_mel
z4_el = 1 - abs(s4_mm)/s4_mel
z5_el = 1 - abs(s5_mm)/s5_mel
z6_el = 1 - abs(s6_mm)/s6_mel
z7_el = 1 - abs(s7_mm)/s7_mel
z_el = min(z1_el,z2_el,z3_el,z4_el,z5_el,z6_el,z7_el)

#z_phi evaluates rotation capacity in plastic range (Class 1,2,3), included if statement to prevent division by zero in some cases
tol = 1E-4
if s1_phicd < tol:
    z1_phi = 1
else:
    z1_phi = 1 - abs(s1_phim)/s1_phicd

if s2_phicd < tol:
    z2_phi = 1
else:
    z2_phi = 1 - abs(s2_phim)/s2_phicd

if s3_phicd < tol:
    z3_phi = 1
else:
    z3_phi = 1 - abs(s3_phim)/s3_phicd

if s4_phicd < tol:
    z4_phi = 1
else:
    z4_phi = 1 - abs(s4_phim)/s4_phicd

if s5_phicd < tol:
    z5_phi = 1
else:
    z5_phi = 1 - abs(s5_phim)/s5_phicd

if s6_phicd < tol:
    z6_phi = 1
else:
    z6_phi = 1 - abs(s6_phim)/s6_phicd

if s7_phicd < tol:
    z7_phi = 1
else:
    z7_phi = 1 - abs(s7_phim)/s7_phicd

z_phi = min(z1_phi,z2_phi,z3_phi,z4_phi,z5_phi,z6_phi,z7_phi)

#Zanchw evaluates bending moment in anchor wall, fixed value used for yield stress
ZAncW = 1 - abs(MMA)/(((2600-170*dtD1)*1E-6)/0.85)*2.4E5)

#Zanc evaluates normal force in anchor, fixed value used for yield stress
ZAnc = 1 - abs(NMA)/((0.25*math.pi*(63.4-2*(1.7*(dtD1/4.65)))**2) * 1E-6 * 3.55E5)

#ZSoil evaluates soil stability
if sumM > 0.995:
    ZSoil = 1
else:
    ZSoil = sumM - 1

#Zstruct evaluates whole structure, note to use either z_pl (no softening) or z_phi (with softening)
ZStruct = min(z_pl, z_el, ZAncW, ZAnc, ZSoil)

```

Table 5.1 Implementation of LSF's in PTK

LSF internal variable	Response parameter	Origine
s1_mm	Section_1.M_max	PLX
s1_mpl	Section_1.M_pl_max	Python
s1_mel	Section_1.M_elas_corr	Python
s1_phim	Section_1.Phi_max	PLX
s1_phicd	Section_1.Phi_CD	Python
s1_rhom	Section_1.Rho_c_max	Python
s2_mm	Section_2.M_max	PLX
s2_mpl	Section_2.M_pl_max	Python
s2_mel	Section_2.M_elas_corr	Python
s2_phim	Section_2.Phi_max	PLX
s2_phicd	Section_2.Phi_CD	Python
s2_rhom	Section_2.Rho_c_max	Python
s3_mm	Section_3.M_max	PLX
s3_mpl	Section_3.M_pl_max	Python
s3_mel	Section_3.M_elas_corr	Python
s3_phim	Section_3.Phi_max	PLX
s3_phicd	Section_3.Phi_CD	Python
s3_rhom	Section_3.Rho_c_max	Python
s4_mm	Section_4.M_max	PLX
s4_mpl	Section_4.M_pl_max	Python
s4_mel	Section_4.M_elas_corr	Python
s4_phim	Section_4.Phi_max	PLX
s4_phicd	Section_4.Phi_CD	Python
s4_rhom	Section_4.Rho_c_max	Python
s5_mm	Section_5.M_max	PLX
s5_mpl	Section_5.M_pl_max	Python
s5_mel	Section_5.M_elas_corr	Python
s5_phim	Section_5.Phi_max	PLX
s5_phicd	Section_5.Phi_CD	Python
s5_rhom	Section_5.Rho_c_max	Python
s6_mm	Section_6.M_max	PLX
s6_mpl	Section_6.M_pl_max	Python
s6_mel	Section_6.M_elas_corr	Python
s6_phim	Section_6.Phi_max	PLX
s6_phicd	Section_6.Phi_CD	Python
s6_rhom	Section_6.Rho_c_max	Python
s7_mm	Section_7.M_max	PLX
s7_mpl	Section_7.M_pl_max	Python
s7_mel	Section_7.M_elas_corr	Python
s7_phim	Section_7.Phi_max	PLX
s7_phicd	Section_7.Phi_CD	Python
s7_rhom	Section_7.Rho_c_max	Python
sumM	Phase_6.MStage	PLX
MMA	AnchorPlate.M2D	PLX
NMA	Anchor.Force	PLX
dtD1	C1.dtD1	PTK

Table 5.2 Explanation of used symbols in Table 5.1

## 6 Calculation results (2<sup>nd</sup> series)

### 6.1 Introduction

As stated in the first chapter it is the ultimate objective of the research to enable probabilistic analyses with the Finite Element Method (FEM) using a probabilistic library/toolkit in an 'easy to use' way, and applicable to realistic soil-structure interaction problems. A stepwise approach is used to reach this objective and within this report a couple important steps have been taken. In the next future phase of the research there are still some important steps to be taken such as the implementation of the enhanced Class 4 strength and the development of a method within the approach for annual probabilities for degrading structures taking in account past performance.

The calculation results presented in this chapter consist of test runs of the various implementation steps as described in the previous three chapters using a realistic sheet pile case. Step by step the impact of these implementations is presented. First a summary of results is presented in paragraph 6.2. Next the results are analysed in paragraph 6.3 along the following steps:

- 1 Compare results with study [Deltares, 2018].
- 2 Consider impact of softening.
- 3 Consider impact of corrosion uncertainty.
- 4 Consider impact of yield stress as a stochastic variable.
- 5 Consider impact of different reference period.

In paragraph 6.4 some additional runs are discussed which have been made as a prelude to the next future phase of this project. Finally, in paragraph 6.5 the performed verification of the created probabilistic approach is discussed.

### 6.2 Summary of results

The results found by [Deltares, 2018] in the previous phase of this research are repeated here in Table 6.1.

Run	Softening	Corrosion	Soil strength	Yield stress	$\beta$	$\beta$ 84-16% interval <sup>8</sup>
2	No	Deterministic	Triaxial	Deterministic	2.02	(2.00-2.05)
4	Yes	Deterministic	Triaxial	Deterministic	2.97	(2.93-3.00)

Table 6.1 Results found by [Deltares, 2018]

The results of the final 2019 test runs in this study are summarised in Table 6.2 and Table 6.3.

<sup>8</sup> This is the 84-16% confidence interval based on Pf +/-Cov

Run	Softening	Corrosion	Soil strength	Yield stress	$\beta$	$\beta$ 84-16% interval <sup>9</sup>
H1	No	Deterministic	Triaxial	Deterministic	2.13	(2.09-2.17)
H2	Yes	Deterministic	Triaxial	Deterministic	3.83	(3.79-3.88)
H3	Yes	$V_c = 0.2$	Triaxial	Deterministic	2.90	(2.86-2.95)
H4	Yes	$V_c = 0.3$	Triaxial	Deterministic	1.94	(1.90-1.99)
H5	Yes	$V_c = 0.5$	Triaxial	Deterministic	1.16	(1.10-1.22)
H6	No	Deterministic	Triaxial	Stochastic	2.96	(2.92-3.01)
H7	Yes	Deterministic	Triaxial	Stochastic	4.19	(4.11-4.32)
H8	Yes	$V_c = 0.3$	Triaxial	Stochastic	1.90	(1.85-1.96)
H9	Yes	$V_c = 0.2$	Triaxial	Stochastic	2.60	(2.55-2.66)

Table 6.2 Summary of results found in this study. All results presented are made for  $T = 75$  years, i.e. at the end of the reference period

All the runs up to H9 were made for  $T = 75$  years, i.e. at the end of the reference period. Next some additional runs were made in which the end of the reference period was changed, i.e.  $T = 74, 50$  and  $49$  years. In these calculations the variables which are assumed to be time dependent have been adjusted to the changed reference period, see chapter 4. For these runs a variation coefficient for loss of thickness due to corrosion  $V_c=0.5$  was chosen because of both calculation time and the expectation that the influence of time will be most pronounced.

Run	Softening	Corrosion	Soil strength	Time	$\beta$	$\beta$ 84-16% interval <sup>9</sup>
H10	Yes	$V_c = 0.5$	Triaxial	74	1.22	(1.16-1.28)
H11	Yes	$V_c = 0.5$	Triaxial	50	2.67	(2.62-2.73)
H12	Yes	$V_c = 0.5$	Triaxial	49	2.78	(2.73-2.84)

Table 6.3 Results found in this study when using a different reference period. Note the yield stress was again set to a deterministic value of  $240 \text{ N/mm}^2$ .

From all the calculation runs the influence factors were derived by the PTK and presented in Table 6.4.

<sup>9</sup> This is the 84-16% confidence interval based on  $Pf \pm \text{Cov}$

	Run H	1	2	3	4	5	6	7	8	9	10	11	12
1 sand medium (SM), unsaturated weight	$\gamma_{\text{unsat\_SM}}$	15	5	1	1	1	10	0	1	1	0	1	2
2 sand medium (SM), saturated weight	$\gamma_{\text{sat\_SM}}$												
3 sand medium (SM), friction angle	$\varphi_{a^*\_SM}$	27	61	6	0	1	25	49	1	3	0	1	1
4 sand medium (SM), effective stiffness	$E'\_SM$	3	2	0	0	1	2	0	0	0	1	0	0
5 clay medium (CM), friction angle	$\varphi_{a^*\_CM}$	6	3	0	0	2	6	1	1	1	1	0	0
6 clay medium (CM), stiffness	$E'\_CM$	31	6	3	1	0	26	5	1	1	0	0	1
7 clay medium (CM), cohesion	$c_{a^*\_CM}$	5	3	1	1	0	5	5	0	0	0	0	1
8 sand dense (SD), friction angle	$\varphi_{a^*\_SD}$	1	9	0	0	0	5	12	0	0	0	0	0
9 canal bottom	$z$	2	1	0	0	0	2	0	1	1	0	0	1
10 outside waterlevel	$h$	8	6	0	0	0	6	18	1	2	0	0	0
11 load zone 1	$q1$	3	3	0	0	0	3	2	0	2	0	0	0
12 load zone 2	$q2$	0	1	0	0	0	0	4	0	1	0	1	0
13 load zone 3	$q3$	0	0	0	0	0	1	0	0	0	1	0	0
14 thickness reduction D1	$\Delta t\_D1$			62	79	84			72	58	83	77	71
15 thickness reduction D2	$\Delta t\_D2$			25	17	10			23	29	12	19	21
16 steel yield stress	$f_y$						8	3	0	1			
17 time	$T$												
	<b>SUM</b>	<b>100</b>	<b>100</b>	<b>100</b>	<b>100</b>	<b>100</b>	<b>100</b>	<b>100</b>	<b>100</b>	<b>100</b>	<b>100</b>	<b>100</b>	<b>100</b>

Table 6.4 Overview of all the calculated Influence factors [%] per run. Note that since the unsaturated weight and the saturated weight are fully correlated the influence factors presented for the unsaturated weight also apply to the saturated weight. Furthermore, note that Time is not used as a stochastic variable in the calculation presented in this paragraph. See paragraph 6.4 for more information on Time as a stochastic variable

### Some notes regarding influence factors

The influence factors are determined using the “centre of gravity” option. In this case the program uses all samples in the failing domain and takes the weighted mean. Also see appendix C and/or the PTK manual for more background information.

Important to realize is that the calculated influence factors are not as accurate as they seem, there is a significant uncertainty. This uncertainty comes from the fact that with the Directional Sampling method does not result in the exact design point (i.e. the point with the highest failure probability and thus closest to the origin in u-space) but only an approximation of this value. Based on the first experiences gathered the values calculated should be rounded to magnitudes of 10% before comparing them.

It is furthermore noted that although a variable may have a large impact on forces in the sheet pile structure and as such determine for a large part the design of the structure, then the influence factor may still be small in case the UNCERTAINTY associated with this variable is relatively small. Example here is the water level which is modelled with a Gumbel extreme minima distribution. As such the minimum water level expected within the service life is quite CERTAIN and as such the influence factor is quite small.

For all the calculation runs it was also analyzed how many failures and the type of failure occurred and how these failures are distributed over the defined LSF. The results are presented in Table 6.5. Note: the number of failures is not a direct measure for the reliability, this is also dependent on the probability of the individual realizations that failed and the number of non-failures and probability of those realizations.

run H	softening?	corrosion	yield stress	Time	z_pl	z_el	z_phi	z_anchwall	z_anc	z_soil	total failures
1	No	Deterministic	Deterministic	75	306					1	307
2	Yes	Deterministic	Deterministic	75			43			10	53
3	Yes	V = 0.2	Deterministic	75		11	53				64
4	Yes	V = 0.3	Deterministic	75		45	60				105
5	Yes	V = 0.5	Deterministic	75		44	50				94
6	No	Deterministic	Stochast	75	190					4	194
7	Yes	Deterministic	Stochast	75			7			7	14
8	Yes	V = 0.3	Stochast	75		42	29				71
9	Yes	V = 0.2	Stochast	75		22	35				57
10	Yes	V = 0.5	Deterministic	74		55	40				95
11	Yes	V = 0.5	Deterministic	50		26	33				59
12	Yes	V = 0.5	Deterministic	49		21	29				50

Table 6.5 Overview of number of failures per mechanism per run [-]

### 6.3 Analyses of results

#### 6.3.1 Comparison with previous study (run 2-4 & run H1-2)

Some results from the Deltares 2018 research are compared with results of the current 2019 study. First two more or less identical calculations without softening are compared. Secondly two runs with softening are compared, but these runs are different as in the 2019 run a refined approach on softening was used. This refined approach on softening is expected to result noticeable/significant positive effect on the reliability.

When comparing run 2 from [Deltares, 2018] with run H1 performed within this study it is concluded that a comparable reliability is calculated, i.e. a  $\beta$  of 2.02 vs. 2.13. The small differences found seem acceptable as some differences occur between the two approaches, i.e. different tools are used (with different random generators for the directions calculated) and a different approach in surcharge loads (the more realistic approach for the load in H1 is effectively lower).

The comparable results between these two calculations give confidence regarding the implementation of the developed approach in this study and as such can be considered a first verification step.

When comparing run 4 from [Deltares, 2018] with run H2 performed within this study it is concluded that with the new approach on softening a significant higher reliability is calculated, i.e. a  $\beta$  of 2.97 vs. 3.83 and their 16-84% confidence interval are widely spaced. The difference found is expected to be dominated by and in line with the foreseen benefit of the refined approach on softening.

#### 6.3.2 Impact of softening (run H1-2)

When comparing results of calculation run H1 and H2 it becomes clear that due to softening a large positive effect is found on reliability. The reliability index  $\beta$  increases from 2.13 to 3.83.

When inspecting the calculated influence factors, the following conclusions are drawn:

- In run H1 no softening and a deterministic corrosion is applied and here most dominant influence factors are the strength  $\phi$  of the top sand layer and the stiffness ( $E$ ) of the middle clay layer.



- In run H2 there is softening applied in combination with a deterministic corrosion, here the most dominant influence factor is the strength ( $\phi$ ) of the top sand layer. It seems the stiffness is of much less importance in this case.

When inspecting the number of failures per mechanism the following conclusions are drawn:

- In run H1 the relative number of soil failures is very small compared with failures of the sheet pile front wall.
- In run H2 the relative number of soil failures is relatively large compared with failures of the sheet pile front wall.
- The above observations match with the expectation that in case softening is applied more strength of the soil can be mobilized, i.e. the soil is now also “allowed” to fail more often.

### 6.3.3 Impact of corrosion uncertainty (run H2-5)

When comparing results of H2, 3, 4 and 5 it becomes clear that an increasing a-priori uncertainty of the corrosion results in an increasing negative effect is found on reliability and hence residual service lifetime of the structure. This also means that when the a-priori uncertainty of corrosion can be reduced by means of inspection a positive effect is found on reliability and hence residual service lifetime of the structure.

When inspecting the calculated influence factors, the following conclusions are drawn:

- In run H2 there is softening applied in combination with a deterministic corrosion, here the most dominant influence factor is the strength ( $\phi$ ) of the top sand layer. Or in a general sense the uncertainty related to the soil is dominant.
- In runs H3, 4 and 5 the uncertainty related to corrosion is added as a stochastic variable. In all cases considered ( $V_c = 0.2, 0.3$  or  $0.5$ ) the corrosion has become the dominant uncertainty. Or in a general sense the uncertainty related to the structure has become dominant.
- Furthermore, note that the calculations are all made for the end of the reference period, i.e. at  $T = 75$  years. Basically, this means that at the start of the reference period the influence of soil is dominant and during the reference period gradually the influence of the structure will become stronger. How quickly the transition goes is dependent on the uncertainty of the corrosion, but at the end of the reference period for all cases considered here ( $V_c = 0.2, 0.3$  or  $0.5$ ) corrosion has become the dominant uncertainty.

When inspecting the number of failures per mechanism the following conclusions are drawn:

- In run H2 a relative large number of soil failures is to occur.
- In runs H3, 4, and 5 no soil failures occur. The soil no longer failing since the structure is the dominant “weakest link” due to the corrosion.
- In runs H3, 4 and 5 one can see the increasing relative number of failures due to LSF  $z_{el}$ . This seems logical since with increasing variation coefficient of the corrosion the chance of a larger corrosion value increases and hence the chance the sheet pile becomes so corroded it becomes a Class 4 profile.

### 6.3.4 Impact of yield stress as a stochastic variable (run H1-9)

When comparing H1 and H6 it becomes clear that in the case no softening is used and corrosion is a determinist the stochastic nature of the yield stress has a positive effect on reliability. Also, when comparing H2 and H7 it becomes clear that in the case softening is used and corrosion is a determinist the stochastic nature of the yield stress has a positive effect on reliability.

When comparing H3 and H4 with respectively H9 and H8 it becomes clear that in the case softening is used AND corrosion is a stochastic variable, the stochastic nature of the yield stress has no influence anymore (or even a small negative effect) on reliability. This is remarkable at first sight. After further analyzing results it however becomes clear there is a positive and a negative effect related to a higher yield stress:

- Positive effect is that, because a higher stress is allowed in the steel sheet pile, a higher capacity is obtained.
- On the other hand, there is a negative effect, this is related to the effect of the yield stress on the ratio " $b/t_f/\epsilon$ " in which  $\epsilon = \sqrt{(235/f_y)}$ . The larger the yield stress  $f_y$  the larger this ratio becomes, indicating that the profile is becoming more and more prone to local buckling effects. Or in other words allowing for more stress in the same (slender) geometry causes more quickly instability effects. As a result, the capacity increase is less than linear with increasing yield stress. This negative effect becomes more dominant for situations with a higher yield stress and/or more corrosion.
- The negative effects are strengthened when moving into the Class 4 area since in this phase of the research a conservative approach for the Class 4 strength is chosen. Actually, in the current approach the strength in the Class 4 area is independent of the actual yield stress. This conservative approach is believed to be responsible for the fact that when comparing H3, H4 with H9, H8 it seems that due to the increase of yield stress even a small reduction in reliability may be found. Reliability is not expected to become less, however the increase in reliability may be insignificant for situations with a higher yield stress and slenderer sheet pile profiles. *Note that in paragraph 5.2.2 an enhanced model for Class 4 is mentioned to be implemented in a future research phase.*
- Less use can be made of the positive effects of softening: due to the higher yield stress we move to a higher bending moment capacity BUT with a lower softening capacity or no softening capacity at all as compared with the situation with a lower yield stress. It seems that the increased bending moment capacity cannot fully account for the loss in rotation capacity.
- The aforementioned positive and negative effects have been further elaborated by means of figures and some example calculations in appendix H.5

When inspecting the calculated influence factors, the following conclusions are drawn:

- In run H6 and H7 the yield stress has a relative small influence factor. This suggests that although the on average higher yield stress, compared with run H1 and H2, has a significant effect on the reliability the uncertainty associated with this stochastic variable is relatively small;
- In run H8 and 9 the on average higher yield stress, compared with run H3 and H4, has no significant effect on the reliability and also the uncertainty associated with this stochastic variable is small.

When inspecting the number of failures per mechanism the following conclusions are drawn:

- In run H6 the relative number of soil failures is very small compared with failure of the sheet pile front wall. In run H7 the relative number of soil failures is relatively large compared with failure of the sheet pile front wall. The above observations match with the expectation that in case softening is applied more strength of the soil can be mobilized, i.e. the soil is now also "allowed" to fail more often. The yield stress as a stochastic variable has no clear effect;
- In run H8 and 9 the relative number of failures due to LSF  $z_{el}$  seems to have increased compared with run H3, 4 and 5. This seems logical since on top of the increasing variation coefficient of the corrosion the increased yield stress adds to a higher ratio " $b/t_f/\epsilon$ " and the sheet pile becomes a Class 4 profile even faster.

## 6.4 Additional runs

### 6.4.1 Modelling with the HS model

The reported calculations (H1 – 12) have made use of the Mohr Coulomb (MC) model within PLAXIS. The MC model is a relatively simple material model. Most notable drawback is the oversimplified way of dealing with soil stiffness, the model just has one stiffness parameter ( $E$ ). To investigate the impact of using a more realistic material model use was made of the Hardening Soil (HS) model within PLAXIS. The HS model makes use of three stiffness parameters ( $E_{50;ref}$ ,  $E_{oed;ref}$  and  $E_{ur;ref}$ ). By means of these stiffness parameters it can account for the non-linearity of soil stiffness in different stress paths and loading and unloading.

The sensitively calculations made with the HS model were done with preliminary versions of the coupling so the results cannot directly be compared with the results reported in this chapter. However, the following experiences have been gathered:

- Challenge when using the HS model is to make sure that a consistent parameter set is send to PLAXIS. When defining the stiffness values of the HS model as a stochastic variable it may be that a parameter set results that is not “accepted” by PLAXIS, i.e. the program returns an error and will not calculate. This is caused by internal model boundaries of the HS material model to prevent unrealistic results. To by-pass this problem a check was included on the consistency of the parameter set. There are multiple ways of including this check. Here the following practical approach was chosen:
  - Define  $E_{50;ref}$  as the stochastic variable and use a fixed ratio with  $E_{ur;ref}$ .
  - For the soils modelled with the HS model the parameter range of  $E_{oed;ref}$  was determined such that an always a consistent parameter set is found;
  - Create a “special command” with the above mentioned fixed ratio and a formula to calculate  $E_{oed;ref}$  such that the parameter set is always consistent.
  - Experience is that in some cases adjustments have to be made to  $E_{oed;ref}$  leading to stiffness values that are considered less realistic. Since however for a retaining wall behavior is mostly controlled by  $E_{50\_ref}$  and  $E_{ur;ref}$  this is assumed to be acceptable for this sensitively analysis.
- The cases calculated with the HS material model suggest that:
  - In case the (uncertainty in) soil parameters is more relevant, for example without softening or at the start of the reference period when corrosion is not yet dominant, the choice of the material model will have a larger impact.

It is recommended to perform further research into the effects of using a more advanced material model on reliability, i.e. are the effects significant and is it necessary to use a more advanced material model?

### 6.4.2 Modelling time as a stochastic variable

In the reported calculations in this chapter (H1 -12) the time ( $T$ ) is set to a fixed value, in most cases  $T = 75$  years (the end of the reference period). The uncertainty in the water level and surcharge load used are determined according to this reference period. The amount of thickness reduction used in the calculations is the value at the end of the reference period.

A thought which occurred during this study is to include time in the calculation as a uniformly distributed stochastic variable on the range [25, 75], i.e. the reference period. The corrosion is

directly coupled to the Time, so the corrosion values used is scaled using the parameter  $(T / 75)$ .

Advantage of this approach should have been that the PTK directly calculates the reliability over the full reference period, which is in line with the Eurocode. However, a downside of this approach was that the contribution of the uncertainty of the soil was overestimated as this was not considered to be a constant over the reference period. This approach was therefore not further investigated.

## 6.5 Verification of results

An important part of software models is the verification that the model does what it is supposed to do. Within the context of the project it has not been possible to make a full extensive review/verification of all parts of the software. Nevertheless, several sanity checks have been made, especially on the created python coupling scripts since the other two pieces of software (PTK and PLAXIS) have their own quality procedures.

Results of the model are in line with results found by [Deltares, 2018] using different software. Furthermore, checks are made on parts of the python scripts using spreadsheets and results of the model are post-processed with python to make them more accessible and allow for a review of results, see appendix G. It is concluded that the developed approach seems to work as expected.

## 7 Calculation results (3<sup>rd</sup> series)

### 7.1 Introduction

In the 3<sup>rd</sup> calculation series performed in 2020 an improved Class 4 strength has been implemented in comparison to the 2<sup>nd</sup> calculation series from 2019. Details about the improved Class 4 strength formulation have been presented in appendix I.

Within the 3<sup>rd</sup> series first the impact of using the improved Class 4 strength has been analysed. Next variations have been made with the reference period for which the reliability is determined: By means of these variations more insight is obtained on the impact of corrosion over the reference period. Finally, a number of calculations have been made using the plane strain soil strength instead of the (3D) triaxial soil strength.

### 7.2 Summary of results

In Table 7.1 a summary is presented of the input and output of the 3<sup>rd</sup> series of calculations. For a more detailed summary of output results, including influence factors and number of failures per mechanism, reference is made to appendix J.

Run	Corrosion	Soil strength	Improved Class 4	$T_c$	$T_{ref}$	$\beta$	$\beta$ 84-16% interval <sup>10</sup>	
H14	$V_c = 0.5$	Triaxial	No	75	50	1.12	1.06	1.18
I1	$V_c = 0.5$	Triaxial	Yes	75	50	1.18	1.12	1.24
I2	$V_c = 0.5$	Triaxial	Yes	50	25	2.71	2.67	2.75
I3	$V_c = 0.5$	Triaxial	Yes	26	1	5.34	5.28	5.43
I4	$V_c = 0.3$	Triaxial	Yes	26	1	5.42	5.35	5.53
I5	Deterministic	Triaxial	Yes	26	1	5.45	5.40	5.51
I6	$V_c = 0.2$	Triaxial	Yes	26	1	5.45	5.37	5.60
I7	$V_c = 0.3$	Triaxial	Yes	50	25	4.54	4.46	4.66
I8	$V_c = 0.3$	Triaxial	Yes	75	50	1.93	1.89	1.98
I9	Deterministic	Triaxial	Yes	50	25	4.65	4.60	4.71
I10	Deterministic	Triaxial	Yes	75	50	3.99	3.91	4.10
I11	$V_c = 0.2$	Triaxial	Yes	50	25	4.59	4.54	4.66
I12	$V_c = 0.2$	Triaxial	Yes	75	50	2.63	2.58	2.69
I13	Deterministic	Triaxial	Yes	75	1	4.78	4.71	4.88
I14	$V_c = 0.2$	Triaxial	Yes	75	1	2.84	2.78	2.91
I15	$V_c = 0.3$	Triaxial	Yes	75	1	2.05	2.00	2.10
I16	$V_c = 0.5$	Triaxial	Yes	75	1	1.38	1.33	1.44
I17	Deterministic	Triaxial	Yes	50	1	5.32	5.28	5.38
I18	$V_c = 0.5$	Triaxial	Yes	50	1	2.83	2.77	2.90
I19	Deterministic	Plane-strain	Yes	75	50	4.62	4.56	4.71
I20	$V_c = 0.2$	Plane-strain	Yes	75	50	2.89	2.81	3.00
I21	$V_c = 0.3$	Plane-strain	Yes	75	50	2.11	2.03	2.20
I22	$V_c = 0.5$	Plane-strain	Yes	75	50	1.38	1.32	1.44

Table 7.1. Summary of results of the 3<sup>rd</sup> series of calculations. Note that in all cases softening is used and  $f_y$  is set as a stochastic variable.

Note:

<sup>10</sup> This is the 84-16% confidence interval based on  $P_f \pm Cov$

$T_c$  is the final year of the reference period  $T_{ref}$ , i.e.  $T_c = 25 + T_{ref}$ .

### 7.3 Analyses of results

#### 7.3.1 Impact using an improved Class 4 strength (run H14 and I1)

The effect of using a more realistic Class 4 strength appears to be small for this Case Study. The increase in  $\beta$ -value is from 1.12 to 1.18. The small increase in reliability is explained by looking in more detail at the results. The calculated design point for run H14 for the dominant variable i.e. the corrosion parameter  $\Delta t_{D1}$  is 6.8 mm, see “C1.dtD1” in Figure 7.1, which effectively is only just in the Class 4 area. Apparently, the sheet pile fails almost directly when ‘entering’ the Class 4 area. The impact of the improved Class 4 formulation is however very limited at ‘the beginning of the Class 4 area’ and only becomes more significant ‘deeper into the Class 4 area’. As such the small increase in reliability found here seems logical. Note however that for different situations the impact of an improved Class 4 formulation may be much more significant. Furthermore, note that the improved Class 4 strength formulation used in this study is only an approximation. Further research is recommended. Also see appendix I for further background details.

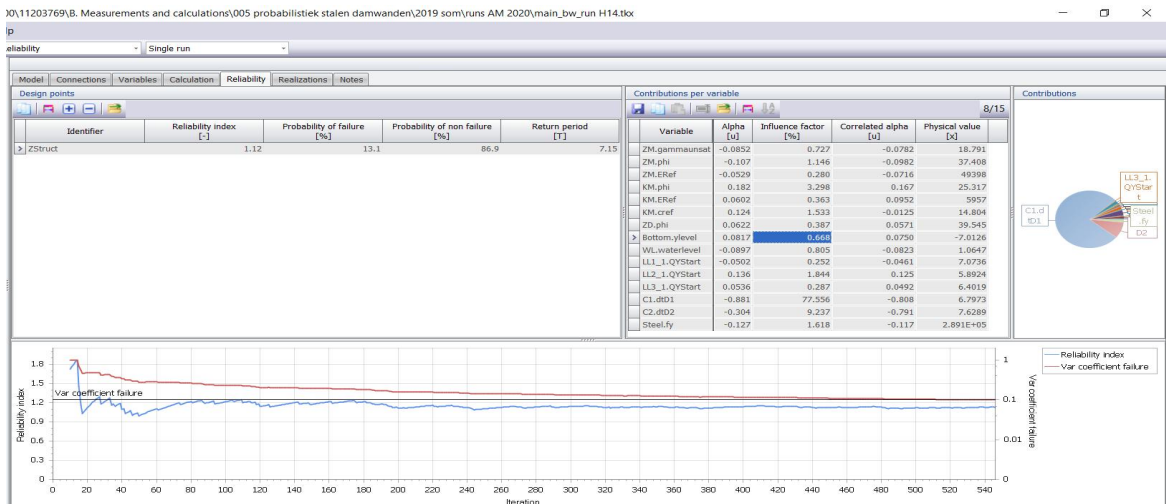


Figure 7.1. Calculation results for run H14

#### 7.3.2 Impact of different reference periods (run I1 – I18)

The results of calculations I1 to I18 are summarized in Figure 7.2. The following observations are made from this figure:

- At  $T_c = 50$  and 75 years there is hardly any difference between the calculation for a  $V_c = 0.5$  with a 1-year reference period and the reference periods of 25 and 50 years. This suggests that the length of the reference period and the connected uncertainty in (time-dependent) loads is not relevant compared to the uncertainty in corrosion. Corrosion is dominant throughout the analyzed reference periods in this case.
- Compared to the previous bullet: there is a difference between the calculation for a  $V_c = 0$  with a 1-year reference period and reference periods up to 50 years. This suggests that the length of the reference period and the connected uncertainty in (time-dependent) loads is relevant compared to the uncertainty in corrosion.

- The reliability determined in the runs with  $V_c = 0, 0.2$  and  $0.3$  and a reference period,  $T_{ref}$ , up to 25 years is (almost) the same. This suggests that corrosion is not relevant to that moment. At  $T_c = 25$  year this also holds for  $V_c = 0.5$ .

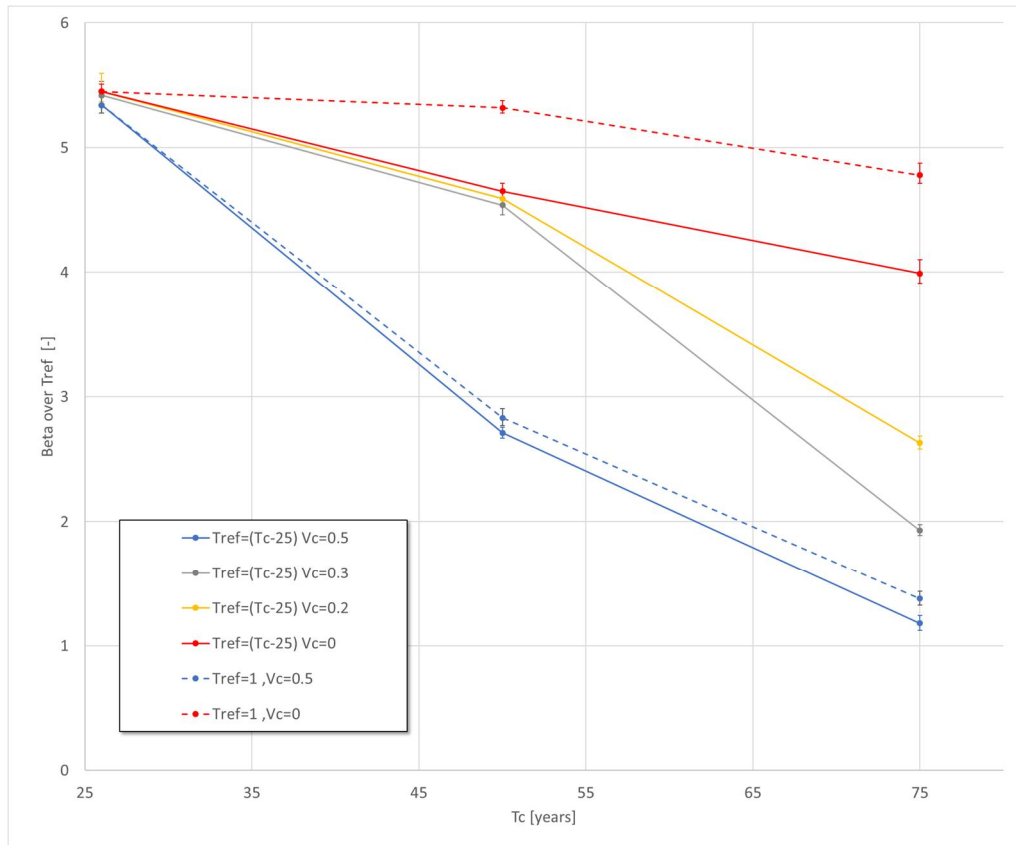


Figure 7.2. Summary of results of run I1 – I18 presented as calculated reliability (Beta) vs. final year of reference period  $T_c$

The following observations are made from the summary of output results in appendix J:

- The uncertainty in soil weight, soil stiffness, bottom level, surcharge load and yield stress in all runs seems to be relatively small compared to the uncertainty in soil strength, water level and corrosion;
- Run I7 ( $T_c = 50$ ,  $T_{ref} = 25$  and  $V_c = 0.3$ ) only has a total of 8 failures found, this seems related to the choice for a 'search depth' of only 6 in the directional sampling method, which appears to be too low in hindsight. The low number of failures found suggests that results are less trustworthy for this run;

7.3.3 Impact of using plastic hinges and corrosion uncertainty (1<sup>st</sup> series and run I1, I8, I10 and I12)  
To gain insight into the positive effect of using plastic hinges in combination with the negative effect of corrosion uncertainty use is made of an adjusted version of the bar chart created in the 1<sup>st</sup> series of calculations [Deltares, 2018] and which is presented in appendix F. The adjusted bar chart is presented in Figure 7.4. and combines results of the 1<sup>st</sup> and 3<sup>rd</sup> series of calculations.

From the figure the following observations can be made:

- The exact formulation of the limit state related to front wall failure has a very large impact on reliability. This can be seen by looking at the four bars at the left side of Figure 7.3, i.e. a formulation that ranges from using (1) elastic capacity, (2) plastic capacity (but no rotation capacity), (3) plastic capacity (with a simplified formulation for rotation capacity) to (4) plastic capacity with a realistic estimate of rotation capacity. The calculated reliability ranges from approximately 1 to 4, which equals a factor 5000(!) difference in reliability;
- The uncertainty in corrosion, taken into account in the calculation, also has a very large impact on reliability. This can be seen by looking at the four bars at the right side of Figure 7.3, i.e. a formulation that uses (1) a coefficient of variation (CoV) for the applied corrosion of 0.5, (2) a CoV = 0.2, (3) a CoV = 0.3 to (4) a CoV = 0.5. The calculated reliability ranges from 4 to approximately 1, which again equals a factor 5000(!) difference in reliability;
- From [Deltares, 2019a and b] it was concluded that a-priori the CoV for corrosion may be in the order of 0.5 on a regional scale. The CoV for corrosion on a local scale however may be in the order of 0.2 to 0.3 as such allowing for reducing the a-priori uncertainty by inspections. As such it seems that the positive effect of a more realistic limit state function for the front wall may outweigh the negative effects of corrosion uncertainty.

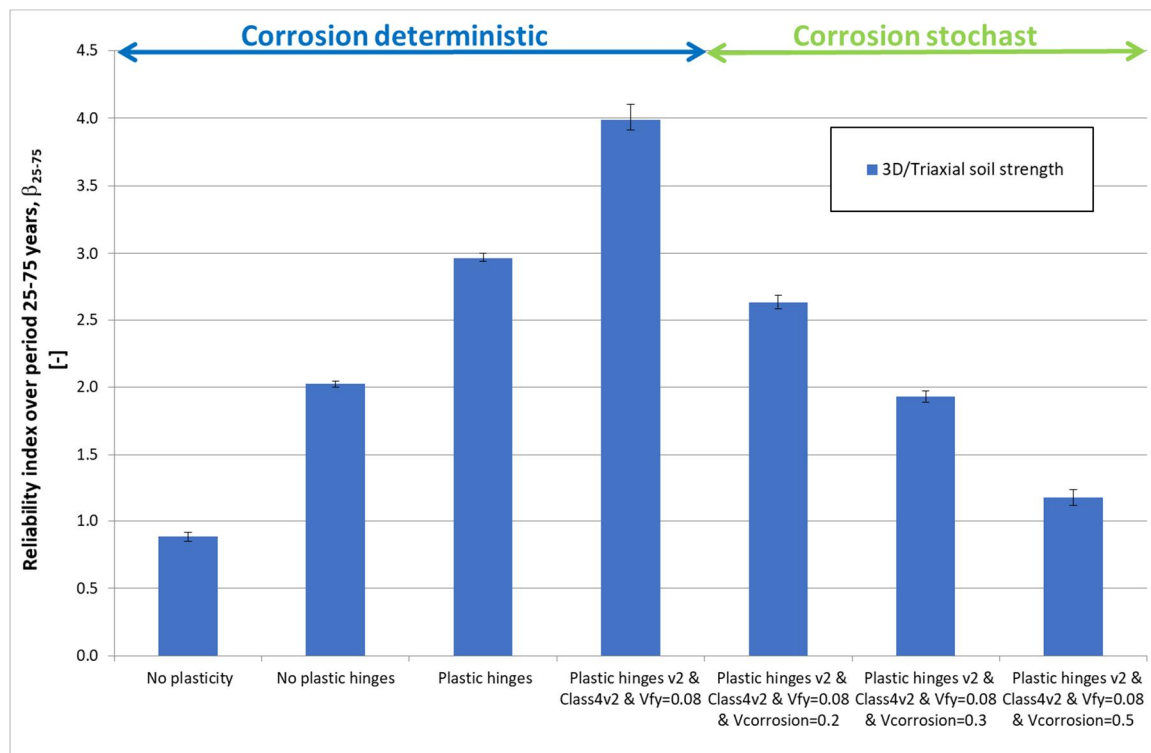


Figure 7.3. Bar chart presentation of results found during 1<sup>st</sup> and 3<sup>rd</sup> series of calculation using 3D/Triaxial soil strength

Note with terms on x-axis in Figure 7.3:

- No plasticity: use is made of the elastic capacity of the sheet pile front wall
- No plastic hinges: use is made of the plastic capacity of the sheet pile front wall, but no rotation capacity is allowed
- Plastic hinges: use is made of the plastic capacity of the sheet pile front wall with a first simplistic implementation of rotation capacity in the 1<sup>st</sup> series of calculations;



- Plastic hinges v2: use is made of the plastic capacity of the sheet pile front wall with a more realistic implementation of the rotation capacity as detailed in this report and used in the 2<sup>nd</sup> and 3<sup>rd</sup> series of calculations;
- Class 4v2: the improved Class 4 formulation as detailed in appendix I of this report;
- V<sub>fy</sub>: the coefficient of variation used for the yield strength
- V<sub>corrosion</sub>: the coefficient of variation used for the corrosion

#### 7.3.4 Impact of using plane strain soil strength (run I19 – I22)

To gain insight into the effect of using plane strain strength parameters use is made of an adjusted version of the bar chart presented in Figure 7.3. which combines results of the 1<sup>st</sup> and 3<sup>rd</sup> series of calculations. Effectively the bar chart is repeated in Figure 7.4 but now also the results of runs I19 – I22 are included using 2D/Plane strain soil strength.

From the figure the following observations can be made:

- The formulation of the limit state related to soil failure has an impact on reliability. Using the 2D plain strain strength results in an increased reliability at the end of the reference period of 50 years,  $T_c = 75$  year, for all runs as expected;
- The impact of the 2D plane strain strength formulation is relatively larger in case the sheet pile can generate a plastic hinge and the impact of corrosion is relatively small. This seems plausible as for low corrosion values the sheet pile will be able to utilize its rotation capacity (it stays in Class 2 – 3 and does not end up in Class 4) and as such more of the extra available 2D soil strength can be mobilized.

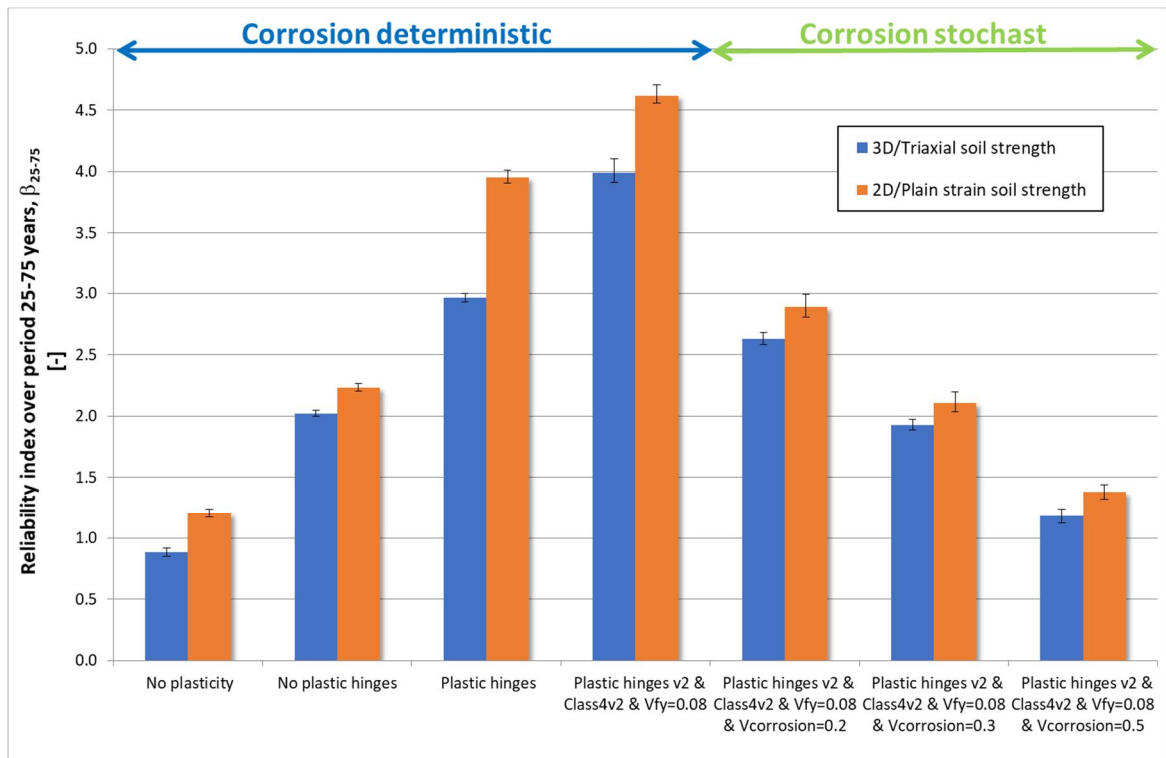


Figure 7.4. Bar chart presentation of results found during 1<sup>st</sup> and 3<sup>rd</sup> series of calculation using 3D/Triaxial and 2D/Plain strain soil strength

Note with terms on x-axis in Figure 7.4:

- No plasticity: use is made of the elastic capacity of the sheet pile front wall
- No plastic hinges: use is made of the plastic capacity of the sheet pile front wall, but no rotation capacity is allowed
- Plastic hinges: use is made of the plastic capacity of the sheet pile front wall with a first simplistic implementation of rotation capacity in the 1<sup>st</sup> series of calculations;
- Plastic hinges v2: use is made of the plastic capacity of the sheet pile front wall with a more realistic implementation of the rotation capacity as detailed in this report and used in the 2<sup>nd</sup> and 3<sup>rd</sup> series of calculations;
- Class 4v2: the improved Class 4 formulation as detailed in appendix I of this report;
- $V_{fy}$ : the coefficient of variation used for the yield strength
- $V_{corrosion}$ : the coefficient of variation used for the corrosion

## 8 Conclusions and recommendations

### 8.1 Objective and scope

In this report the results are reported of research performed in the period 2019 - 2021 within the framework of the research program on Hydraulic Structures (Dutch abbreviation: *KpNK*).

The objective of this research is twofold:

1. To make probabilistic methods practically applicable to FEM based analysis of soil-structure interaction, allowing for a more rational assessment;
2. To come to a more realistic and balanced physical model for steel sheet pile structures by including two aspects known to be lacking: a more realistic corrosion model and softening of the steel sheet pile.

The scope of this research phase is focussed on setting-up and gaining experience with a more generic and “easy to use” coupling between the program PLAXIS and the Deltares software Probabilistic Toolkit (PTK) by means of a case study. The case study is further used to gain experience with the impact of modelling corrosion as a stochastic variable, to improve on mechanical behaviour by including plastic hinges, rotation capacity and softening, to gain experience with the impact of modelling the yield stress as a stochastic variable and to record the mentioned experiences.

### 8.2 Results and conclusions

The following main results have been reached in this study:

- a generic coupling between the PTK and external models using neutral files has been developed. This generic coupling is here applied to the FE model PLAXIS;
- The developed “probabilistic approach” is applied to a case study of a steel sheet pile retaining wall;
- A specific python “softening module” for steel sheet piles has been developed and applied in the case study;
- A more realistic corrosion model is applied in the case study based on data collected and analysed within previous studies within the context of *KpNK*;
- By adding softening and a more realistic corrosion model a more realistic and balanced physical model has been achieved. A more realistic and balanced physical model will allow for less conservative assessment of existing hydraulic structures;
- First insights have been gathered with the more realistic and balanced model regarding amongst others the transition of sheet piles from Class 3 to Class 4 due to corrosion effects, the workings of softening and the transition from dominant soil influence on reliability to a dominant structural influence on reliability.

The results and conclusions are presented in more detail hereafter.

#### Coupling of PTK and PLAXIS

The Deltares software product Probabilistic Toolkit (PTK) is a probabilistic library with numerical tools dedicated to the treatment of uncertainties. Within this project the PTK coupling option was added to interact with any program using so-called neutral files. Within this project the new coupling option of the PTK has been applied to the commercial FE package PLAXIS by means of a python interpreter. The “resulting probabilistic approach” allows for analyzing reliability of generic soil-structure interaction problems.

Main advantages of the approach are that it allows the use of the probabilistic library of the PTK, including all common distribution functions and all common reliability integration methods. The PTK is a user friendly and intuitive software package. The approach allows the use of the FE principles through PLAXIS, combining the most relevant geotechnical and structural failure mechanisms in one model and allowing for realistic soil-structure interaction behavior. Moreover, it allows taking direct advantage of research developments by TUDelft and Deltares, since it also allows for coupling with (experimental new) python-based reliability methods, such as the ERRAGA package [Van den Eijnden et al, 2019].

For specific soil-structure problems (e.g. slope stability, settlements, retaining walls) it may be necessary to develop some specific “special commands”, i.e. python scripts dealing with some specific pre -and post processing tasks that cannot be dealt with directly in the PLAXIS command line. In the long term it is feasible to develop a database with these kinds of “problem-specific” special commands.

Checks have been performed on the developed approach (and recorded in this report) to verify its intended behavior. The developed approach for the coupling with PLAXIS can, due to the vast calculation time of weeks, be considered a research approach and can be used in pilot projects for e.g. research, code calibration or advanced assessment of existing structures.

In this report a number of practical tips and tricks have been reported on both operating this coupling and the setup of the FE-analysis for the purpose of running probabilistic analysis.

#### Softening module

It is well-known that the EN1993-5:2008 allows for incorporating plastic hinges, rotation capacity and softening into design and assessment of steel sheet pile structures. Nevertheless, this is still not common practice. To explore the impact on reliability a special python command (i.e. “softening” module) has been created allowing for plastic hinges, rotation capacity and softening within the case study used here.

Using plastic hinges, rotation capacity and softening has multiple advantages. The bending moment capacity of a plastic hinge is larger than the commonly used elastic capacity. Furthermore, if a plastic hinge develops in a statically indeterminate structure the structure will start deforming while allowing for forces to redistribute within the structure. At the same time the soil will also deform (following the sheet pile) while mobilizing more of the soil strength, effectively reducing and redistributing the load on the sheet pile.

Based on the case study it is concluded that using plastic hinges, rotation capacity and softening has a large positive influence on reliability.

#### Impact of corrosion uncertainty

Using the case study, the impact was studied of adding corrosion as a stochastic variable and varying the (a-priori) uncertainty (i.e. the variation coefficient). Results found by [Deltares, 2019b] suggest that the a-priori uncertainty in corrosion may be large. Using these large uncertainties results in a large negative impact on (calculated) reliability and as such results in a shorter (residual) service life. By means of inspection it is however to be expected that the a-priori uncertainty can be substantially reduced resulting in a significant increase in (calculated) reliability and a longer (residual) service life.

From the influence factors it was concluded that for this case study the corrosion was THE dominant uncertainty near end of technical life at 75 years. Although this conclusion may not be directly generalized for other situations it may be argued that in any “economic” design the

corrosion will be at least one of the more dominant uncertainties near end of technical service life.

#### Impact of yield stress uncertainty

Next the impact of modelling the yield stress as a stochastic variable was investigated using the case study. It is known that a steel sheet pile is a “factory product” with a certain minimum quality. For the yield stress this means that the “yield stress from the brochure” is a minimum value. In reality this value is (much) higher. It is interesting to quantify the effect of the real yield stress on reliability. From literature a distribution was chosen and incorporated into the case study.

From the results it was concluded that using a stochastic yield stress can have a positive influence on reliability. However, the positive effect will become less for increasingly slender (more corroded) sheet pile profiles. This is caused by the fact that these slender profiles are more susceptible for local buckling effects, or in other words the maximum allowable stress in the geometry is not limited by the yield stress anymore but by the stability of the profile. The latter effect is non-linear especially when sheet pile profiles become so corroded they move towards Class 4. Eventually the positive effects of the stochastic yield stress may become insignificant.

#### Impact of improved Class 4 strength formulation

To investigate the effect of using a more realistic (and less conservative) Class 4 strength the formulation is adjusted in the 3<sup>rd</sup> series of calculations compared to the 2<sup>nd</sup> series. For a number of different yield stresses and different corrosion values ArcelorMittal provided the Class 4 strength for an AZ26 profile according to a critical stress calculation in line with Eurocode 3 guidelines. Deltares used the provided numerical values to make a better approximation of the real Class 4 strength. To this end a polynomial surface was fitted through the provided numerical values to generate a continuous representation of the Class 4 strength in the calculations.

The effect of using a more realistic Class 4 strength appears to be small for this Case Study. This seems related to the relatively small attribution of failures ‘deep into’ the Class 4 area, where the improved strength formulation is most relevant, to the overall reliability for this Case Study. For other situations the impact of the improved strength formulation may be more significant.

#### Impact of different reference periods

For the Case Study used here more insight is obtained in the moment the situation will change from a dominance in soil uncertainty to a dominance in structure uncertainty. The turning point for this Case Study seems mostly dependent on the used coefficient of variation for the corrosion. For the situation of an a-priori  $V_c = 0.5$  the situation is fully dominated by the uncertainty in corrosion for all reference periods analysed after an age of  $T_c = 25$  years. For the situation with an a-priori  $V_c = 0.2$  or  $0.3$  the turning point however seems to be roughly around an age of  $T_c = 50$  years with a reference period of 25 years were corrosion starts to be of some significant influence and at an age of  $T_c = 75$  years corrosion is also dominant.

It is concluded that by analyzing different reference periods a better insight can be obtained in for example the optimum moment of corrosion inspection, i.e. a moment as late as possible in time, but before the (calculated) reliability becomes too low, i.e. the moment that the uncertainty in corrosion starts becoming dominant.

#### Impact of using plane strain soil strength

Using the higher (2D) plain strain strength results in an increased reliability for all cases compared to using the (3D) triaxial strength as expected. Interesting however to note is that the relative impact of the plane strain strength is larger in case the sheet pile can generate a plastic hinge and the impact of corrosion is relatively small. This seems plausible as for low corrosion values the sheet pile will be able to utilize its rotation capacity (it stays in Class 2 – 3 and does not end up in Class 4) and as such more of the extra soil strength can be mobilized.

### 8.3 Recommendations

The following recommendations are made:

- To include, in end of service life assessments of thin walled existing sheet piles structures, a more realistic physical model of the strength of steel sheet piles, the so-called Class 4 (i.e. the area where sheet piles become so thin walled due to corrosion effects, they experience local instability effects). The more realistic physical model should replace the currently in daily practise used conservative approach. Use can be made for example of finite strip analysis, as implemented in the open source software CUFSM [ref. 29]
- To investigate the potential of recently developed reliability analysis methods using surrogate (or response surface) modelling, e.g. [Van den Eijnden et al, 2019], allowing for a significant reduction of calculation times while maintaining a robust analysis.
- To investigate the potential of using other (open-source) FE programs, such as Kratos.Geo [Deltares, 2021], allowing for performing large numbers of calculations at the same time instead of one by one calculation to reduce calculation times;
- To investigate the potential to derive annual reliability taking in account past performance of a degrading structure from a limited set of FE calculations with the developed approach;
- To investigate the potential for reliability updating by incorporating survived loads and other performance or monitoring data;
- Perform calculations at multiple moments of time during the reference period to gain more insight in the transition from a dominant uncertainty in soil parameters to a dominant uncertainty in thickness reduction. These calculations will provide more insight into the moment that thickness inspections are most efficient.
- Investigate the positive influence of soil embedment on bending moment capacity and rotation capacity for thin walled sheet piles in the transition zone from Class 3 to Class 4 and in Class 4. The benefit could be that in class 3/4 the bending moment capacity might be increased and/or (some) additional rotation capacity is available. It is expected that the gain of some “plastic” rotation capacity can have a significant positive effect on the reliability.
- To try and gain more experience with the developed coupling within a pilot project;
- To further investigate how to deal with influence of numerical (in)stability of FE-codes on the performance of the reliability methods.

## 9 References

- [1] CUR 166, Damwandconstructies, 2012.
- [2] CUR 211, Handboek Kademuren, 2013.
- [3] E. Calle. Veiligheid van damwandconstructies, Deltares, 1991.
- [4] T. Schweckendiek. Structural Reliability Applied To Deep Excavations – Coupling Reliability Methods with Finite Elements, MSc Thesis, TU Delft, 2007a.
- [5] H. J. Wolters. Reliability of Quay Walls, MSc Thesis, TU Delft & Gemeentewerken Rotterdam, 2012.
- [6] W. Courage, H. Steenberg, Prob2B variables, expressions and Excel; Installation and getting started, TNO report 2007-D-R0887/A Prob2B, 2007.
- [7] <http://www.openturns.org/>, 2015.
- [8] P. Waarts, A. Vrouwenvelder, Structural Reliability using the finite element method, 2000.
- [9] K. Roscoe, F Diermanse, A. Vrouwenvelder. System reliability with correlated components: Accuracy of the Equivalent Planes method. Structural Safety 57, 53–64. 2015.
- [10] T. Schweckendiek, W. Courage, P van Gelder. Reliability of Sheet Pile Walls and the Influence of Corrosion - Structural Reliability Analysis with Finite Elements. Proceedings of ESREL 2007, Stavanger Norway, 2007b.
- [11] A. Rippi. Structural reliability analysis of a dike with a sheet pile wall – Coupling Reliability methods with Finite Elements, MSc Thesis, TU Delft, 2015.
- [12] H. Larsen, P. Lubking, J. Breedevel. Ontwerp stabiliteitsschermen (type II) in primaire waterkeringen (groene versie), referentie 1205887-000-GEO-0016, Deltares, 2013.
- [13] Richtlijnen Ontwerpen Kunstwerken ROK 1.2. Doc.nr.: RTD 1001:2013, versie 1.2 (status definitief) van Rijkswaterstaat Ministerie van Infrastructuur en Milieu, 2013.
- [14] ENW. Corrosietoets van stalen damwandplanken in de grond, memo aan Leden van ENW Techniek, referentie 1209030-GEO-007, Deltares, 2014.
- [15] Eurocode 3: Ontwerp en berekening van staalconstructies - Deel 5 Palen en damwanden, Nederlands Normalisatie-instituut.
- [16] J. Boero et al. Modélisation de champs stochastiques de corrosion à partir de données: application au secteur portuaire, 1st Congrès Français de Mécanique [article in English, title French], 2009.
- [17] P. Osório et al. Failure Probability of Marine Steel Sheet Pile Structures with Special Consideration of the Corrosion Impact, 2011.
- [18] P. Osório, M. Greger, A.C.W.M. Vrouwenvelder. Corrosion effects on the safety of sheet pile walls in marine environment, 2011.
- [19] CUR 190, Kansen in de civiele techniek – Deel 1: Probabilistisch ontwerpen in theorie, 1997.
- [20] H.M.G.M. Steenberg, B.L. Lassing, A.C.W.M. Vrouwenvelder and P.H. Waarts. Reliability analysis of flood defence systems. HERON, Vol. 49, No. 1, 2004.
- [21] ArcelorMittal 2017, Durability\_3.5.2.145.exe, version July 2017
- [22] Deltares, Natte kunstwerken van de toekomst, Soil-structure interaction – reliability analysis of a retaining wall 2015, v4. Final, February 2016a  
[https://www.nattekunstwerkenvandetoekomst.nl/upload/documents/tinymce/NKvdT\\_gond-constructie-interactie\\_report\\_20160315.pdf](https://www.nattekunstwerkenvandetoekomst.nl/upload/documents/tinymce/NKvdT_gond-constructie-interactie_report_20160315.pdf)
- [23] Deltares, presentatie bijeenkomst Kennis programma Natte Kunstwerken, 2018
- [24] Deltares, manual Probabilistic Toolkit, version May 2016b

- [25] Deltares, Corrosie van damwanden in zoetwater. Deel 1: Literatuurstudie, 2019a.  
[https://www.nattekunstwerkenvandetoekomst.nl/upload/documents/tinymce/KpNK-2019-BKW-02a002-D-v1\\_Corrosie-damwanden-in-zoetwater-Literatuurstudie.pdf](https://www.nattekunstwerkenvandetoekomst.nl/upload/documents/tinymce/KpNK-2019-BKW-02a002-D-v1_Corrosie-damwanden-in-zoetwater-Literatuurstudie.pdf)
- [26] Deltares, Corrosie van damwanden in zoet water. Deel 2: Analyse verzamelde diktemetingen, 2019b  
[https://www.nattekunstwerkenvandetoekomst.nl/upload/documents/tinymce/KpNK-2019-BKW-02a003-D-v1\\_Corrosie-damwanden-in-zoetwater-Analyse-metingen.pdf](https://www.nattekunstwerkenvandetoekomst.nl/upload/documents/tinymce/KpNK-2019-BKW-02a003-D-v1_Corrosie-damwanden-in-zoetwater-Analyse-metingen.pdf)
- [27] Houyoux, C. (2004), Design Method for Steel Structures in Marine Environment Including the Corrosion Behaviour, ESCS, 2004
- [28] Van den Eijnden, A.P., Schweckendiek, T., Hicks, M.A. (2020). Metamodelling for geotechnical reliability analysis with noisy and incomplete models. Draft submitted to Structural Safety (under review), November 2019.
- [29] John Hopkins University, Professor Ben Schafer's thin-walled structures research group, open source software CUFSM - constrained and unconstrained finite strip method, <https://www.ce.jhu.edu/bschafer/cufsm/>
- [30] ArcelorMittal, design note on Class 4 AZ26 Sheet Pile, 2019
- [31] Deltares. (2021). Kratos.Geo – a geomechanical application based on KRATOS, an open source multi-physics finite element platform



## A Background on soil properties

### A.1 Non associatieve soil properties

The values in Table 1 are based on [TUD 2012] with one exception, the dilatancy angle is taken as  $\psi' = \phi' - 30$ .

**Table 1** Non associative grondeigenschappen, layer averages

code	Soil type	$\gamma$	$\gamma_{\text{sat}}$	$c'$	$\phi'$	$\psi'$	$E_{50;\text{ref}}$	$E_{\text{oed};\text{ref}}$	$E_{\text{ur};\text{ref}}$	$R_{\text{int}}$	$m$
[#]	[-]	[kN/m <sup>3</sup> ]	[kN/m <sup>3</sup> ]	[kN/m <sup>2</sup> ]	[°]	[°]	[MN/m <sup>2</sup> ]	[MN/m <sup>2</sup> ]	[MN/m <sup>3</sup> ]	[-]	[-]
1	SM	18,5	20,7	0	38,9	8,9	69,2	69,2	207,7	0,9	0,5
2	CM		17,4	14,8	26,9	-	7,69	5,27	15,38	0,67	1,0
3	SD		21,8	0	41,9	11,9	115,4	115,4	346,2	0,9	0,5

### A.2 Model

#### A.2.1 Drained

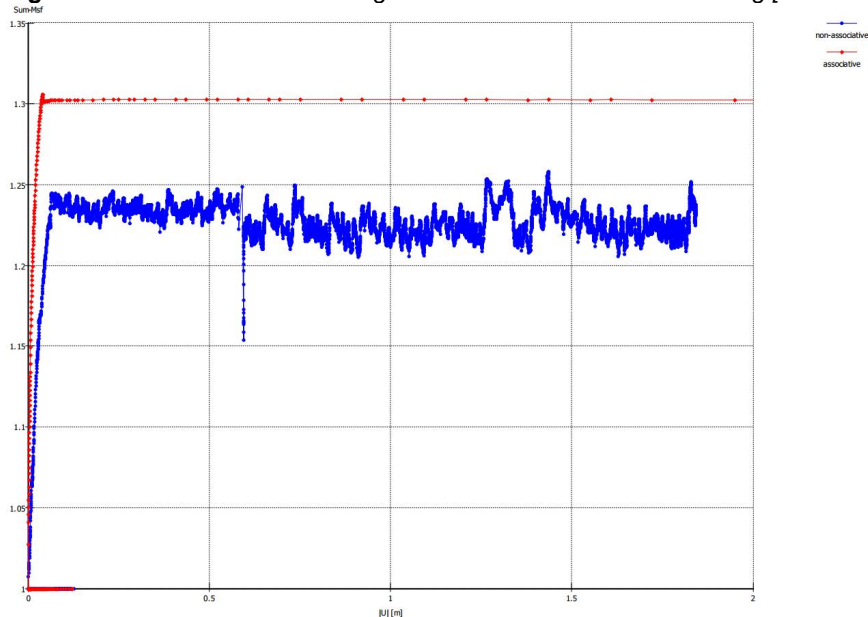
Er is gekozen een voor een gedraineerde analyse. In de praktijk wordt de grondsterkte in EEM analyses meestal met een niet associatieve parameterset beschreven dit impliceert dat voor de dilatantiehoek een waarde ongelijk aan de inwendige wrijvingshoek wordt aangehouden. Deze beschrijving stemt overeen met het fysieke grondgedrag. Als in een EEM-analyses echter situaties met doorgaand bezwijken worden beschouwd, dan schiet de mathematische beschrijving van de huidige constitutieve modellen qua eenduidigheid tekort.

In een gedraineerde analyse moet onderscheid worden gemaakt tussen de piek- en reststerkte van een materiaal. De pieksterkte is de maximale sterkte die bereikt kan worden en de reststerkte is de sterkte die overblijft bij doorgaand vervormen. Er is een verschil tussen deze sterktes als de wrijvingshoek 25° of hoger is. De sterkte bij doorgaand bezwijken, de reststerkte, is lager dan de maximale sterkte. In de eindige elementen simulaties betekent dit dat het materiaal in schuifvlakken zal willen bezwijken. Tegelijkertijd met de schuifvlakvorming neemt de spanning loodrecht op schuifvlak af en komt er energie vrij. Dit mechanisme van schuifvlakvorming met het bijbehorende energieverlies maakt dat deze berekeningen zeer lastig uit te voeren zijn. Dit speelt zich vooral af bij materialen met een hoge wrijvingshoek en een kleine dilatantiehoek. Dit zijn de sterkteparameters die overeenkomen met de kritieke sterkte in het Camclay model en zoals deze meestal toegepast worden in de praktijk

Het verdient daarom aanbeveling om met een associatief model te rekenen. Hiertoe zullen echter de niet associatieve parameters welke overeenkomt met het werkelijke fysische gedrag dien te worden getransformeerd naar een associatieve parameterset met equivalente sterkte, een zogenaamd *equivalent associatieve parameterset*.

Het verdient daarom aanbeveling om met een equivalent associatief model te rekenen.

In figuur 2 wordt typisch voorbeeld gegeven waar binnen een EEM berekening met een niet een associatieve parameterset de fysische werkelijke sterkte niet wordt bereikt en bij gebruikt van een equivalent associatieve parameterset wel. Een equivalent associatieve parameterset is alleen toepasbaar in situaties die niet opsloten zijn dit zijn situaties waar omspanning ten gevolge van dilatantie geen significante rol speelt. De onderhavige damwandconstructie voldoet hieraan.

**Figuur 2** Voorbeeld de ontwikkeling van de MSF in PLAXIS berekening [Deltares 2009]

Gekozen is om te rekenen met het zogenaamde “Best Guess Equivalent model” dat op dit moment standaard voor constructies in waterkeringen wordt toegepast [Deltares 2013]. Hierdoor wordt enerzijds de werkelijke sterkte significant beter benaderd en anderzijds zijn de berekeningen numeriek veel stabielier wat leidt tot significant kortere reketijden.

#### A.2.2 Best Guess Equivalent model

Vervolgens dienen de niet-associatieve rekenwaarden ( $c'$ ,  $\varphi'$ ,  $\psi' \neq \varphi'$ ) naar equivalent associatieve rekenwaarden ( $c_a^*$ ,  $\varphi_a^*$ ,  $\psi_a^* = \varphi_a^*$ ) te worden getransformeerd, gebruik makende van het Best Guess Equivalent model. Hiervoor geldt [Deltares 2013].:

$$\sin \varphi_a^* = \frac{R}{\sin 2\beta - R \cos 2\beta}$$

$$\text{met } \beta = 45^\circ + \frac{\varphi' + 4\psi'}{10}$$

$$R = \frac{\cos \psi' \sin \varphi'}{1 - \sin \varphi' \sin \psi'} \quad (1)$$

$$\psi_a^* = \varphi_a^*$$

$$c_a^* \cot \varphi_a^* = c' \cot \varphi'$$

Op basis van (1) zijn voor de niet associatieve grondeigenschappen in tabel 2 associatieve grondeigenschappen bepaald en deze zijn gegeven in tabel 3. De waarden van de grondeigenschappen in tabel 2 dienen in de PLAXIS analyses te worden toegepast.

**Table 2** Associative soil parameters, average values of each layer, for Hardening soil

code	Soil type	$\gamma$	$\gamma_{\text{sat}}$	$c_a^*$	$\varphi_a^*$	$\psi_a^*$	$E_{50;\text{ref}}$	$E_{\text{oed};\text{ref}}$	$E_{\text{ur};\text{ref}}$	$R_{\text{int}}$	$m$
[#]	[-]	[kN/m <sup>3</sup> ]	[kN/m <sup>3</sup> ]	[kN/m <sup>2</sup> ]	[°]	[°]	[MN/m <sup>2</sup> ]	[MN/m <sup>2</sup> ]	[MN/m <sup>3</sup> ]	[-]	[-]
1	SM	18,5	20,7	(1,0 <sup>1</sup> )	37,0	37,0	69,2	69,2	207,7	0,9	0,5
2	CM		17,4	14,1	25,8	25,8	7,69	5,27	15,38	0,67	1,0
3	SD		21,8	(1,0 <sup>1</sup> )	39,8	39,8	115,4	115,4	346,2	0,9	0,5

<sup>1</sup>)Ten behoeve van PLAXIS berekeningen is 1 kPa cohesie toegevoegd

### A.2.3 Materiaal model

Voor de eerste berekeningen om het rekenschema uit te proberen kan het simpele Mohr-Coulomb model worden gehanteerd met als stijfheden: matig gepakt zand  $E = 50 \text{ MN/m}^2$ , matige vaste klei  $E=6,5 \text{ MN/m}^2$  en dichtgepakt zand  $E=125 \text{ MN/m}^2$ .

Geadviseerd wordt om te trachten ervaring op te doen met gebruik van het Hardening Soil model.

### Referenties

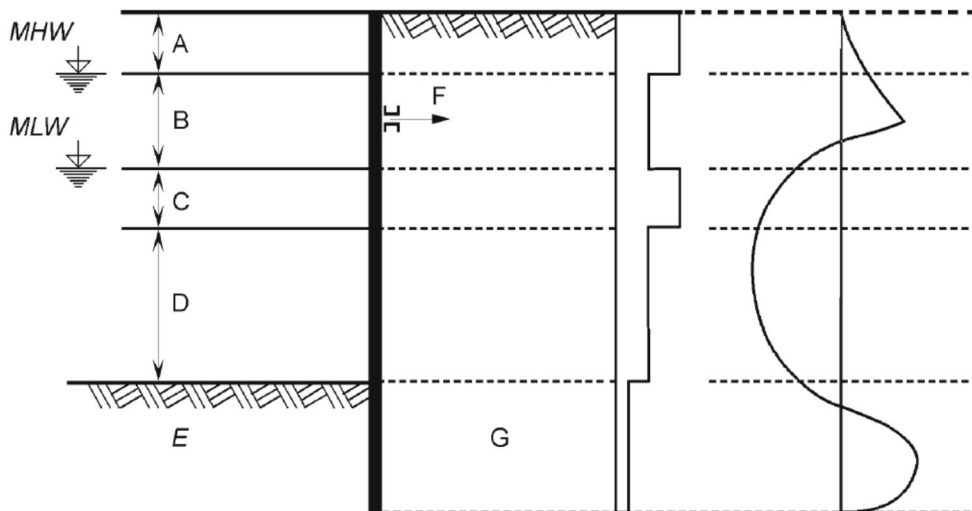
- [NEN-EN 1993-5 ] Eurocode 3: Ontwerp en berekening van staalconstructies - Deel 5 Palen en damwanden, Nederlands Normalisatie-instituut
- [NEN 9997-1] Geotechnisch ontwerp van constructies Deel 1: Algemene regels, Nederlands Normalisatie-instituut
- [TUD 2012] Reliability of Quay Walls, MSc Thesis, H.J. Wolters, TU Delft & Gemeentewerken Rotterdam, 2012
- [RWS 2013] Richtlijnen Ontwerpen Kunstwerken ROK 1.2 Doc. nr. : RTD 1001:2013 versie 1.2 status definitief van Rijkswaterstaat Ministerie van Infrastructuur en Milieu, 2013
- [Deltares 2009] SBW Analyse macrostabiliteit van dijken met Eindige Elementen Modellen Achtergronden bij Activiteit EEM 04.a: Opstellen stappenplan 1001463-013-GEO-0001, Deltares, 23-09-2009
- [Deltares 2013] Ontwerp stabiliteitsschermen (type II) in primaire waterkeringen (groene versie) Ontwerprichtlijn voor WSRL, ref. 1205887-000-GEO-0016, Deltares 03-03-2013
- [Deltares 2014] Corrosietoeslag van stalen damwandplanken in de grond, memo aan Leden van ENW Techniek, referentie 1209030-GEO-007, Deltares, 9-4-2014

## B Corrosion

This appendix presents an overview of recommended corrosion zones according to [NEN-EN 1993-5] and values for thickness-reduction on the side without soil recommended by [RWS, 2013] and on the side of the soil as proposed by [Deltares, 2014].

### B.1 Definition of corrosion zones [NEN-EN 1993-5]

EN 1993-5: 2007 (E)



a) Vertical zoning of sea water aggressivity

b) Corrosion rate distribution at side exposed to sea water

c) Typical bending moment distribution

A	Zone of high attack (splash zone);	B	Intertidal zone;
C	Zone of high attack (Low water zone);	D	Permanent immersion zone;
E	Buried zone (Water side);	F	Anchor;
G	Buried zone (Soil side)		
MHW	Mean high water;	MLW	Mean low water

## B.2 Thickness reduction due to corrosion [RWS 2013]

### 7.14 Deel 5: Palen en damwanden

Aanvullingen op NEN-EN 1993-5 + NB.

4.4 (2)	Eis
---------	-----

NEN-EN 1993-5, Tabel 4-2 moet voor eroderende omstandigheden veroorzaakt door afspoeling, zoals bij sluizen, worden vervangen door tabel 7-3.

**Tabel 7-3: Dikteverlies door corrosie bij eroderende omstandigheden veroorzaakt door afspoeling, zoals bij sluizen (zones volgens NEN-EN 1993-5, fig. 4-1)**

Ontwerplevensduur [jaar]	5	25	50	75	100
<b>expositie</b>					
zoet water, zone tussen laagste en hoogste schutpeil (zone B)	0,1	0,5	1,0	1,5	2,0
zoet water, zone boven hoogste schutpeil en zone onder laagste schutpeil (zones A en C)	0,25	1,25	2,5	3,75	5,0
zout water, zone tussen laagste en hoogste schutpeil (zone B)	0,25	1,25	2,5	3,75	5,0
zout water, zone boven hoogste schutpeil en zone onder laagste schutpeil (zones A en C)	0,75	3,75	7,5	11,25	15,0

Bij sluizen loopt zone C tot op de bodem; zone D is daar niet van toepassing.

#### Toelichting:

Aangezien in sluizen een door afspoeling eroderende omgeving aanwezig is, is de corrosiesnelheid in tabel 7-3 constant in de tijd. De waarden komen overeen met de 'Handreiking rekenmethodieken NIC, groene versie', de interne bureaurichtlijn die tot 2006 bij de afdeling Constructie Waterbouw van de Bouwdienst Rijkswaterstaat werd gehanteerd.

## B.3 Thickness reduction due to corrosion of soil embedded steel sheet pile sections [Deltares 2014]

		Corrosietoeslag (dubbelzijdig) (mm)	
		50 jaar	100 jaar
1	Ongeroerde, schone grond en permanent beneden de grondwaterspiegel	1,2	2,4
2	Geroerde grond, of ligging in zone met fluctuatie van grondwaterspiegel, of ligging boven de grondwaterspiegel	2,4	4,4

<sup>1</sup> In de uitdrukking 'ongeroerde grond' betekent ongeroerd dat de grond niet op enige manier is omgewoeld, dus 'vast' is. Het tegengestelde van ongeroerd is geroerd of los (<http://www.encyclo.nl/begrip/ongeroerd>). Voor het bepalen van de diepte kan gebruik worden gemaakt van de ontgravingsdiepte samen met de aanvullingshoogte.

## C The Probabilistic Toolkit

### C.1 Introduction

The Probabilistic Toolkit (PTK) can perform probabilistic analysis and/or automated sensitivity analysis on an arbitrary internal or external model. The user can enter his/her model within the model (internal) or link to an existing model (external). For more information on the PTK the user is referred to the manual [Deltares, 2016b].

### C.2 Theoretical background of reliability methods

A basic introduction to reliability analysis, such as follows, can be found for example in [CUR, 1997], [Steenbergen, 2004].

In reliability analysis limit state functions, here denoted by  $Z$ , are defined such that:

$$\begin{cases} Z < 0 \text{ corresponds to failure and} \\ Z \geq 0 \text{ corresponds to no failure} \end{cases} \quad (38)$$

And  $Z$  generally takes the form of:

$$Z = R - S \quad (39)$$

where  $R$  stands for resistance (capacity) and  $S$  for solicitation (load). Consequently,  $Z < 0$  corresponds to the load being larger than the capacity and hence to a failure state.  $R$  and  $S$  will be either stochastic parameters themselves or functions of a number of stochastic parameters  $X$ :

$$Z = R(X) - S(X) \quad (40)$$

In structural reliability, one then wants to be reassured that a design - given the stochastic nature of e.g. the materials, handling, operation and loads - has an acceptable low level of failure probability. Hence the need for methods to calculate these probabilities. The probability of failure follows from:

$$P_f = \int_{Z < 0} f(x) dx \quad (41)$$

Here  $f(x)$  is the joint probability distribution function of the set of stochastic parameters  $X$ .

In words, eq.(4) is the total probability as obtained by integrating this probability density function over that part of its domain that corresponds with  $Z < 0$ .

Instead of the probability of failure one usually refers to the reliability index  $\beta$ . It is related to the probability of failure by:

$$\beta = \Phi^{-1}(1 - P_f) \quad (42)$$

in which  $\Phi$  is the standard normal distribution. The reliability index  $\beta$  is easier and more intuitive to use and is directly related to the safety level, i.e. the safety/reliability increases as the index increases.

For solving the integral, a number of methods are available such as plain numerical integration, Crude Monte Carlo, Importance Sampling (IS) and Directional Sampling (DS), First Order

Reliability Method (FORM), Second Order Reliability Method (SORM, not in PTK available) and response surface methods like DARS.

The Monte Carlo method consists of randomly sampling the  $X$  values from their distributions and calculating the relative number of simulations for which  $Z < 0$ :

$$P_f = N_f/N \quad (43)$$

where  $N$  is the total number of calculations and  $N_f$  the number of failed states found.

In DS the basic variables are transferred into polar coordinates ( $\lambda, \underline{\vartheta}$ ) The unit vector  $\underline{\vartheta}$  defines the direction and the scalar quantity  $\lambda$  defines the length of the vector in standard normal  $u$ -space. For each uniformly sampled direction  $\underline{\vartheta}_i$  the value of  $\lambda_i$  is determined for which the limit state function equals zero:

$$Z_i = Z(\lambda_i, \underline{\vartheta}_i) = 0 \quad (44)$$

An estimate of the probability of failure  $P_f$  is obtained by performing  $N$  directional Monte Carlo simulations of the  $\underline{\vartheta}$  vector. Every direction results in a sample value  $P_{fi}$ :

$$P_{fi} = P \left[ Z(\lambda_i, \underline{\vartheta}_i) < 0 \right] = 1 - \chi_n^2(\lambda_i^2) \quad (45)$$

in which  $\chi^2$  is the chi-squared cumulative distribution function and  $n$  the number of random variables.

The estimate for the probability of failure is calculated as the weighted mean value of the sample values  $\chi_n^2$ :

$$P_f = \frac{1}{N} \sum_{i=1}^N \chi_{n_{fi}}^2 \quad (46)$$

FORM is an iterative method that makes use of stepwise linearization of the limit state function. FORM is a fast method, especially when compared to e.g. Monte Carlo and when small probabilities need to be calculated. A drawback, however, is that depending on the nature of the function, convergence might not always be achieved or a local minimum (instead of a global minimum) may be found. In case the failure domain is curved the resulting failure probability is under or overestimated, which can be mitigated by using SORM, a second order counterpart of FORM. The benefits of FORM (speed) thus always have to be weighed against the knowledge one has with respect to the nature and behaviour of the target function.

A more dedicated method is DARS [Waarts et al, 2000] which is a combination of DS with a Response Surface<sup>11</sup> that is created and updated during sampling. The response surface enables efficiency in calculation time as, under appropriate conditions, intermediate samples can be taken from this surface instead of from expensive model calculations.

FORM and SORM are not suited to directly investigate multiple limit states or mechanisms at once, i.e. doing a system analysis. A work around would be to quantify the failure contribution of each mechanism separately with FORM or SORM when possible, taking advantage of the calculation efficiency of these methods and afterwards combine the results in a system analyses of series and/or parallel systems/mechanisms according to [Roscoe et al, 2015].

<sup>11</sup> In statistics, response surface methodology (RSM) explores the relationships between several explanatory variables and one or more response variables. The main idea of RSM is to use a sequence of designed experiments to obtain an optimal response.

FORM is an approximate method, while ordinary Monte Carlo or DS are pure probabilistic methods with higher accuracy. The Monte Carlo is a very straightforward method, while FORM has limitations when complex  $Z=0$  are necessary and/or it is not possible to approximate with Normal distributions.

Important by-product of the probabilistic methods is that next to the probability of failure also the influence coefficients ( $\alpha$  or  $\alpha^2$ ) and design point are computed. The design point is defined as the point with the highest probability density in the failing domain. With the influence coefficients, one can assess the influence of each random variable and choose the necessary number of basic variables of a problem (random variables can be reduced without compromising the accuracy of the reliability calculation).

#### Direction Sampling used in this report

In this report it was decided to use DS as it seems to gather important advantages with respect to other methods:

- Most importantly the method is very robust while analysing highly non-linear computation models with complex z-functions. This in contrast to FORM – like methods.
- It allows for a stop-continue option in case a crash occurs (which may be expected to happen with long calculation times)
- it is a fully probabilistic method (taking into account all characteristics of the random variables);
- the method is able to return the influence coefficients which are an important part of the result and can be used to gain insight in the results;
- The computational time is very optimised in comparison with (crude) Monte Carlo simulations. However still calculation times may be in the order of weeks (depending on the failure probability of problem at hand). Note: alternatives using response surface techniques (like ref.[28]) are expected to become available on relative short notice in the PTK allowing for a significant reduction of calculation times.

### C.3 Coupling the Probabilistic Toolkit and PLAXIS

In this paragraph some more detailed background information is presented belonging to chapter 2 “Coupling the Probabilistic Toolkit and PLAXIS”.

In more detailed steps, the reliability analysis is carried out the following way:

1. After pressing start in the PTK a first simulation is made (based on the input and correlation of the stochastic variables)
2. PTK adjusts a prepared \*.txt file which already contains relevant PLAXIS input commands
3. The python script reads the \*.txt file and executes the commands such that the first PLAXIS simulation is performed
4. After the calculation the python scripts executes the relevant output commands to retrieve the relevant results and send the results to the PTK
5. The PTK computes the limit state functions
6. PTK prepares the next simulation (based on the results of 6.)
7. Carry out steps 4 to 7 until the, user specified, convergence criteria of the selected reliability integration method is reached. The PTK then presents the relevant results such as the reliability (Beta value) and influence factors.



It is essential that the PLAXIS simulation converges to the desirable criteria, and under the physical boundary conditions that have been determined. Likewise, the convergence criteria of the reliability methods shall be manipulated to enable the optimization algorithms to converge efficiently.

Related to Table 2.1 is the table below which gives a more detailed overview of the created special commands within this research project.

Special command	Does what?
MaxAngular Distortion Sheetpile	Derives from the PLAXIS deformations output of the plates per specified zone/section the maximum (absolute) rotation difference between node pairs. For this the special command organizes the nodes, removes double nodes and calculates the rotation differences between consecutive node pairs.
MaxBendingMoment	Derives from the PLAXIS forces output of the plates per specified zone/section the maximum absolute bending moment
Corrosion Reduction SheetPile	Determines based on the (stochastic) corrosion values as provided by the PTK the initial input properties for a sheet pile section and transforms these into the required PLAXIS input (EA, EI, w, Mp, Np). These are the properties required for the elasto-plastic plate elements with plastic hinge option. Note that these initial properties are without softening.
CorrosionReductionAnchor	Determines based on the (stochastic) corrosion values as provided by the PTK the initial input properties for the anchor rod and transforms these into the required PLAXIS input (EA).
SofteningModule	Extracts from PLAXIS Output per section $M_{max;i}$ and $\Phi_{i;max;i}$ . If section is Class 1/2/3 it makes a check on rotation capacity, if section is Class 4 it makes a check on bending moment capacity. This command can lower the $M_{max;i}$ and at the same time increase $\Phi_{i;CD}$ , and determine new PLAXIS Input. Also see appendix E.4 for more information on this module.
CorrosionReductionSheetPileElastic	Command works the same as "Corrosion Reduction SheetPile" however it always sends $M_p = 1E12$ to PLAXIS to make sure the plate element behaves elastic (no plastic hinge)
OutputValues	Extracts from PLAXIS Output per section $M_{max;i}$ . Command can be used in case no softening is applied.

Table C.1 Explanation of special commands developed for the case study of a retaining wall

Hereafter in more detail the challenges and limitations to consider are described.

### Challenges to consider

A number of challenges were found during the research:

- What if PLAXIS fails in a phase before the last phase? Current implementation: a check is included in the generic python coupling files to see if the last phase is reached. If the last phase is not reached an exception is raised and the calculation is stopped so the USER notices this behaviour. Note: during this research the case study was set up in such a way the last phase was reached in all calculation runs.
- What if the last phase fails (i.e. does not reach  $SUMMStage = 1$ )? In the current implementation the last phase is then recalculated with arc length control switched off.

This is done to doublecheck it is not a numerical issue. If the phase does still not reach  $SUMstage = 1$  then results are accepted and assumed to be a soil failure and used to calculate the LSF.

- It was decided to use the numerical integration method Directional Sampling. Although this is a robust method, it takes long calculation times. Typical calculation times found with the case study are in the order of weeks. Ideally calculation times can be reduced to order of days to make the approach more practical.

### Limitations

There are a number of limitations with the current implementation.

Related to generic python coupling files

- Some installation paths are hardcoded in the python files, they can however easily be generalised
- For the python file "Distortion":
  - The calculated rotation between node pairs of the plate elements representing the sheet piles is the total rotation (i.e. elastic + plastic), which is a conservative assumption.
  - The file makes use of a linearization for the deformations in between the FE nodes. The rotations outputted by PLAXIS per node are based on the more advanced beam theory used for the plate elements. Hence differences occur in results. Ideally more sensitivity analysis is performed to gain more insight in the possible differences and the impact on results. For now it is believed that results are acceptable as long as the mesh size (and thus the node distance) is relatively small.

Related to LSF and SpecialCommands

- Effects of normal force and shear force are not included for sheet piles;
- The mechanical properties, the effect of corrosion and the effect of softening are currently only implemented for an AZ26 sheet pile profile
- For the anchor a fixed yield stress of 355 N/mm<sup>2</sup> is used
- For the anchor wall a fixed yield stress of 240 N/mm<sup>2</sup> is used.
- The current LSF for the anchorwall is only intended for Class 1, 2 or 3 behaviour and as such not suitable for very large corrosion values on the anchor wall as it would then fall into Class 4 and require a different LSF. Within this case study it was double checked that corrosion values were so low that only Class 1, 2 or 3 behaviour was relevant.

Related to PLAXIS

- The original ambition was to carry out calculations with the 'Hardening soil' soil model. However, due to some unknown randomness in the calculation method, for the same input parameters the output results (such as deformations and stresses) differ up to 5%. While for a deterministic or semi-probabilistic (partial factor based) calculation such differences can be negligible, in a probabilistic calculation, where failure 'directions' are to be identified, these inherent 'randomness' in the output of the FEM calculation jeopardise the results. As such, PLAXIS 'Hardening soil' soil modelling was not used for the main calculations. Note: during the project it became clear that the randomness of

the HS model can be diverted by forcing the calculation on a single thread. To gain experience some runs were performed with the HS model, see paragraph 6.4.1.

- It became clear during this project while using the PLAXIS version 2018.00 that a PLAXIS exception occurred in a random manner. It was confirmed by PLAXIS support that this indeed was a known issue in the software. Result of this known issue is that an exception window is opened in the software which has to be closed manually. Since this is not possible during an automated loop the calculation hangs until the user restarts the calculation. PLAXIS supports indicated that also here a work around would be to force the calculation on a single thread. For this a so called “toggles” folder needs to be created in the PLAXIS installation folder and a file named: `TASKS_FORCE_SINGLE_THREAD` should be placed in this toggles folder. As a result the calculation kernel will only use a single calculation thread. This work around proved to work ok during this research.

#### C.4 Experiences using Directional sampling in the PTK

When making use of the DS method in the PTK it is good to be aware of the different calculation options. In this paragraph the gathered experiences during this project have been reported with these calculation options.

Method	
Method	Directional sampling
Random sequence type	Repeatable random
Seed	0
Design point determination	Center of gravity
Realizations	
Min directions [#]	2
Max directions [#]	5000
Realizations calc together [#]	1
Direction	
Max u in direction [u]	6
Step size [u]	1
Precision u in direction [u]	0.1
Precision limit state value [x]	0.1
Limit state behaviour	Varying
Convergence	
Var coefficient failure [-]	0.1

Figure C.1 Calculation options with method Directional sampling

It is good to be aware of the following terms used:

- Direction = when using the method Directional sampling the program randomly selects a vector in the variables [u] space. Along this vector it searches for the point where the LSF equals zero ( $z = 0$ ), i.e. the boundary between non-failure and failure.
- x-space = the stochastic variables are defined by the user in the physical “x-space” according to a certain reliability distribution with a mean and standard deviation. The PTK automatically transfers the stochastic variables into the so-called “u-space”.
- u-space = In u-space all variables are transformed into standard normal distribution with mean = 0, standard deviation = 1. This mathematical transformation simplifies the reliability analysis. In u-space the origin (i.e. Beta = 0, Pf = 0.5) is formed by the point where all the variables are equal to the 50% quantile value.
- Design point = the point in u-space which is the closest to the origin and as such has the highest failure probability density and thus the largest contribution to the calculated probability of failure

The calculation options shown in Figure C.1 are further explained hereafter:

### Method

Here the user can select the desired reliability analysis method: FORM, DS, etc.

### Random sequence type

- Random = directions are chosen in a non-repeatable manner
- Repeatable random = directions are chosen in a repeatable manner (when adding or removing stochastic variables the repeatable manner however is changed)
- Repeatable random per variable name = directions are chosen in a repeatable manner per variable

### Seed

a collection of predefined but random set of numbers. When the seed is not changed, exactly the same samples are generated and thus results are reproducible.

### Design point determination: nearest to mean / center of gravity

With the default option “nearest to mean” the program takes the direction with the largest contribution to the probability of failure as decisive for the influence factors. This approach is an approximation of the influence factors.

More accurate approximation of the influence factors can be made by use the “centre of gravity” option. In this case the program uses all samples in the failing domain and takes the weighted mean.

Note: with the desired accuracy used during this study the influence factors found while using the DS method were considered a first indication. The accuracy of the influence factors is dependent on the amount of directions calculated (and thus how close we come to the real design point).

### Limit state behavior: varying or monotone

Varying = the PTK will always continue to search up to the specified “max u in direction”

Monotone = the PTK will stop searching in a direction if the value of the limit state function is increasing instead of decreasing.

With the current implementation of the softening module it may happen that there is a strong non-linear and non-monotonous behavior around  $z = 0$ . As such the option “varying” should be used instead of “monotone” or else it could happen that the search in this direction stops too soon due to increasing  $z$ -function where-as in reality there is still some  $z < 0$  space behind it;

### Parallel chunk size

The program allows for running parallel calculation using multiple cores. At this moment this is not recommended for PLAXIS calculations.

### Min. directions [-]

The minimum number of directions to be searched by the program. For a more complex model this number will not be so relevant.

### Max. directions [-]

The maximum number of directions to be searched by the program. For a more complex model this number might be used to force the program to stop before the convergence criteria are reached.

### Maximum [u] in direction

The maximum length of the vector to be explored in u-space. As a rule of thumb: this value should be chosen at least a value of 2 larger than the expected/calculated Beta value.

### Step size

The PTK allows for specifying the step size used per direction. When the step size is too big, variations and non-monotonous behavior within the step are overlooked. Default step size is 1. A number of runs have been tried using a larger step size. It is concluded that for a model with a strongly non-linear behavior around  $z = 0$  this may lead to inaccurate results since the PTK is using a linear interpolation between the point with  $z > 0$  and the point with  $z < 0$ . Recommended is to use the default step size when using softening.

Two examples are shown:

- run B11, direction 693 with step size of 1
- run A11, direction 2287 with step size of 3

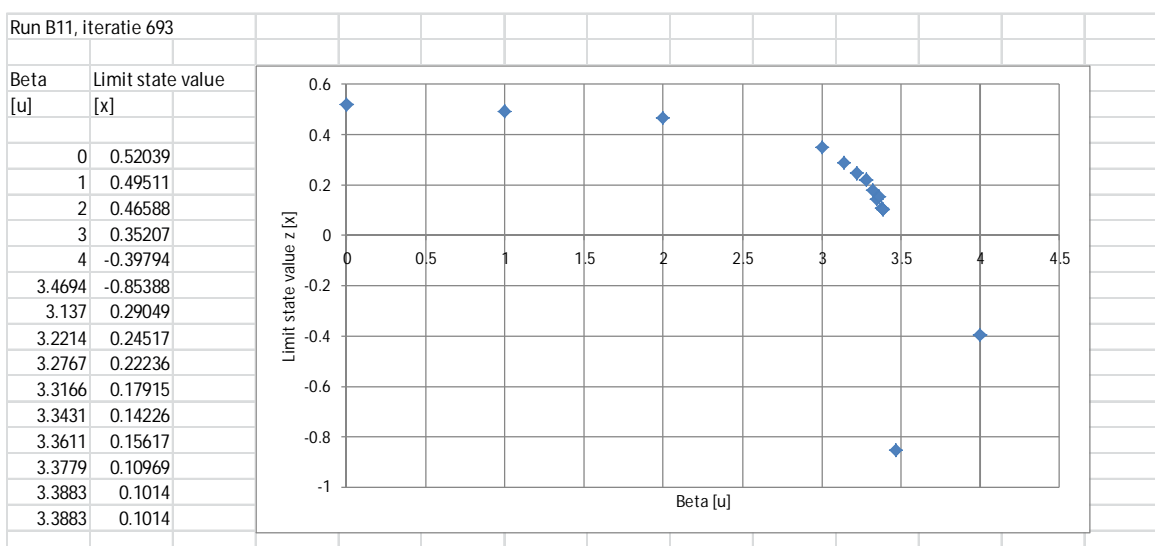


Figure C.2 Example step size of 1. On the left side the numerical values from the PTK, on the right side the graphical representation of these numerical values

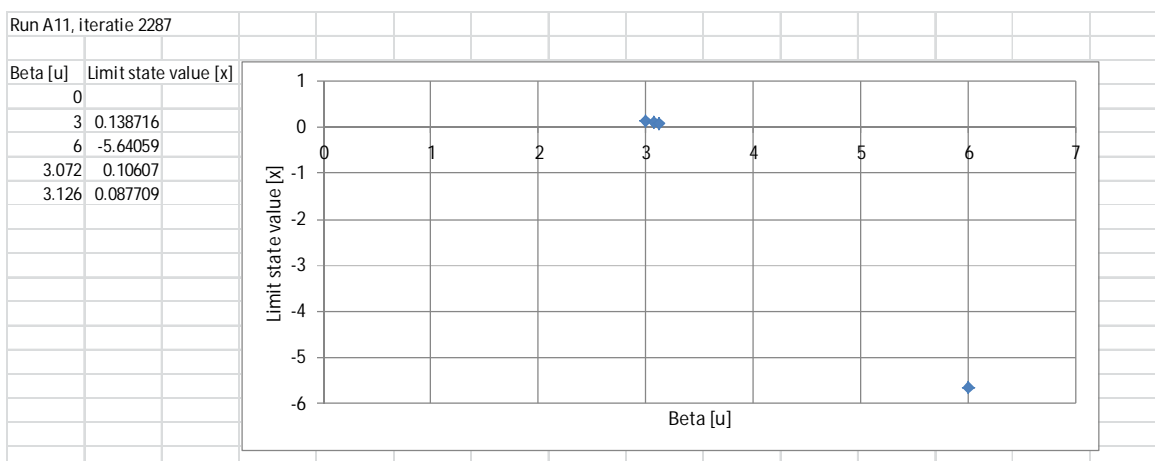


Figure C.3 Example step size of 3. On the left side the numerical values from the PTK, on the right side the graphical representation of these numerical values

**Example of strong non-linear behavior around  $z = 0$**

In Figure C.4 an example has been shown of the strong non-linear convergence around  $z = 0$  in the case of using softening. For a Beta [u] = 4 the program calculates a limit state value close to zero (even within the specified tolerance). However no failure is found. This is the results of the fact that the PTK first needs to cross the  $z\_phi = 0$  line (and thus a negative  $z$  value calculated) in order to classify something as failure.

Or in other words the way the softening module has been implemented (in combination with the behavior of the PTK) it will make sure that first all (remaining) strength/rotation capacity is mobilized ( $Rho\_min = 0.85$ ). In the PLX file we make use of elasto-plastic plate elements for which the maximum capacity  $Mpl\_hinge$  is specified. PLX will make sure that the bending moments are limited in the plastic hinge and forces are redistributed inside the structure. Within the python module there is a check on rotation capacity  $phi\_max < phi\_CD$ . As long as this condition is not satisfied the python module will try to soften even further and see if equilibrium of rotations can be found. In case this criterium is satisfied the LSF on rotation capacity  $z\_phi$  is by definition  $> 0$ . In case this criterium can no longer be satisfied then by definition  $Rho$  has reached the minimum value of 0.85 for at least one of the sheet pile sections and  $z\_phi$  is beneath 0.

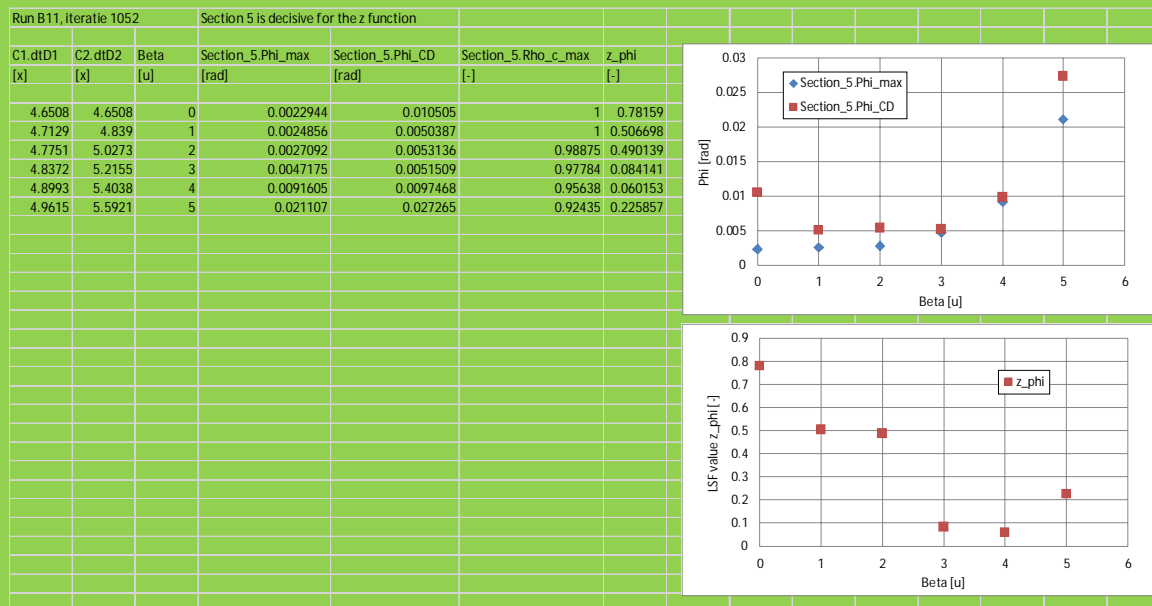


Figure C.4 Example of the non-linear behavior of implemented SofteningModule

**Diff u per direction [u] / precision limit state value [x]**

The difference allowed in u-space / x-space for a certain direction between the calculated value and the LSF = 0 such that the programs considers the result as sufficiently converged. In a trial and error way it was found that a value of 0.1 seems to give reasonable results for this project.

**Var coefficient failure [-]**

Based on the results over all directions the program determines a probability of failure (and the corresponding Beta value) and the variation coefficient in the physical x-space. The variation coefficient determined by the PTK relates to the probability of failure  $P_f$  and **NOT** the Beta value. For this case study a variation coefficient of 0.1 seemed sufficiently accurate.

As an example, a coefficient of variation of 0.1 belonging to a Beta value of 1.9 gives:

- $\text{Beta} = 1.90 \Rightarrow \text{Pf} = 2.87\text{E-}2$
- $\text{Pf plus one st.dev.} = 2.87\text{E-}2 + 0.1 * 2.87\text{E-}2 = 3.16\text{E-}2 \Rightarrow \text{Beta} = 1.86$
- $\text{Pf minus one st.dev.} = 2.87\text{E-}2 - 0.1 * 2.87\text{E-}2 = 2.58\text{E-}2 \Rightarrow \text{Beta} = 1.95$

As an example, a coefficient of variation of 0.3 belonging to a Beta value of 1.9 gives:

- $\text{Beta} = 1.90 \Rightarrow \text{Pf} = 2.87\text{E-}2$
- $\text{Pf plus one st.dev.} = 2.87\text{E-}2 + 0.3 * 2.87\text{E-}2 = 3.73\text{E-}2 \Rightarrow \text{Beta} = 1.78$
- $\text{Pf minus one st.dev.} = 2.87\text{E-}2 - 0.3 * 2.87\text{E-}2 = 2.01\text{E-}2 \Rightarrow \text{Beta} = 2.05$

## D PLAXIS model

### D.1 PLAXIS base model

The following construction phases are used

1.  $K_0$ -procedure for the generation of the initial stresses under horizontal groundwater level at NAP -1 m and with surface level of the soil at NAP +5 m;
2. Excavation of the soil to NAP +2 m and set up in ground water level to NAP +1 m, head is NAP 0 m in deep sand and interpolation of pore pressures over layer KM;
3. Installation (activation) of the sheet pile wall, anchor and anchor wall;
4. Fill on the right side (anchor side) of the sheet pile to NAP +5 m;
5. Excavation (complete) on the left side of the sheet pile;
6. Lower the water level (apply expected water level conditions) on the left side of the sheet pile and application of the (expected) surface load on the right side of the sheet pile;

A screenshot of the relevant phases has been shown below

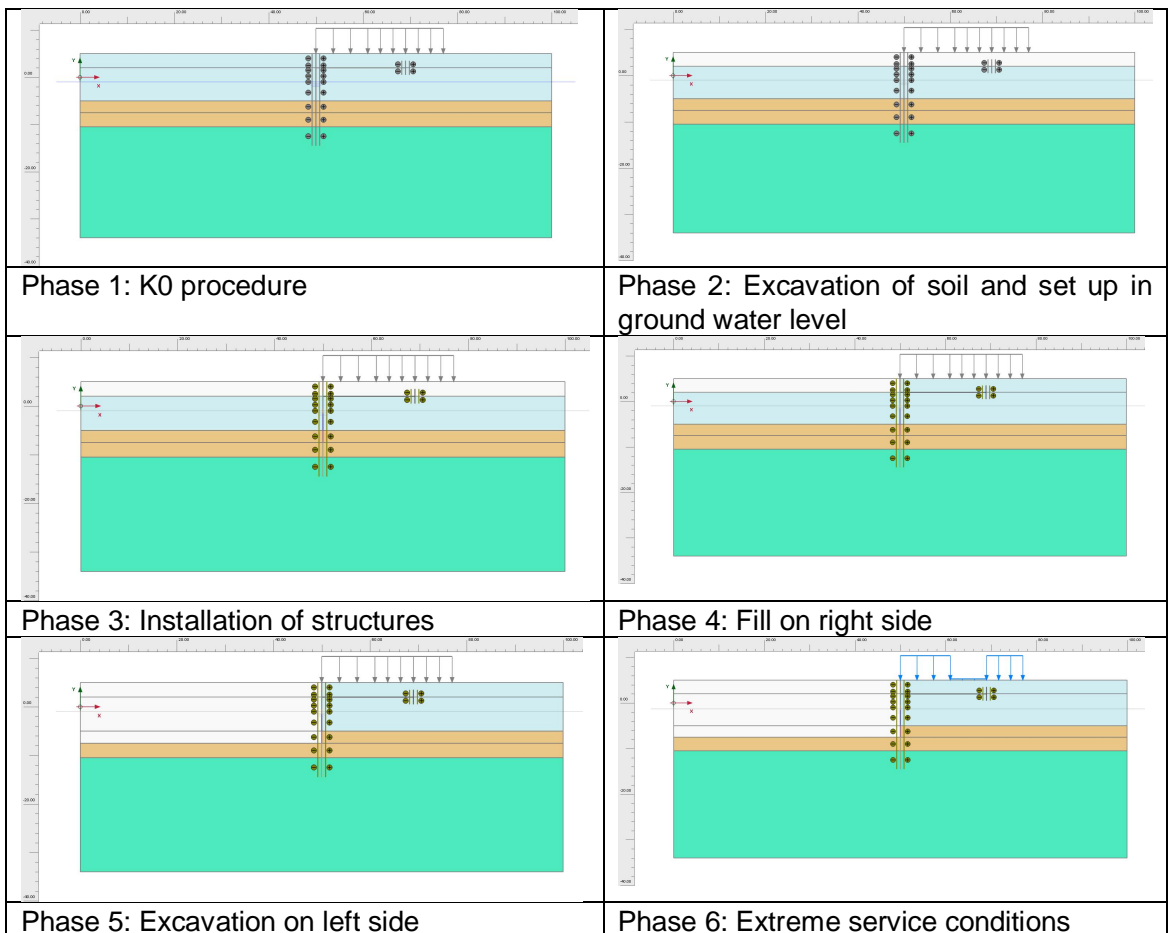


Figure D.1 Screenshots of relevant phases



ID	Calculation t...	Loading type...	Pore pressur...	Time interval	Estimated en...	Ignore undr....	Reset displa...	Updated me...	Max.steps (D)
Initial phase [InitialPhase]				0.000 day	0.000 day	<input checked="" type="checkbox"/>	<input type="checkbox"/>	<input type="checkbox"/>	250
<b>Ontgraven en water [Phase_2]</b>				<b>0.000 day</b>	<b>0.000 day</b>	<input type="checkbox"/>	<input type="checkbox"/>	<input type="checkbox"/>	<b>1000</b>
Plaatsen constructies [Phase_3]				0.000 day	0.000 day	<input type="checkbox"/>	<input checked="" type="checkbox"/>	<input type="checkbox"/>	1000
Aanvullen tot +5m rechts [Phase_4]				0.000 day	0.000 day	<input type="checkbox"/>	<input type="checkbox"/>	<input type="checkbox"/>	1000
ontgraven [Phase_5]				0.000 day	0.000 day	<input type="checkbox"/>	<input type="checkbox"/>	<input type="checkbox"/>	1000
bovenbelasting + verlagen ws (arc ON) [Phase_6]				0.000 day	0.000 day	<input type="checkbox"/>	<input type="checkbox"/>	<input type="checkbox"/>	1000

Figure D.2 Screenshot of calculation settings used

Note: within the PLAXIS file all these construction phases are considered/ added in order to model the stresses in the soil, and the structures, given a certain set of properties/parameters. Also, if considered, these phases are used to model the ground water. Even though the carried out reliability analysis concerns the assessment of an existing structure, the current/existing soil stresses, at the time of the assessment, are necessary to perform the analysis, as they are ‘built’ during the construction phase. This is especially true when soil parameters are being considered as random, where for example a change in soil unit weight will change the soil stresses.

Note: during preparation of the PLAXIS file it was noticed that if phase 6 was split in first lowering the water level (phase 6) and then applying the surface load in a next phase (phase 7) it could happen that failure would occur in the fore last phase 6. This would complicate the python code as it should be able to handle failure in both phase 6 and 7. It was chosen for this study to combine the loads in one phase. It was checked that combining the loads in one phase would generate the same results as two separate phases. Furthermore it was doublechecked that failure during phases prior to the last was highly unlikely. As a backstop a break was included in the python code that would stop the calculation loop in case the PLAXIS calculation would fail/stop in a phase before last.

## D.2 InputCommand file (i.e. change file)

The PLAXIS base model has been described in the previous paragraph. Now during the reliability analyses changes are to be made to (the stochastic variables in) this base model.

For this a so called InputCommand file has to be created by the user. This file consists of basic PLAXIS commands (as can be found in the PLAXIS manuals) to change the Input or to extract output. Additionally so called special commands (SC) can be created. These SC allow for more complicated tasks to be completed (i.e. tasks that cannot be performed using the default PLAXIS commands). For example: to generate the Input properties for a plate element (EA, EI, Mpl\_hinge) based on the amount of corrosion and the yield stress.

An example of an InputCommand file used in this study has been shown in figure below.

```

keywords
#input
_gotostructures
sps ZM "gammaunsat" %ZM.gammaunsat=18.5% "gammamat" %ZM.gammamat=18.5%
sps ZM "phi" %ZM.phi=30.0% "psi" %ZM.psi=30.0%
sps ZM "Eref" %ZM.Eref=5000%
sps KM "phi" %KM.phi=30.0% "psi" %KM.psi=30.0%
sps KM "Eref" %KM.Eref=5000%
sps KM "cref" %KM.cref=5%
sps ZD "phi" %ZD.phi=37.0% "psi" %ZD.psi=37.0%
_set Point_21.y %Bottom.ylevel=-7.5%
_set Point_8.y %Bottom.ylevel=-7.5%
_set Point_24.y %Bottom.ylevel=-7.5%
_gotomesh
_mesh 0.06
_gotostages
_movepoint UserWaterLevel_2.Points[0] -5 -%WL.waterlevel=1.3%
_movepoint UserWaterLevel_2.Points[1] 105 -%WL.waterlevel=1.3%
_set LineLoad_1_1.qy_start Phase_6 -%LL1_1.QYStart=40%
_set LineLoad_2_1.qy_start Phase_6 -%LL2_1.QYStart=15%
_set LineLoad_3_1.qy_start Phase_6 -%LL3_1.QYStart=35%
*CorrosionReductionSheetPile("AZ26_plas_240_75y_ECcorr_secA", %C1.dtD1=2%, [2.1E8, %Steel.fy=2.4E5%, 0.356, 13.0], [%Time.time=50%, 75], [2.45, 4.65])
*CorrosionReductionSheetPile("AZ26_plas_240_75y_ECcorr_secB", %C1.dtD1=2%, [2.1E8, %Steel.fy=2.4E5%, 0.356, 13.0], [%Time.time=50%, 75], [3.2, 4.65])
*CorrosionReductionSheetPile("AZ26_plas_240_75y_ECcorr_secC", %C1.dtD1=2%, [2.1E8, %Steel.fy=2.4E5%, 0.356, 13.0], [%Time.time=50%, 75], [2.4, 4.65])
*CorrosionReductionSheetPile("AZ26_plas_240_75y_ECcorr_secD1", %C1.dtD1=2%, [2.1E8, %Steel.fy=2.4E5%, 0.356, 13.0], [%Time.time=50%, 75], None)
*CorrosionReductionSheetPile("AZ26_plas_240_75y_ECcorr_secD2", %C2.dtD2=2%, [2.1E8, %Steel.fy=2.4E5%, 0.356, 13.0], [%Time.time=50%, 75], None)
*CorrosionReductionSheetPile("AZ26_plas_240_75y_ECcorr_secD3", %C1.dtD1=2%, [2.1E8, %Steel.fy=2.4E5%, 0.356, 13.0], [%Time.time=50%, 75], None)
*CorrosionReductionSheetPile("AZ26_plas_240_75y_ECcorr_secE", %C1.dtD1=2%, [2.1E8, %Steel.fy=2.4E5%, 0.356, 13.0], [%Time.time=50%, 75], [1.8, 4.65])
*CorrosionReductionSheetPile("AZ26_plas_240_75y_ECcorr_secF", %C1.dtD1=2%, [2.1E8, %Steel.fy=2.4E5%, 0.356, 13.0], [%Time.time=50%, 75], [3.4, 4.65])
*CorrosionReductionAnchor("Anchor", %C1.dtD1=2%, [2.1E8, 63.4], [%Time.time=50%, 75], [1.7, 4.65])
_calculate
$6
#output
*SofteningModule("Phase_6", ["Plate_1", "Plate_2", "Plate_3", "Plate_4", "Plate_8", "Plate_9", "Plate_5"], [%C1.dtD1=2%, %C1.dtD1=2%, %C1.dtD1=2%, %C1.dtD1=2%, %C2.dtD2=2%, %C1.dtD1=2%, %C1.dtD1=2%], [[2.1E8, %Steel.fy=2.4E5%, 0.356, 13.0], [2.1E8, %Steel.fy=2.4E5%, 0.356, 13.0], [2.1E8, %Steel.fy=2.4E5%, 0.356, 13.0], [2.1E8, %Steel.fy=2.4E5%, 0.356, 13.0], [2.1E8, %Steel.fy=2.4E5%, 0.356, 13.0], [%Time.time=50%, 75], [%Time.time=50%, 75], [%Time.time=50%, 75], [%Time.time=50%, 75], [%Time.time=50%, 75], [%Time.time=50%, 75], [%Time.time=50%, 75], [%Time.time=50%, 75], [%Time.time=50%, 75], [2.45, 4.65], [3.2, 4.65], [2.4, 4.65], None, None, None, [1.8, 4.65]])
echo Phase_6.Reached.SumMstage
getsingleresult Phase_6 ResultTypes.Plate.M2D (69 2) True
getsingleresult Phase_6 ResultTypes.NodeToNodeAnchor.AnchorForce2D (69 2) True

```

Figure D.3 Example of InputCommand file, consisting of regular PLAXIS commands and special commands

### Explanation

- **Keywords** = this word is required for the PTK to be able to read the text file
- **#input** = required for python interpreter that code below deals with Input and can directly be "fired" to PLAXIS Input
- **%..%** = these so called "flags" are used by the PTK and indicate that all text between the percentage signs is first read by PTK to recognise the stochastic variables and will later on be replaced by a numerical value (the drawn stochastic value)
- **\*** = flag used by python interpreter to recognise a so called Special Command which triggers a python function allowing for more complex pre -and post processing tasks to be executed

- \$ = symbol used by python interpreter to understand from which PLAXIS phase the relevant output should be extracted. If this phase is not reached the calculation loop should be stopped
- #output = required for python interpreter that code below deals with Output and the commands can be “fired” to PLAXIS Output

Note 1: for more information on the special commands see Table C.1.

Note 2: a tip is to define every parameter that is potentially used as a stochastic variable with the %..% in the InputCommand file. This way it can be easily switched between stochastic or deterministic in the PKT without later adjustments to the InputCommand file.

Note 3: keep in mind whether a value is positive or negative (in line with the definition in PLAXIS). It is possible to define a value as positive in the PTK and then by including a minus sign in the InputCommand file to revert the sign (-%..%) while setting this value in PLAXIS. This approach is used here for defining the waterlevel. The intention is to use a Gumbel extreme minima distribution, this however is not directly supported by the PTK. Therefore we define a Gumbel extreme maxima distribution in the PTK and by adding the minus sign switch to a Gumbel extreme minima in PLAXIS.

### D.3 PLAXIS settings

In this paragraph additional information is presented on the settings in the PLAXIS base model.

- As mentioned before, the Mohr Coulomb (associative) soil model is used for modelling the soil.
- Elastic-perfectly plastic behaviour is used to model the sheet pile structure (to allow for plastic hinges and hence softening to occur).
- Elastic behaviour is assumed for the anchor (no plasticity allowed).
- For the anchor wall plasticity is allowed but no plastic hinges are allowed.
- The arc-length control is switched off in all phases prior to last to prevent numerical issues (spontaneous unloading). Arc-length control is set ON in the last phase and the maximum number of steps is set to 1000.
- Changes are made to the geometry (i.e. excavation level) in the INputCommand file, as such the program needs to remesh. During remeshing the program also automatically will start with automatic regeneration of phases in relation to variation of geometry. The program tries to see if due to the changes in geometry the specified phasing can still be used or (when relevant) updates the phasing. Based on experience it is found that with small geometrical changes (i.e. intersection of a line with a soil cluster as used here) the program is robust and updating of the phases works ok. It is recommended to carefully consider results if more complex geometry changes are made during automated calculations;
- In general the recommendation is to carefully “condition” the PLAXIS base model. Things to consider are to simplify the model as much as possible (to reduce calculation times, chance of numerical issues), to inspect model behaviour for more extreme stochastic values and to choose robust numerical settings.
- While using the InputCommand script note that it is possible to change multiple (soil) parameters with one “sps” command. Advantage of this approach that this prevents Input errors due to inconsistent parameter combinations. It may else happen that when changing parameters one at a time that PLAXIS returns an error.
- It became clear during this project while using the PLAXIS version 2018.00 that a PLAXIS exception occurred in a random manner. It was confirmed by PLAXIS support that this indeed was a known issue in the software. Results of this known issue is that an exception

window is opened which has to be closed manually. Since this is not possible during an automated loop the calculation hangs until the user restarts the calculation. PLAXIS supports indicated that also here a work around would be to force the calculation on a single thread. For this a so called toggles folder needs to be created in the PLAXIS installation folder and a file named: TASKS\_FORCE\_SINGLE\_THREAD should be placed in this toggles folder. As a result the calculation kernel will only use a single calculation thread.

- It also became clear during the project that after running the coupling for a number of days (and hundreds of PLAXIS calculations) inevitable a crash or issue will occur with PLAXIS. It is for this moment not clear whether this an inevitable effect of running so many PLAXIS calculations after each other or an effect of the developed python code. However the PTK can simply be stopped and the run can be saved. After rebooting the computer the run can simply be continued.
- It is furthermore recommended that use is made of the python version installed with the PLAXIS installation.

### Arc-length control

Considering the arc-length option, assume a certain geometry and load, and that during the calculation the load to be applied is larger than the failure load. The calculation would then try to apply the load defined by the user over and over again without converging to a solution as the load can simply not be applied. Hence, the calculation will keep iterating. When using the arc-length control the calculation will in fact accurately find how much of the load can really be applied (see figure D.3.).

In principle using arc-length control or not makes no difference for the result of the calculation if no failure occurs. However, in case of failure the results will differ because without arc-length control there is no accurate determination of the failure load. Generally, without using arc-length control the failure load is overestimated. Since arc-length control is meant to determine failure accurately, it's recommended to always do Safety analysis with arc-length control switched on.

It may happen in some situations that use of the arc-length control results in numerical failure as this option triggers "spontaneous unloading". In this case it is justified to switch the option off.

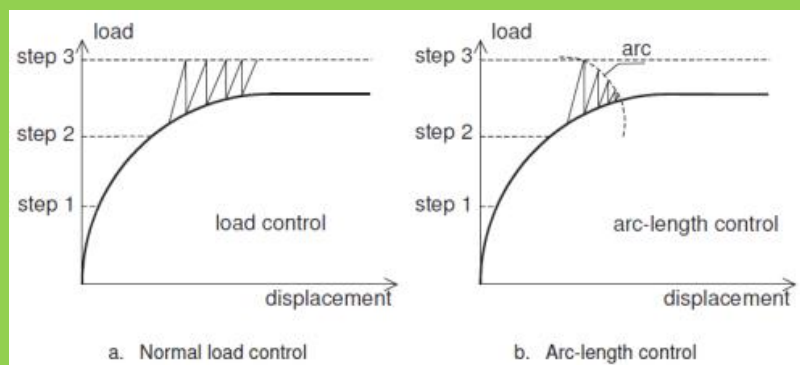


Figure D.3. Arc-length control effects (PLAXIS)

## E Plastic rotation capacity

### E.1 Classification of cross sections

EN1993-5:2008, Design of steel structures – Part 5 : Piling, provides principles and application rules for the structural design of bearing piles and sheet piles made of steel.

The code distinguishes between so called Classes of cross-sections:

- Class 1 cross-sections for which a plastic analysis involving moment redistribution may be carried out, provided that they have sufficient rotation capacity;
- Class 2 cross-sections for which elastic global analysis is necessary, but advantage can be taken of the plastic resistance of the cross-section;
- Class 3 cross-sections which should be designed using an elastic global analysis and an elastic distribution of stresses over the cross-section, allowing yielding at the extreme fibres;
- Class 4 cross-sections for which local buckling affects the cross-sectional resistance, see Annex A.

Classification of cross-sections may be done in accordance with Table 5-1 from EN 1993-5:2008. Table 5-1 has been repeated here in Table E.1. Relevant parameters in the classification are the width and thickness of the compressed flange of the steel sheet pile as well as the yield stress in relation to a reference yield stress (235 MPa). The ratio " $b/t_f/\epsilon$ " basically states that the slenderness of the sheet pile profile becomes the more prone it becomes to local buckling effects. Also, the higher the allowable yield stress the more prone it becomes to local buckling effects, since a higher stress in the same (slender) cross section also leads more quickly to local buckling effects.

Table 5-1: Classification of cross-sections

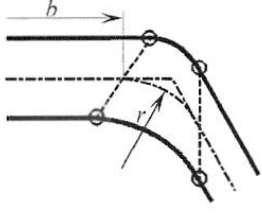
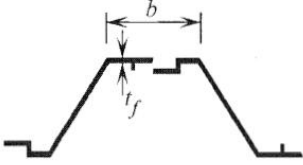
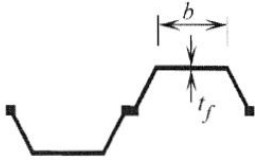
Classification		Z-profile				U-profile	
							
Class 1		<ul style="list-style-type: none"> <li>- the same boundaries as for class 2 apply</li> <li>- a rotation check has to be carried out</li> </ul>					
Class 2		$\frac{b/t_f}{\epsilon} \leq 45$				$\frac{b/t_f}{\epsilon} \leq 37$	
Class 3		$\frac{b/t_f}{\epsilon} \leq 66$				$\frac{b/t_f}{\epsilon} \leq 49$	
$\epsilon = \sqrt{\frac{235}{f_y}}$	$f_y$ [N/mm <sup>2</sup> ]	240	270	320	355	390	430
	$\epsilon$	0,99	0,93	0,86	0,81	0,78	0,74
<b>Key:</b>							
<p><math>b</math>: width of the flat portion of the flange, measured between the corner radii, provided that the ratio <math>r/t_f</math> is not greater than 5,0; otherwise a more precise approach should be used;</p> <p><math>t_f</math>: thickness of the flange for flanges with constant thickness;</p> <p><math>r</math>: midline radius of the corners between the webs and the flanges;</p> <p><math>f_y</math>: yield strength.</p>							
<p><b>Note:</b> For class 1 cross-sections it should be verified that the plastic rotation provided by the cross-section is not less than the plastic rotation required in the actual design case. Guidance for this verification (rotation check) is given in Annex C.</p>							

Table E.1 Classification of cross-sections according to EN 1993-5:2008

The principles from EN 1993-5:2008 Table 5-1 are also shown in Figure E.1. For a ratio " $b/t_f/\epsilon \leq 45$ " the full 100% of the  $M_{pl;Rd}$  can be used. This area is referred to as Class 1 / 2. Depending on the exact value of " $b/t_f/\epsilon$ " even some rotation capacity may be used in the design. For Class 3 the  $M_{el;Rd}$  can be used without any rotation capacity. For Class 4 the capacity is lower than  $M_{el;Rd}$  and a separate (buckling) analysis has to be made to quantify the capacity.

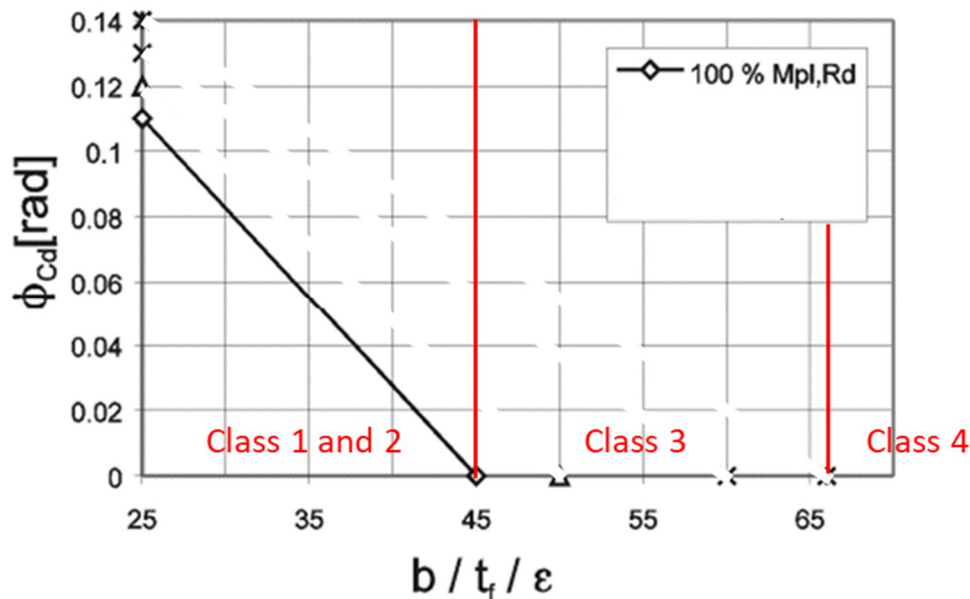


Figure E.1 Graphical representation of principles from [EC3-5:2008] Table 5-1

## E.2 Rotation capacity according to annex C of [EC3-5:2008]

Guidance for design of the steel sheet piling allowing for plastic global analysis is given in Annex C of EN 1993-5:2008. In Annex C it is explained how to deal with a plastic design with moment redistribution.

EN1993-5:2008 Paragraph C.1.2. in Annex C "Verification of Class 1 and Class 2 cross-sections" indicates that the classification of a cross-section may be carried out according to one of the following procedures :

- classification according to Table 5-1:  $b/t_f$  ratios determined for the full plastic moment resistance;
- classification according to Table C-1 in which the  $b/t_f$  ratios are given for 85 % to 100 % of the full plastic moment resistance, in steps of 5 %.

Classification may be performed according to Table C-1 from EN1993-5:2008, see Table E.2. In this case use is to be made of a reduced yield strength (resulting in a reduced  $M_{pl,Rd}$ ). By reducing the strength however use can be made of additional rotation capacity. The principle of exchanging bending moment capacity with rotation capacity is shown in Figure E.2.

**Table C-1: Classification of cross-sections in bending on a reduced  $M_{pl,Rd}$  level**

Type of pile	$M_{pl,Rd}$	100 %	95 %	90 %	85 %
	Reduction factor $\rho_c$	1,0	0,95	0,90	0,85
U-piles	Class 1 or 2	$\frac{b/t_f}{\epsilon} \leq 37$	$\frac{b/t_f}{\epsilon} \leq 40$	$\frac{b/t_f}{\epsilon} \leq 46$	$\frac{b/t_f}{\epsilon} \leq 49$
Z-piles	Class 1 or 2	$\frac{b/t_f}{\epsilon} \leq 45$	$\frac{b/t_f}{\epsilon} \leq 50$	$\frac{b/t_f}{\epsilon} \leq 60$	$\frac{b/t_f}{\epsilon} \leq 66$

Table E.2 Classification of cross section in bending on a reduced  $M_{pl,Rd}$  level

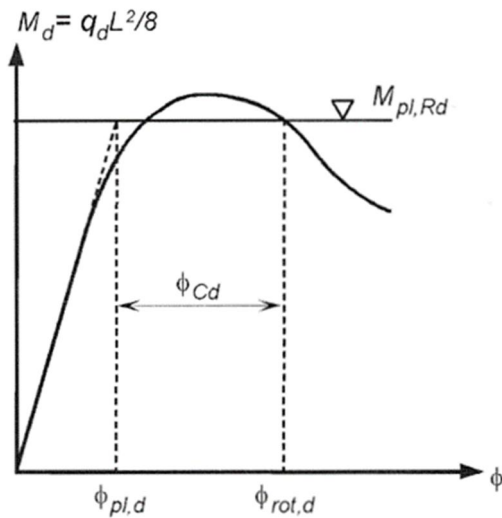


Figure E.2 Principle of reducing yield stress (i.e.  $M_{pl,Rd}$ ) in exchange for additional rotation capacity

Now with using the values indicated in EN 1993-5:2008 Table C-1, an updated graph can be made of Figure E.1, see Figure E.3. Note that in this case there is no Class 3 anymore. Only a Class 1 and 2 area exists where we can make use of a plastic moment capacity and rotation capacity. Or above a certain threshold there is a Class 4 profile with a certain moment capacity and NO rotation capacity anymore.

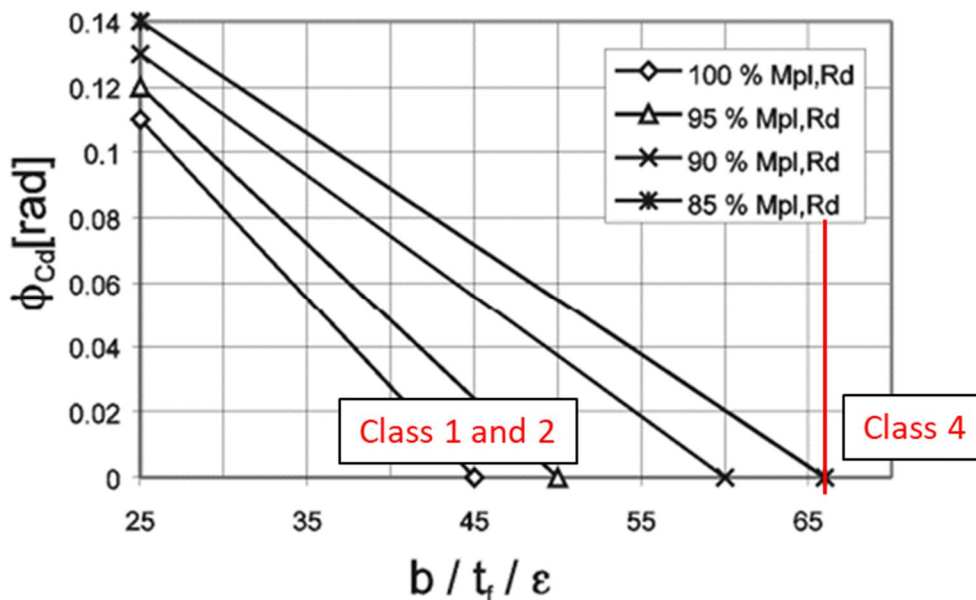


Figure E.3 Plastic rotation angle of a z-section  $\phi_{Cd}$  provided by the cross-section at different levels of reduced plastic moment capacity  $M_{pl,Rd}$  [EC3-5:2008 Figure C-1b)

For this research the principles explained in Figure E.3 are applied to an AZ26 sheet pile profile which is used in the case study. In this research a linear interpolation will be applied in between the lines in Figure E.3.

In Figure E.4 for an A26 S240GP the linear part and the nonlinear part of effect on moment capacity and plastic rotation capacity is presented.



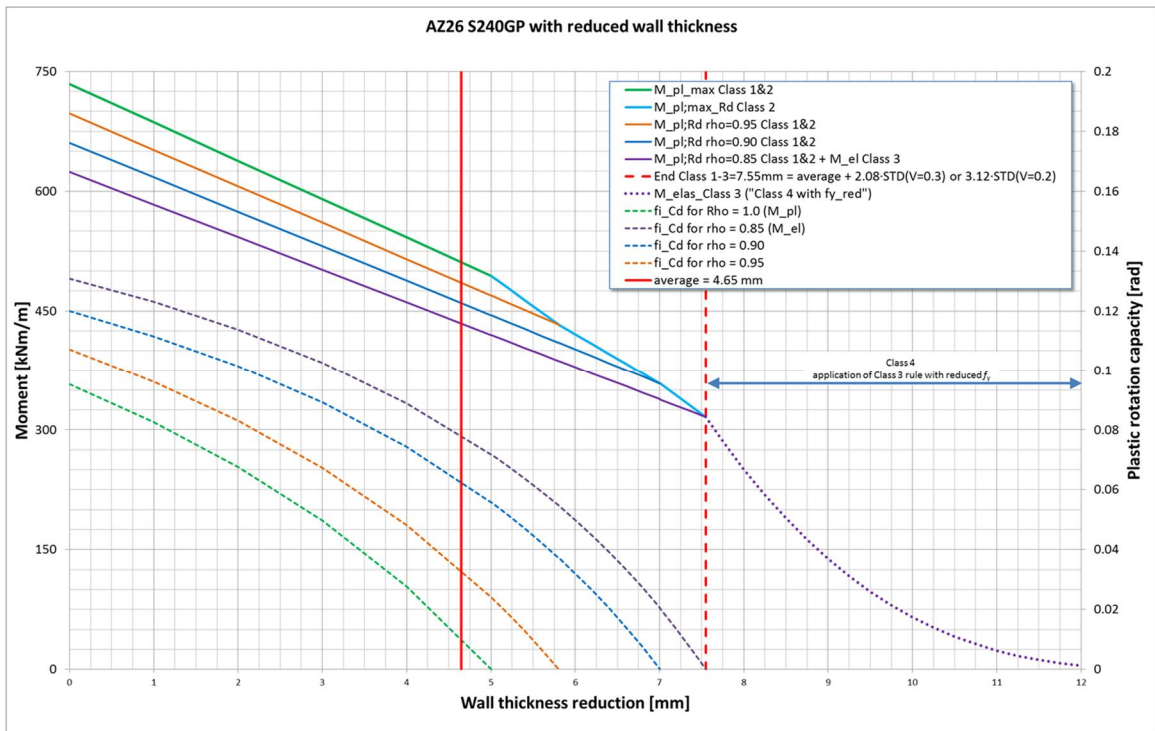


Figure E.4 Effect of thickness reduction on moment capacity and plastic rotation capacity of an AZ26 S240GP

When adding the yield stress also as a stochastic variable we can extend the above figure to three dimensions, see Figure E.5. Note that in this figure only the maximum (plastic) moment capacity is presented and not the capacity including some softening. The rotation capacities are also not presented.

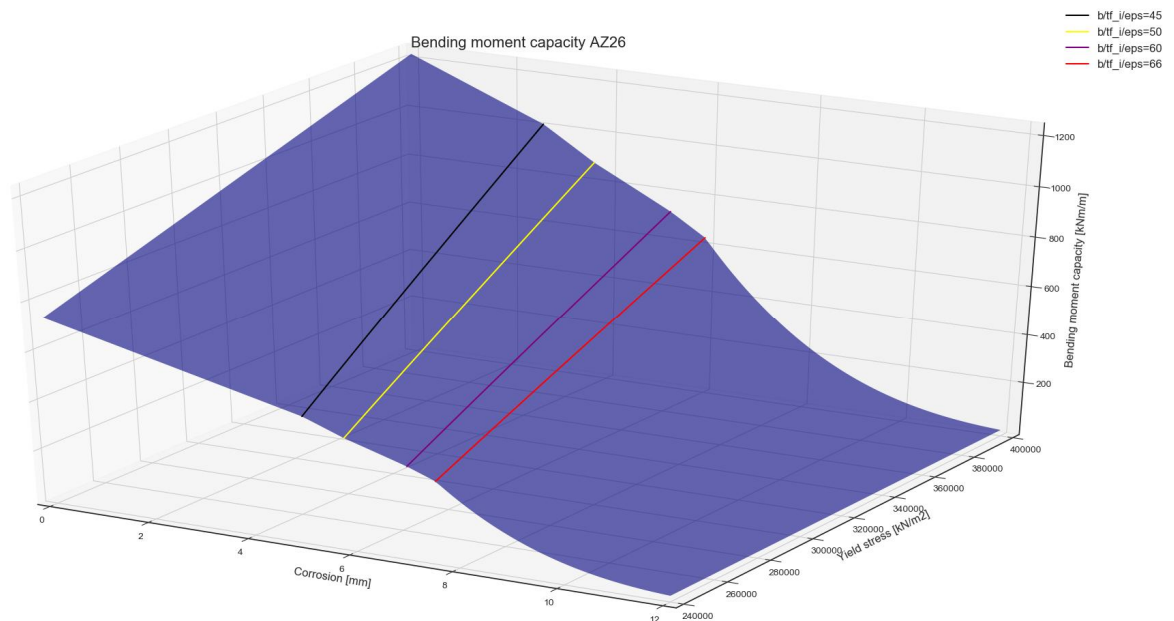


Figure E.5 Extension of the Bending moment – corrosion relation as shown in Figure E.4 with a third parameter (yield strength). Note that in this figure only  $M_{pl,max}$  is shown.

### E.3 Principles of softening: moment capacity vs rotation capacity

Basically what the EN 1993-5:2008 allows in its Annex C is to exchange bending moment capacity with rotation capacity during the softening that takes place after reaching the peak capacity.

The described Softening process has been illustrated in Figure E.6 and Figure E.7. Figure E.6 may be seen as a 3D plot. The third axis in this case is then perpendicular to the figure and displays the bending moment capacity  $M_{pl,Rd}$ . If we would make 4 cross-sections of this 3D figure (i.e. the 4 colored lines in the figure) these would look like the lines in Figure E.7. In Figure E.7 use has been made of "softening steps" of 1% just like the way it has been implemented into the python script SofteningModule (see Table C.1).

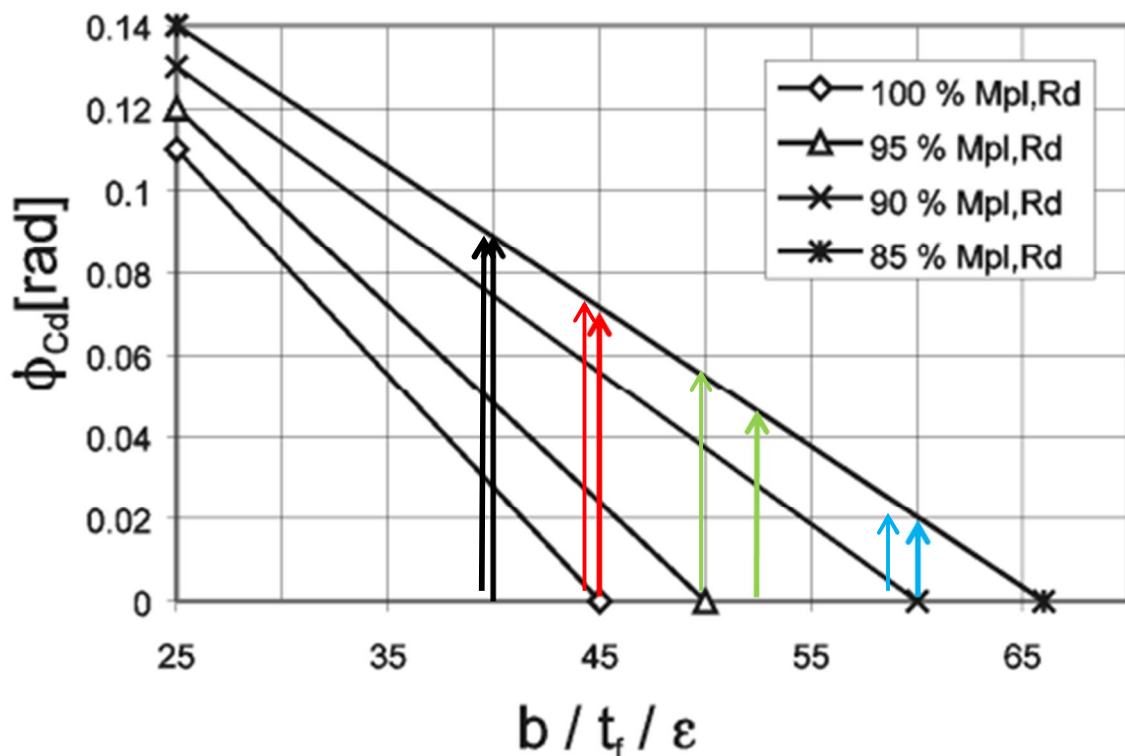


Figure E.6 This figure is a copy of Figure 3.4. showing the plastic rotation angle of a z-section  $\phi_{cd}$  provided by the cross-section at different levels of reduced plastic moment capacity  $M_{pl,Rd}$  EN 1993-5:2008 Figure C-1b. Indicated with four coloured lines are the cross-sections presented in Figure E.7.

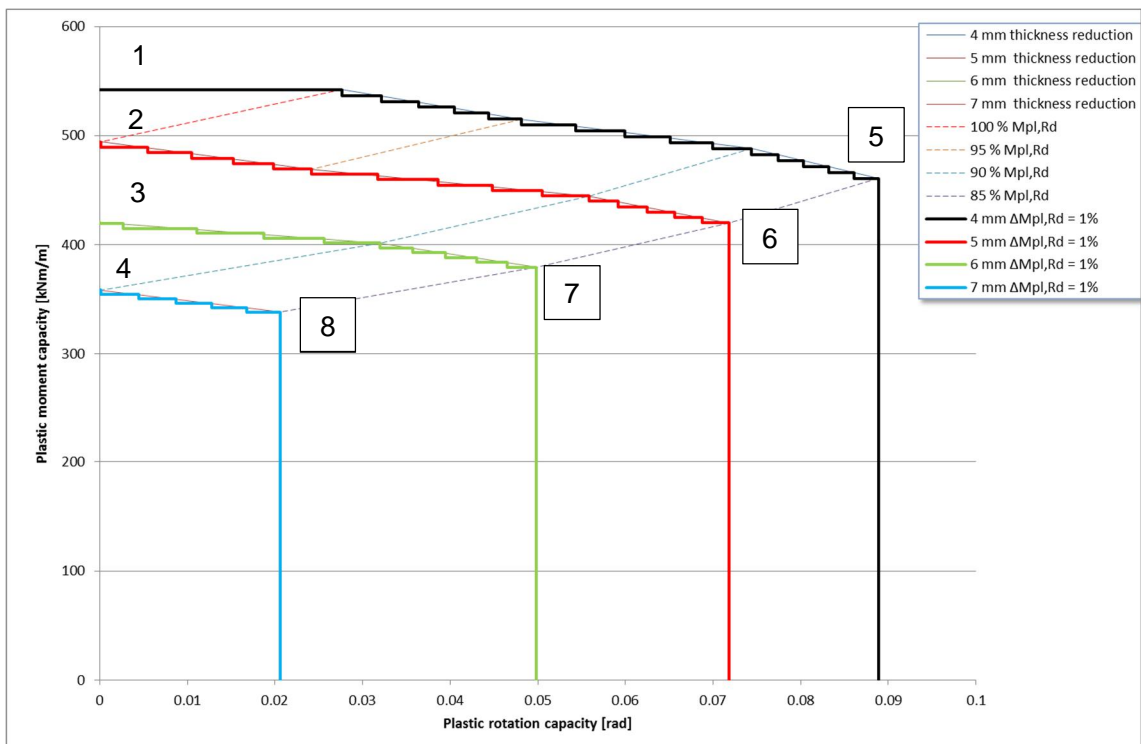


Figure E.7 The relationship between plastic rotation capacity and plastic bending moment capacity, using softening steps of 1%, for the four cross-sections shown in Figure E.6.

The values of the bending moment capacity indicated within the graph with the numbers 1 - 8 are quantified in Table E.3. The values of the numbers 1 – 4 can be calculated using the formulas in paragraph 3.7. The values for numbers 5 – 8 follow from numbers 1 – 4 using a factor of 0.85.

Nr	Bending moment [kNm/m]	Nr	Bending moment [kNm/m]
1	542	5	$542 * 0.85 = 461$
2	494	6	$494 * 0.85 = 420$
3	$446 * 0.943 = 421$	7	$446 * 0.85 = 379$
4	$398 * 0.90 = 358$	8	$398 * 0.85 = 338$

Table E.3 Quantification of the bending moment capacities at numbers 1 – 8 in Figure E.7.

#### E.4 Implementation of Softening module

The special command SofteningModule is called after each PLAXIS run. Let's assume a certain PLAXIS run has been made and call this run 0. The following procedure is followed when the special command is called:

- Gather all Input and Output of all sheet pile sections in PLAXIS run 0
- Enter WHILE loop:
  - Check for PLAXIS run 0 for all sections:
    - IF section is Class 4: check  $M_{max,i} \leq M_{elas\_corr,i}$ ; IF OK continue with next section, ELSE break while loop and stop SofteningModule and give results back to PTK (with comment: "elastic wall failure")

- IF section is Class 1/2/3: check  $\Phi_{\max_i} \leq \Phi_{CD_i}$  ; IF OK continue with next section, ELSE reduce  $Rho_{c\_max_i}$  with 1% for this section (minimum value is 0.85) and determine new input properties for this section.
  - WHEN all sections are OK, break while loop and give results back to PTK;
  - ELSE start PLAXIS run 1 with new set of input properties for the relevant sections.
- Start PLAXIS run 1 (with comment “Softening calculate”). After calculation gather all Input and Output of all sheet pile sections of PLAXIS run 1
  - Check for all sections IF the used input value of  $Rho_{c\_max_i} \leq \mathbf{0.851}$  (a value slightly larger than 0.85 is used) IF so break the while loop and stop SofteningModule and give results back to PTK (with comment “section has reached 0.85”), ELSE (none of the sections has reached 0.85 yet), continue;
  - IF section is Class 4: check  $M_{\max_j} \leq M_{elas\_corr_j}$ ; IF OK continue with next section, ELSE break while loop and stop SofteningModule and give results back to PTK (with comment “elastic wall failure”)
  - IF section is Class 1/2/3: check  $\Phi_{\max_i} \leq \Phi_{CD_i}$  ; IF OK continue with next section, ELSE reduce  $Rho_{c\_max_i}$  with 1% for this section (minimum value is 0.85) and determine new input properties for this section.
  - WHEN all sections are OK, break while loop and give results back to PTK
  - ELSE start PLAXIS run 2 with new set of input properties for the relevant sections.
- Start PLAXIS run 2:
  - Etcetera until one of the break criteria is reached and the while loop is exited, and results are given back to PTK. Maximum amount of softening loops is 15 (in case initial  $Rho_{c\_max_i} = 1$  and going down to 0.85).

In the above:

- $M_{\max_i}$  = calculated max (absolute) bending moment in PLAXIS per section
- $M_{elas\_corr_i}$  = allowable max bending moment for a Class 4 section
- $\Phi_{\max_i}$  = calculated max (absolute) rotation in PLAXIS per section
- $\Phi_{CD_j}$  = allowable rotation for a Class 1/2/3 per section. Value dependent on  $Rho_{c\_max_i}$  and ratio of “ $b/t_f/\epsilon$ ” for this section
- $Rho_{c\_max_i}$  = allowable percentage of plastic peak capacity ( $W_{pl,i} * f_y$ ) per section
- $W_{pl,i}$  = plastic section modulus per section
- $f_y$  = yield stress

Note: in the above softening procedure it has been chosen NOT to include a separate check on plastic bending moment capacity for a Class 1/2/3 with rotation capacity since within the PLAXIS model we make use of elastic-plastic plate elements and the plastic value of the plate element is set to the calculated value of  $M_{hinge}$ . When using elasto-plastic plate elements PLAXIS automatically limits the bending moments in the sheet pile to the specified maximum (=  $M_{hinge}$ ).

During the project it was found that this implementation was working OK. However, it did require in cases with a ratio between 45 and 66 at least 1 softening step since by default (in this implementation) in the initial step  $\Phi_{CD} = 0$  for a ratio between 45 and 66 . In that sense the

algorithm can be optimised by including a check on plastic moment capacity (if OK no need to check rotation capacity and softening). Attention point in this case is the tolerance in PLAXIS on the calculated bending moment in a plastic hinge.

### E.5 Calculation of rotation angle ( $\Phi_{max}$ ) from PLAXIS

The rotation angle is determined per plate section and is calculated as the difference in rotation between any consecutive node pair within a plate section. The principle is indicated in Figure E.8. The python routine has been generalised to deal with random deformations patterns of the sheet piles (represented by plate elements in the PLAXIS model) and is checked with a number of testcases., also see paragraph H.3.

In the chosen approach no distinction has been made between elastic and plastic rotations. Although the EN 1993-5:2008 allows to take only the plastic part of the rotation, here the sum of the elastic and plastic rotations are extracted from PLAXIS since it is more complex to exclude the elastic part from the PLAXIS results. This approach is conservative. In general the elastic rotations however are relatively small compared to the plastic rotations so the approach is not expected to be over conservative.

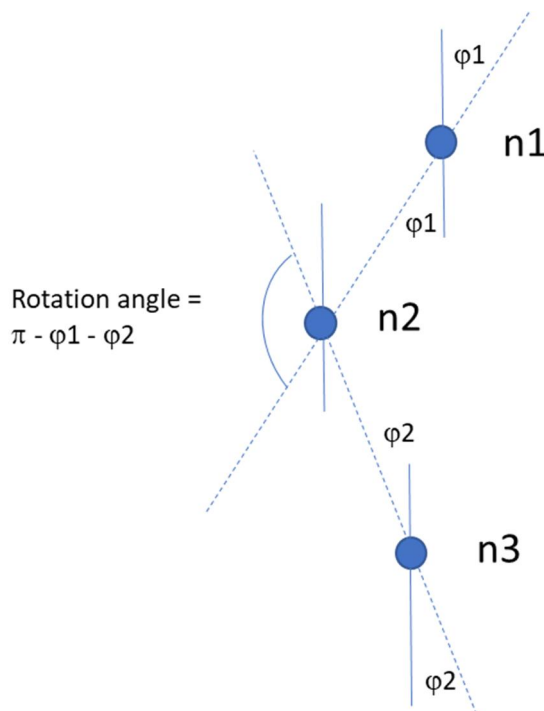


Figure E.8 Principle of determination of rotation angle  $\Phi_{max}$  (in radians) between consecutive node pairs ( $n1+n2$  and  $n2+n3$ ) in a plate element in a PLAXIS calculation

## F Summary of results of [Deltares, 2018] (1<sup>st</sup> series)

[#]	Calculation				Reliability index, $\beta$ [-]		
	Section modulus	Plastic hinges	Plain strain soil strength	$U_{max}$ [mm]	$-\sigma$	Mean	$+\sigma$
1	Elastic	No	No	No	0.85	<b>0.88</b>	0.92
2	Plastic	No	No	No	2.00	<b>2.02</b>	2.05
3	Plastic	No	Yes	No	2.21	<b>2.23</b>	2.27
4	Plastic	Yes	No	No	2.93	<b>2.97</b>	3.00
5	Plastic	Yes	Yes	No	3.91	<b>3.95</b>	4.01
6	Plastic	Yes	Yes	0.30	3.91	<b>3.96</b>	4.02
7	Plastic	Yes	Yes	0.20	3.78	<b>3.83</b>	3.88
8	Plastic	Yes	Yes	0.15	2.69	<b>2.72</b>	2.75
9	Plastic	Yes	Yes	0.13	1.90	<b>1.93</b>	1.97
10	Plastic	Yes	Yes	0.10	0.38	<b>0.41</b>	0.43

Table F.1 Numerical results of previous study [Deltares, 2018]

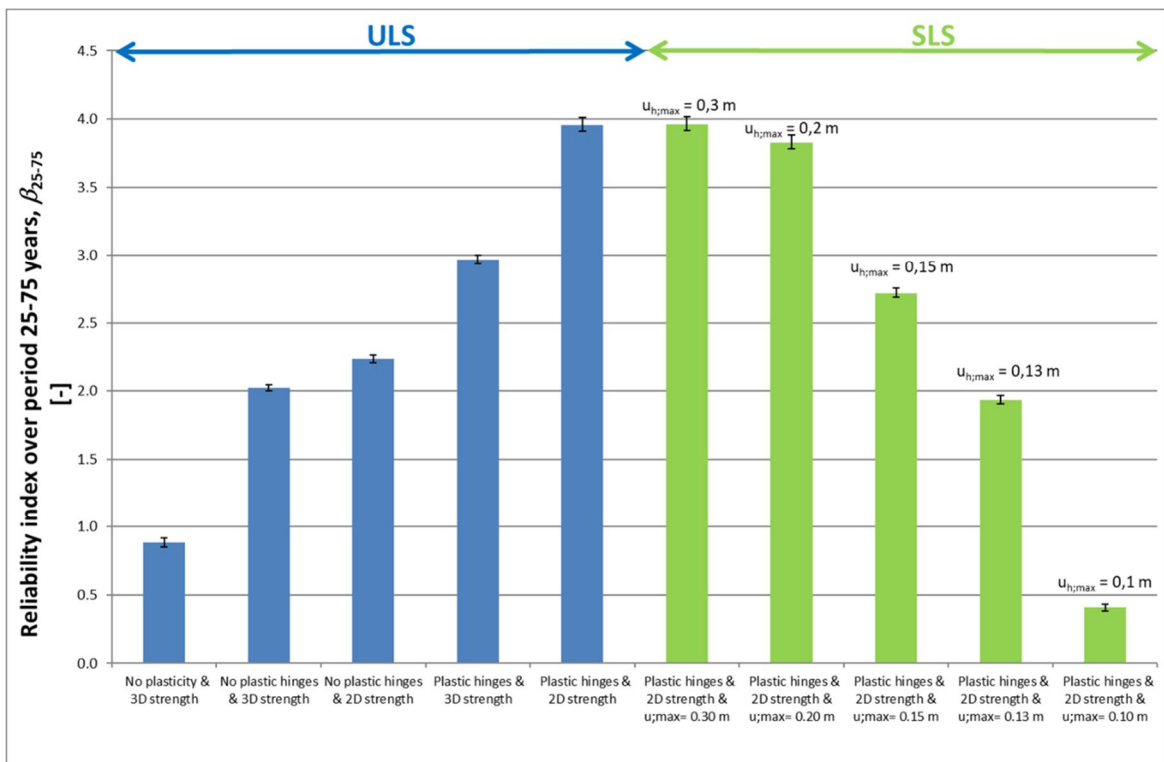


Figure F.1 Graphical results of previous study [Deltares, 2018]

## G Results of calculations (2<sup>nd</sup> series)

### Summary of calculation results

Run	Origin	Node	Model settings			Diff u per direction	Var. coeff.		Time	Softening	model behaviour	Depth	Step size
			material model	corrosion	method		Failure	fy					
H1	like A10	121	MC	deterministic	DS	0.1	0.1	No	75	No	Varying	6	1
H2	like A10	122	MC	deterministic	DS	0.1	0.1	No	75	Yes	Varying	6	1
H3	like B3	124	MC	stochast V = 0.2	DS	0.1	0.1	No	75	Yes	Varying	5	1
H4	like B4	126	MC	stochast V = 0.3	DS	0.1	0.1	No	75	Yes	Varying	4	1
H5		134	MC	stochast V = 0.5	DS	0.1	0.1	No	75	Yes	Varying	4	1
H6	like A10	134	MC	deterministic	DS	0.1	0.1	Yes	75	No	Varying	6	1
H7	like A10	126	MC	deterministic	DS	0.1	0.1	Yes	75	Yes	Varying	6	1
H8	like H4	126	MC	stochast V = 0.3	DS	0.1	0.1	Yes	75	Yes	Varying	4	1
H9	like H5	134	MC	stochast V = 0.2	DS	0.1	0.1	Yes	75	Yes	Varying	5	1
H10	like H5	124	MC	stochast V = 0.5	DS	0.1	0.1	No	74	Yes	Varying	4	1
H11	like H5	122	MC	stochast V = 0.5	DS	0.1	0.1	No	50	Yes	Varying	5	1
H12	like H5	124	MC	stochast V = 0.5	DS	0.1	0.1	No	49	Yes	Varying	5	1

Run	Results		Calculation time				Versions used						Input Commands
	Beta	var. coeff. Failure	start	stop	days	nr. Iterations	nr. Runs	PLAXIS	PLX model	Python script	PTK		
H1	2.13	0.1	2-10-2019	14-10-2019	12	1879	13770	2018.00	v1.0	v8.1	v1.9.22.1134	TimeList, no softening	
H2	3.83	0.188	2-10-2019	2-11-2019	31	5000	35202	2018.00	v1.0	v8.1	v1.9.22.1134	TimeList	
H3	2.90	0.15	2-10-2019	29-10-2019	27	4815	29301	2018.00	v1.0	v8.1	v1.9.22.1134	TimeList	
H4	1.94	0.1	2-10-2019	14-10-2019	12	2275	11895	2018.00	v1.0	v8.1	v1.9.22.1134	TimeList	
H5	1.16	0.1	2-10-2019	5-10-2019	3	569	3368	2018.00	v1.0	v8.1	v1.9.22.1134	TimeList	
H6	2.96	0.14	7-10-2019	29-10-2019	22	3350	23846	2018.00	v1.0	v8.1	v1.9.22.1134	TimeList, no softening	
H7	4.19	0.433	29-10-2019	21-11-2019	23	2659	18664	2018.00	v1.0	v8.1	v1.9.22.1134	TimeList	
H8	1.90	0.121	17-10-2019	29-10-2019	12	1578	8327	2018.00	v1.0	v8.1	v1.9.22.1134	TimeList	
H9	2.6	0.157	30-10-2019	16-11-2019	17	2348	14477	2018.00	v1.0	v8.1	v1.9.22.1134	TimeList	
H10	1.22	0.1	11-11-2019	14-11-2019	3	641	3586	2018.00	v1.0	v8.1	v1.9.22.1134	TimeList	
H11	2.67	0.164	30-10-2019	11-11-2019	12	2130	13069	2018.00	v1.0	v8.1	v1.9.22.1134	TimeList	
H12	2.78	0.17	30-10-2019	11-11-2019	12	2619	15965	2018.00	v1.0	v8.1	v1.9.22.1134	TimeList	

## H Verification of results

### H.1 Check on Input values

A check was made if the stochastic values determined by the PTK are correctly transferred to PLAXIS. In an arbitrary manner run H11 was chosen for this check.

Succeeded	Reused	Beta [u]	Limit state value [x]	Weight [-]	ZM.gammaunsat [x]	ZM.gammasat [x]	ZM.phi [x]	ZM.ERef [x]	KM.phi [x]	KM.ERef [x]	KM.cref [x]	ZD.phi [x]	Bottom.ylevel [x]	WL.waterlevel [x]	LL1_1.QYStart [x]	LL2_1.QYStart [x]	LL3_1.QYStart [x]	C1.dtD1 [x]	C2.dtD2 [x]	Steel.fy [x]	Time.time [x]
<input checked="" type="checkbox"/>	<input checked="" type="checkbox"/>	0	0.61699		19.7	20.7	37	47891	25.8	6225.9	14.513	39.8	-7	0.96295	6.0704	6.0704	6.0704	3.1442	3.1442	2.4E+05	75
<input checked="" type="checkbox"/>	<input checked="" type="checkbox"/>	1	0.60867		18.979	20.979	38.336	50912	25.688	5737.1	13.924	39.395	-7.0256	1.0405	6.2877	7.1506	4.5078	2.5706	2.9119	2.4E+05	75
<input checked="" type="checkbox"/>	<input checked="" type="checkbox"/>	2	0.59792		19.258	21.258	39.671	54123	25.575	5286.7	13.359	38.99	-7.0513	1.1343	6.5084	8.3032	2.7081	2.0087	2.6809	2.4E+05	75
<input checked="" type="checkbox"/>	<input checked="" type="checkbox"/>	3	0.58385		19.537	21.537	41.007	57537	25.463	4871.6	12.817	38.585	-7.0769	1.2483	6.7325	9.5195	1.5975	1.4693	2.4516	2.4E+05	75
<input checked="" type="checkbox"/>	<input checked="" type="checkbox"/>	4	0.56309		19.816	21.816	42.942	61167	25.35	4489.1	12.297	38.18	-7.1025	1.3858	6.9598	10.791	0.85431	0.97353	2.2243	2.4E+05	75
<input checked="" type="checkbox"/>	<input checked="" type="checkbox"/>	5	0.53957	0	20.095	22.095	43.678	65025	25.238	4136.7	11.798	37.774	-7.1281	1.5497	7.1903	12.111	0.41087	0.55778	1.9998	2.4E+05	75

Table H.1 Input of Run H11, Iteration 1182, Beta [u] = 5 (screenshot) as visualized in PTK

Stochastic variable	Value
ZM.gammaunsat	20.095
ZM.gammasat	22.095
ZM.phi	43.678
ZM.ERef	65025
KM.phi	25.238
KM.ERef	4136.7
KM.cref	11.798
ZD.phi	37.774
Bottom.ylevel	-7.1281
WL.waterlevel	1.5497
LL1_1.QYStart	7.1903
LL2_1.QYStart	12.111
LL3_1.QYStart	0.41087
C1.dtD1	0.55778
C2.dtD2	1.9998
Steel.fy	2.40E+05
Time.time	75

Table H.2 Run H11, Iteration 1182, Beta [u] = 5 (numerical values of stochastic variables)

As a check the “fired” PLAXIS commands are listed below in Table H.3 It is verified that all numerical values are according to the values in the PTK as listed in Table H.2. Note that the values of the Waterlevel and the Lineloads are negative values due to the fact that a minus sign is added in the InputCommands file.



```

0961> ##~ running PLAXIS2DXInput.exe 2018.0.0.0
OK
0962> _gotostructures
OK
0963> sps ZM "gammaunsat" 20.0954547665503 "gammamat" 22.0954547665503
Edited ZM
0964> sps ZM "phi" 43.6778654151577 "psi" 43.6778654151577
Edited ZM
0965> sps ZM "Eref" 65024.7213932754
Edited ZM
0966> sps KM "phi" 25.237530025545 "psi" 25.237530025545
Edited KM
0967> sps KM "Eref" 4136.69858194129
Edited KM
0968> sps KM "cref" 11.7982770391948
Edited KM
0969> sps ZD "phi" 37.7744504603992 "psi" 37.7744504603992
Edited ZD
0970> _set Point_21.y -7.12813390177813
OK
0971> _set Point_8.y -7.12813390177813
OK
0972> _set Point_24.y -7.12813390177813
OK
0973> _gotomesh
OK
0974> _mesh 0.06
Generated 805 elements, 6708 nodes
0975> _gotostages
OK
0976> _movepoint UserWaterLevel_2.Points[0] -5 -1.54972863472179
OK
0977> _movepoint UserWaterLevel_2.Points[1] 105 -1.54972863472179
OK
0978> _set LineLoad_1_1.qy_start Phase_6 -7.19025109989275
OK
0979> _set LineLoad_2_1.qy_start Phase_6 -12.1108193400246
OK
0980> _set LineLoad_3_1.qy_start Phase_6 -0.410874745674318
OK

```

Table H.3 Run H11, Iteration 1182, Beta [u] = 5, check on input of soil, water and surcharge properties in PLX

Depending on the stochastic value of the corrosion and the yield stress the sheet pile properties are determined per section by the Special command "Corrosion Reduction SheetPile". As a check the input values are recalculated using a spreadsheet for zone D1 for Run 11, iteration 1182, Beta [u] = 5, see

AZ26 initial properties				
fy	2.40E+05	kN/m2		
b	3.56E-01	m	= width of flange	
$\epsilon$	0.98953	-	=sqrt(235000/fy)	
tf	1.30E+01	mm		
E	2.10E+08	kN/m2		
AZ26 with corrosion				
dt	0.55778	mm	= corrosion C1.dtD1	
b/tfi/eps	28.915	[-]		
tfi	12.44222	[mm]		
A	1.90E-02	m2/m		
I	5.35E-04	m4/m		
Wel	2.51E-03	m3/m		
Wpl	2.95E-03	m3/m		
PLX input values				
<i>in case ratio "b/tfi/eps" &lt; 45</i>				
EA	3.994E+06	kN/m		
EI	1.1226E+05	kNm2/m		
w	1.4930	kN/m/m		
Mp	707.34	kNm/m		
Np	1.0.E+12	kN/m		

Table H.4 Run H11, Iteration 1182, Beta [u] = 5, check on PLX input properties for zone D1

It is verified that the values calculated with the spreadsheet are the same as the values send to PLAXIS, see the table below. Note that only the relevant commands for section D1 are shown here to reduce the size of the table.

```

...
1000> set AZ26_plas_240_75y_ECcorr_secD1.EA 3994012.478325225
AZ26_plas_240_75y_ECcorr_secD1.EA: 3994012.47832522 kN/m
1001> set AZ26_plas_240_75y_ECcorr_secD1.EI 112260.4708588345
AZ26_plas_240_75y_ECcorr_secD1.EI: 112260.470858834 kN·m²/m
1002> set AZ26_plas_240_75y_ECcorr_secD1.w 1.4929999026120484
AZ26_plas_240_75y_ECcorr_secD1.w: 1.49299990261205 kN/m/m
1003> set AZ26_plas_240_75y_ECcorr_secD1.NP 1000000000000.0
OK
1004> set AZ26_plas_240_75y_ECcorr_secD1.MP 707.3441741323297
AZ26_plas_240_75y_ECcorr_secD1.Mp: 707.34417413233 kN·m/m
...
1030> _calculate
OK

```

Table H.5 Input of plate properties (per section) in PLX (only input for section D1 shown)

## H.2 Check on output / softening values

Verification is done by post processing results of run H5 (with  $v=0.5$ ) as this run is expected to make a significant number of calls to the softening module.

### Note for inspecting the plots in this paragraph

Note that Run H5 is a directional sampling run which consists of multiple iterations (i.e. directions) and an iteration consists of multiple calculation results (belonging to  $u = 0, 1, 2, 3$  etc. up to the specified “depth”). The PTK tries to find, if possible, in each iteration a calculation result with a LSF result within the specified accuracy around  $z = 0$ . This calculation result then determines the attribution to the overall probability of failure  $P_f$  (or Beta) of the Run.

Due to the softening module, “behind” each individual calculation result shown in the PTK a maximum of 15 additional softening calculations may be “hidden” (these intermediate results are not stored or shown).

In the plots presented in this paragraph all the calculation results are shown using blue dots. The individual calculation results per iteration that have converged within the specified accuracy around  $z = 0$ , and thus attribute to the overall result, are presented using a different color (see figure title).

First an inspection of the results of the stochastic variables is made. To get a feeling whether all the results are according the specified distribution type, mean and standard deviation. See Figure H.1. It is concluded that results are in line with expectations based on the distributions of the stochastic variables.

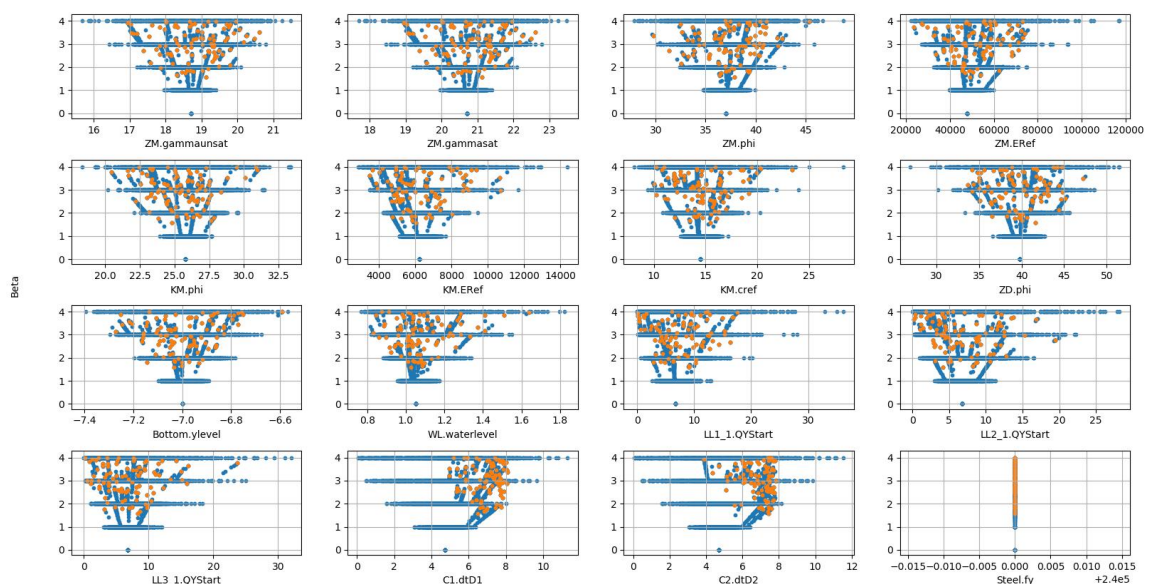


Figure H.1 Run H5 ( $V = 0.5$  on corrosion); overview of stochastic input values for all calculation results (displayed in blue dots) and only those calculation results converged within the required accuracy around  $z = 0$  (orange dots).

Next it is verified that the results of the softening module are according to expectations. For this the following plots are made:

- the calculated bending moment capacity vs the amount of corrosion in the zones defined
- the softening factor  $\rho_c$  vs the ratio " $b/t_f/\epsilon$ "
- the maximum rotation capacity  $\Phi_{CD}$  vs the ratio " $b/t_f/\epsilon$ "

Note that in all these plots per corrosion zone (i.e. zone A – F) the corresponding corrosion value (i.e. dt\_D1 or dt\_D2) has been linked to the corresponding bending moment,  $\rho_c$  or  $\Phi_{CD}$  for that zone.

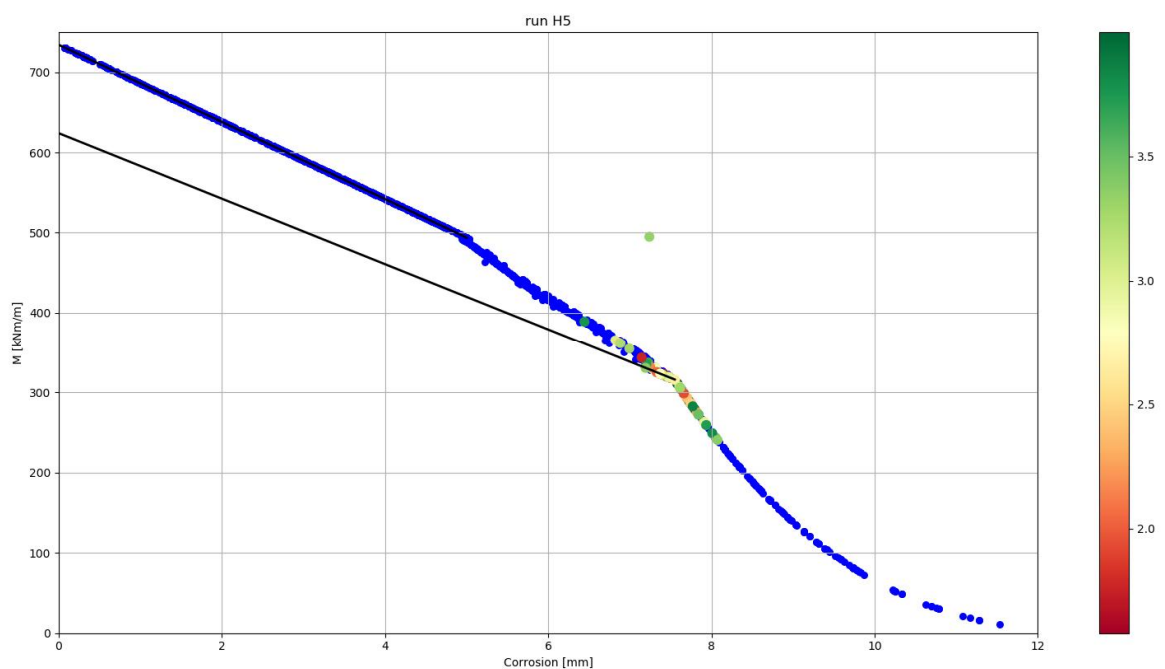


Figure H.2 Run H5; plot of the, by the python module, calculated maximum bending moment capacity ( $M_{pl\_max}$ , before softening) vs the amount of corrosion per zone defined in the sheet pile wall. The blue dots represent all calculation results. The (non-blue) coloured dots represent the individual calculation results per iteration with a LSF value within the specified accuracy around  $z = 0$ . The color legend indicates the reached Beta value of these individual calculation results

Notes to Figure H.2:

- Note 1: One point jumps out. Results have been checked. This is iteration 17. Here section D3 is decisive for the failure (i.e.  $z < 0$ ). But while the PTK searches for  $z = 0$  due to the allowed tolerance on results section B just becomes decisive over section D3 in the final  $z$ -value. So, the fact that the value of Section B is presented is a drawback of the current python post-processing code. It has been doublechecked that the values of section D3 for this case fall exactly on the line (corrosion = 7.2 mm and  $M = 336$  kNm/m)
- Note 2: Results in blue dots are all the intermediate values of the different iterations (so not the converged values of the iterations around  $z = 0$  adding to the overall reliability). So basically, the blue dots are a collection of all results with both  $z > 0$  and  $z < 0$ . It has been randomly checked that results with a large amount of corrosion (i.e.  $> 8$  mm and thus well within Class 4) are indeed failing as expected (i.e.  $z < 0$ ).

- Note 3: as a reference two black continuous lines have been added, they represent the lines  $M_{pl\_max}$  Class 1&2 and  $M_{pl;Rd}$  rho=0.85 Class 1&2 +  $M_{el}$  Class 3 from Figure H.3.

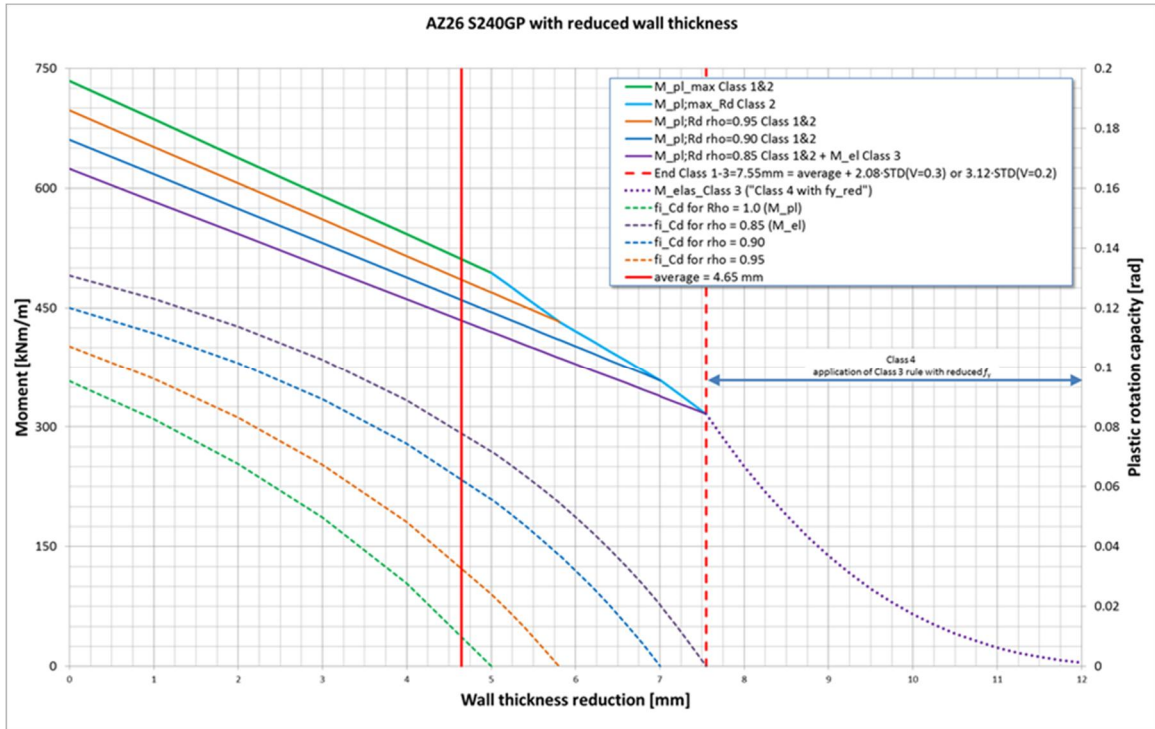


Figure H.3 Copy of Figure 3.5, the figure displays the interaction between (reduced) plastic moment capacity and (increased) rotation capacity

The conclusions from inspection of Figure H.2 and Figure H.3 are:

- The results in Figure H.2 are matching with the intended lines in Figure H.3 as expected;
- Most of the calculations which have a LSF results within the specified accuracy around  $z = 0$  seem located around the Class 3 to 4 transition zone (i.e. corrosion of 7 to 8 mm).
- It seems that in the Class 1&2 range (with corrosion values up to 5 mm) not one softening calculation was made;

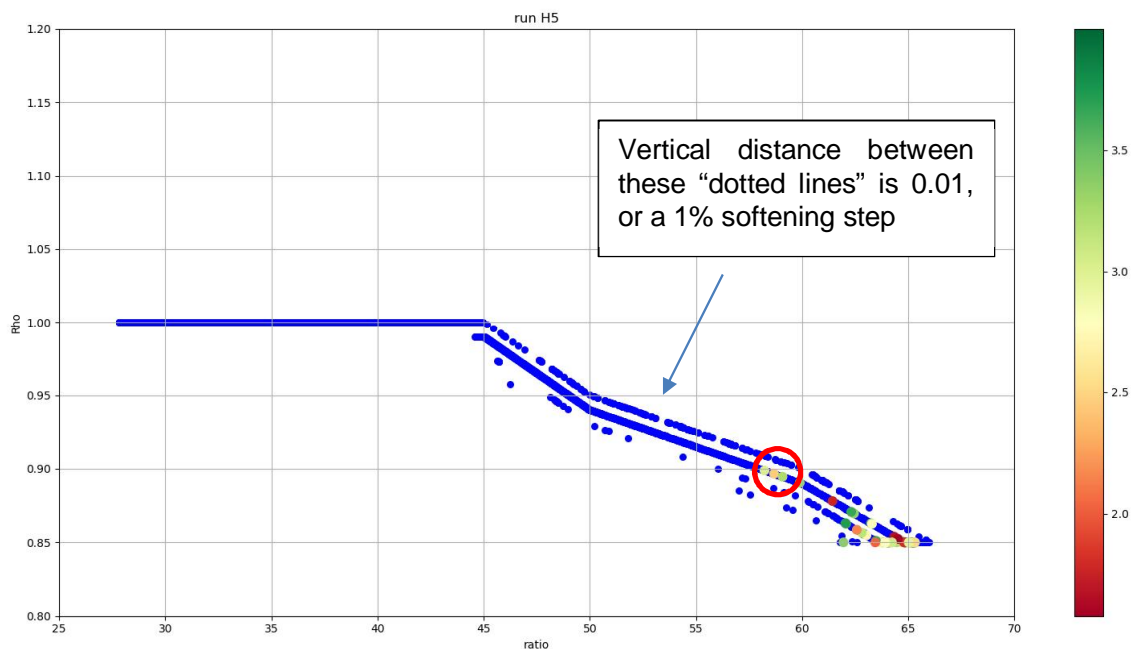


Figure H.4 Results of Reduction factor  $\rho_c$  vs ratio " $b/t_f/\epsilon$ ". The blue dots represent all calculation results. The non-blue coloured dots represent the individual calculation results per iteration that have converged within the specified accuracy around  $z = 0$ . The legend displays the reached Beta value of these individual calculation results

#### Conclusions from Figure H.4:

- Minimal  $\rho_c$  is 0.85 as expected.
- Maximum  $\rho_c$  is 1 as expected
- It seems that in the Class 1&2 range (with corrosion values up to 5 mm) not one softening calculation was made;
- For a ratio " $b/t_f/\epsilon$ " in the range of 45 and 66 (with corrosion values in between 5 and 7.5 mm) the following conclusions are made:
  - The differences between the parallel lines here is 0.01 (1%) as expected.
  - In most cases just one softening step occurs, this seems logical since for the  $M_{pl\_max}$  in first instance  $\Phi_{CD}$  is zero, so at least one softening step is needed to generate some rotation capacity. In most cases this seems to be sufficient to reach equilibrium.
  - In some cases, more softening steps are needed. Especially for ratios " $b/t_f/\epsilon$ " closer to a value of 66 it seems more softening steps are needed.
  - In some cases, it seems no softening is needed. In that case  $\Phi_{CD} = 0$  for that section. This sounds strange. It has however been checked that in these cases the softening loop is stopped due to another section in which elastic failure (Class 4) is detected and as such there is no need to continue the calculation as the sheet pile overall fails. In this case  $M_{pl\_max}$  and  $\Phi_{CD} = 0$  are reported for the relevant zones.

An additional check is made with regarding the results in the red circle in Figure H.4:

- Iteration 15 results in a failure with a  $Rho_{c\_max} = 0.899$  and a ratio = 58.2 in section D2 (section\_5). Logical question: why did it not soften down to 0.85? After checking the results, it becomes clear that during the calculation/iteration it did reach 0.85 as the PTK first needs to cross the  $z = 0$  line before an iteration is considered failing. After crossing the  $z = 0$  line the PTK tries to find  $z = 0$  within a certain (user specified) accuracy. In this case the allowed tolerance allows the PTK to come to a final value with  $\rho = 0.899$ .

During this study a sensitivity analysis has been with a reduced tolerance per iteration (0.01 instead of 0.1), results suggest a limited influence on overall reliability.

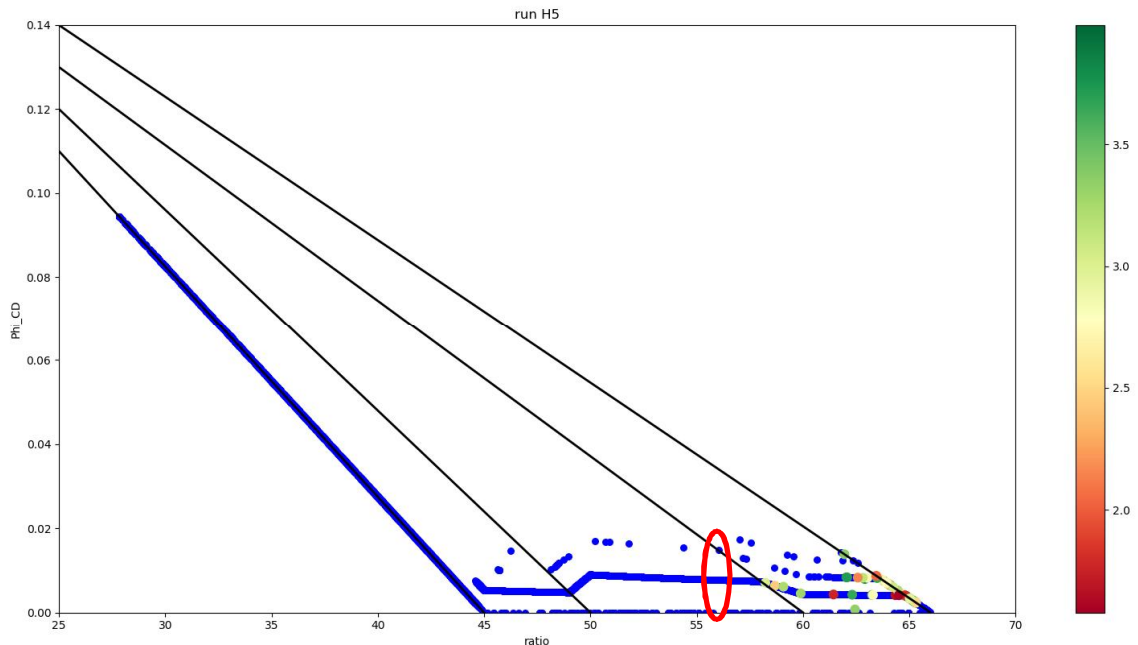


Figure H.5 Rotation capacity vs ratio ( $b/t/\epsilon$ ). The blue dots represent all calculation results. The non-blue coloured dots represent the individual calculation results per iteration that have converged within the specified accuracy around  $z = 0$ . The legend displays the reached Beta value of these individual calculation results. The four black continuous lines represent the lines of 100, 95, 90 and 85% capacity according to Figure 3.4.

Conclusions from Figure H.5:

- Figure H.5 can be seen as complementary to Figure H.4.
- This figure confirms conclusions made with Figure H.4.

A doublecheck is made on the calculated value from the python script using a spreadsheet. In an arbitrary matter some values within the red circle in Figure H.5 were selected and recalculated.

Starting points:

- Corrosion value is 6.58 mm
- $t_f = 13$  mm
- $b = 356$  mm
- $f_y = 240$  N/mm<sup>2</sup>
- ratio = approximately 56 (see red circle in Figure H.5).

With the spreadsheet the values from Table H.6. are calculated. It is verified that the calculated rotation capacities at different softening moments indeed match the results of the python module. The used spreadsheet is shown in Table H.7.

Rho <sub>i</sub>	M <sub>pl,max</sub>	Φ <sub>CD</sub>
[-]	kNm/m	[rad]
0.92	385	0
0.91	381	0.0078
0.90	376	0.0148

Table H.6 Results for Φ<sub>CD</sub> for different Rho values and a ratio ~ 56

AZ26 initial properties							
fy	2.40E+05	kN/m <sup>2</sup>					
b	3.56E-01	m	= width of flange				
ε	0.98953	-	=sqrt(235000/fy)				
tf	1.30E+01	mm					
E	2.10E+08	kN/m <sup>2</sup>					
AZ26 with corrosion							
dt	6.58	mm	= corrosion C1.dtD1				
b/tfi/eps	56.039	[-]					
tfi	6.42	[mm]					
A	1.06E-02	m <sup>2</sup> /m					
I	3.13E-04	m <sup>4</sup> /m					
Wel	1.48E-03	m <sup>3</sup> /m					
Wpl	1.74E-03	m <sup>3</sup> /m					
PLX input values							
in case ratio "b/tfi/eps" < 45				in case 45 < ratio "b/tfi/eps" < 50		in case 50 < ratio "b/tfi/eps" < 60	
EA	2.223E+06	kN/m					
EI	6.5721E+04	kNm <sup>2</sup> /m					
w	0.8312	kN/m/m					
Rho;max;i	1.0000	[-]	Rho;max;i	NA	Rho <sub>i</sub> max	0.92	
Mp_max	418.28	kNm/m	Mp_max	#VALUE!	Mp_max	384.73	
Np	1.0.E+12	kN/m					
plastic rotation capacity Phi_CD							
			1 > Rho > 0.95		0.95 > Rho > 0.90		
			Rho <sub>i</sub> with soften	0.95	Rho <sub>i</sub> with soften	0.90	
			Phi_CD	NA	[rad]	Phi_CD	0.0148
			Mp with softening		Mp with softening		376

Table H.7 Spreadsheet used for verification on Φ<sub>CD</sub>

### H.3 Check on calculated rotations (Φ<sub>max</sub>)

A check is made on the calculated rotations ((Φ<sub>max</sub>) by the special command "MaxAngularDestortionSheetPile". For this the following calculation was selected: Run H5, iteration 198, Beta [u] = 3.2244. The choice was random, however a calculation was selected in which a plastic hinge occurs and hence some softening.

Use is made of the option in PLAXIS to extract the deformations of the plate element (representing the sheet pile) per node and the option to extract the rotations per node.



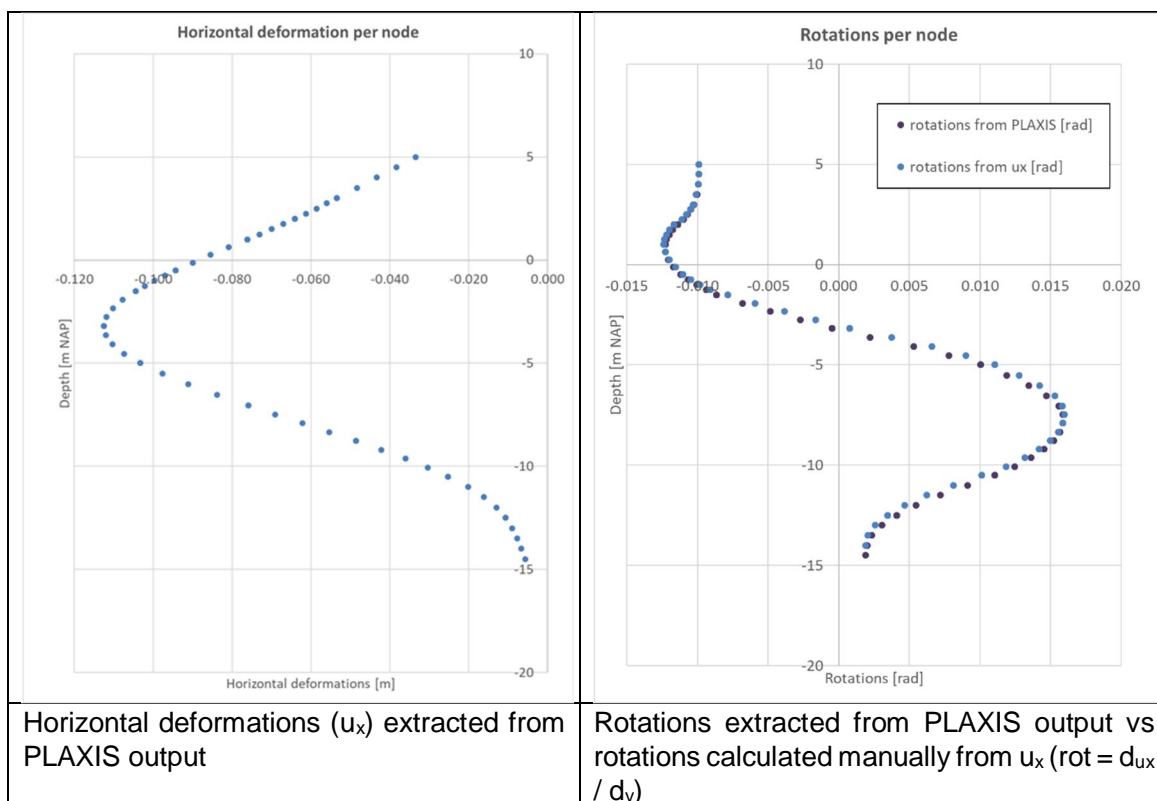


Figure H.6 Run H5, iteration 198, Beta [ $u$ ] = 3.2244. Horizontal deformations and rotations per node

Zone	Level	
	Top [m NAP]	Bottom [m NAP]
A: Above upper lockage level	+5.0	+3.0
B: Upper lockage level-GWL	+3.0	+1.0
C: GWL- lower lockage level	+1.0	-0.5
D1: Lower lockage level-bottom	-0.5	-1.5
D2: Lower lockage level-bottom	-1.5	-5.0
D3: Lower lockage level-bottom	-5.0	-7.0
E: Below bottom	-7.0	-14.5

Table H.8 Defined zones/sections in sheet pile

Section_1.Phi_max	0.00020	rad
Section_2.Phi_max	0.00055	rad
Section_3.Phi_max	0.00052	rad
Section_4.Phi_max	0.00126	rad
Section_5.Phi_max	0.00298	rad
Section_6.Phi_max	0.00205	rad
Section_7.Phi_max	0.00201	rad

Table H.9 Run H5, iteration 198, Beta [ $u$ ] = 3.2244. Extracted values of  $\Phi_{max}$  per zone/section from PTK.

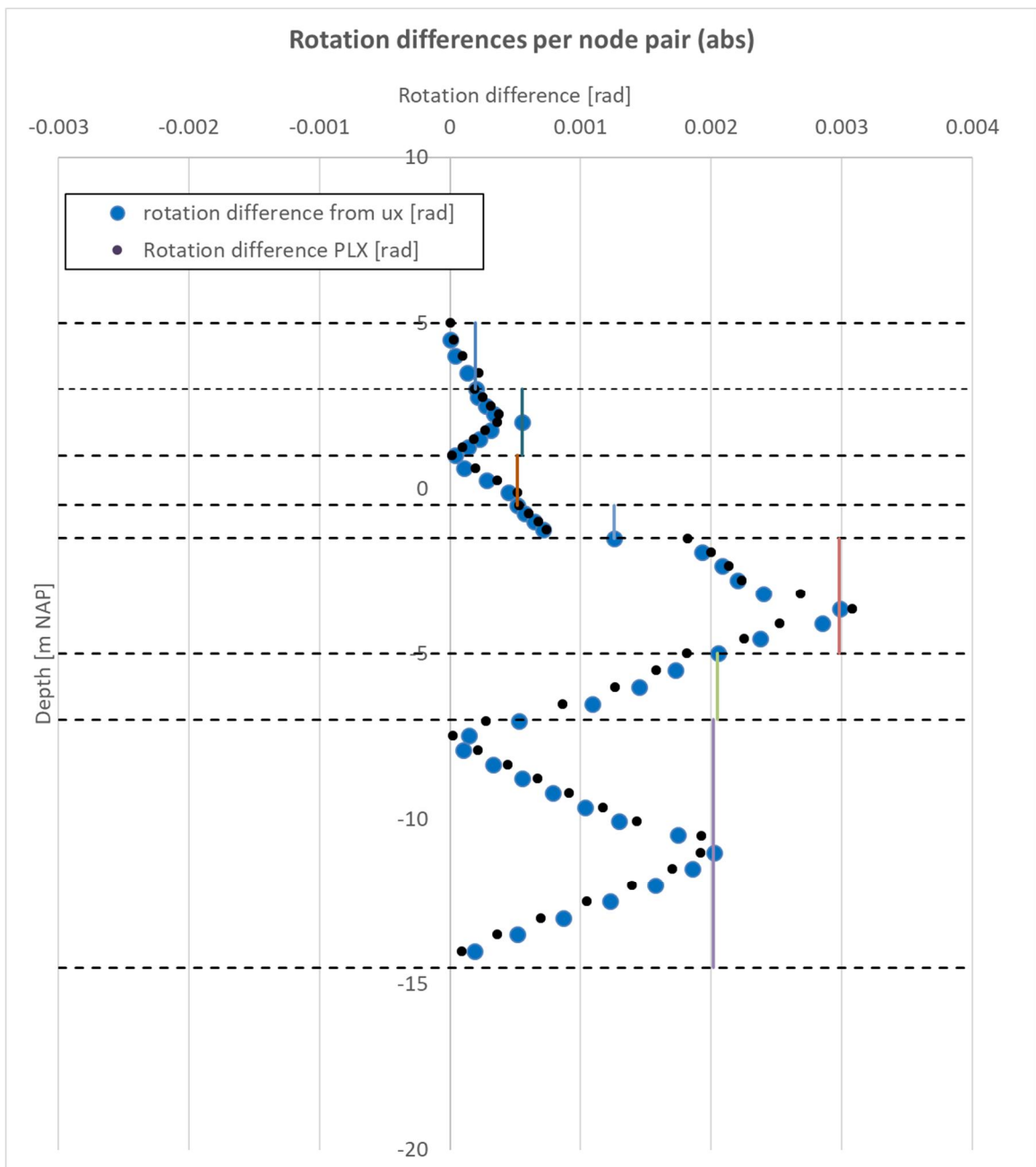


Figure H.7 Run H5, iteration 198, Beta [u] = 3.2244. Comparison of rotation differences per node pair. Black dashed horizontal lines indicate the defined zones/sections in the sheet pile. The coloured vertical continuous lines per zone/section indicate the extracted values of  $\Phi_{max}$  from the PTK. Blue dots are the calculated rotation differences per node pair (calculated in analogy with the special command). As a comparison the black dots are included which are the rotation differences determined based on the rotation per node as extracted from PLAXIS output.

It is concluded that the results of the special command can be exactly reproduced. The rotation differences directly obtained from the PLAXIS output are in general only slightly different. However, at some locations differences are larger. This is caused by the linearization in between the nodes that is made in the special command. The rotations outputted by PLAXIS per node are based on the more advanced beam theory used for the plate elements. Ideally more sensitivity analysis is performed to gain more insight in the possible differences and the

impact on results. For now, it is believed that results are acceptable as long as the mesh size (and thus the node distance) is relatively small.

#### **H.4 Check on LSF values**

The by the PTK calculated LSF values based on the results per calculation are checked. In a random manner a calculation is selected, i.e. Run H5, direction 62, Beta [u] = 3.8389, and recalculated with a spreadsheet. It is verified that the calculated LSF values indeed are the same as found in the PTK.

Run H5			Results of calculation		LSF values	
ID	316		Section_1.M_max	69.57472054	z1_pl	0.871309
Iteration	61		Section_1.M_pl_max	540.6343897	z2_pl	0.599894
dt_D1	7.650486		Section_1.M_elas_corr	10000000000	z3_pl	0.735288
			Section_1.Phi_max	0.000256403	z4_pl	1
			Section_1.Phi_CD	0.02688473	z5_pl	0.086532
			Section_1.Rho_c_max	1	z6_pl	1
			Section_2.M_max	189.7033063	z7_pl	0.40116
			Section_2.M_pl_max	474.1321857	z_pl	0.086532
			Section_2.M_elas_corr	10000000000		
			Section_2.Phi_max	0.000844258		
			Section_2.Phi_CD	1.39E-17	z1_el	1
			Section_2.Rho_c_max	0.98489289	z2_el	1
			Section_3.M_max	144.1576933	z3_el	1
			Section_3.M_pl_max	544.5830276	z4_el	0.195768
			Section_3.M_elas_corr	10000000000	z5_el	1
			Section_3.Phi_max	0.000573146	z6_el	-0.02902
			Section_3.Phi_CD	0.028889792	z7_el	1
			Section_3.Rho_c_max	1	z_el	-0.02902
			Section_4.M_max	241.5542524		
			Section_4.M_pl_max	10000000000		
			Section_4.M_elas_corr	300.3537635	z1_phi	0.990463
			Section_4.Phi_max	0.001370178	z2_phi	1
			Section_4.Phi_CD	-0.12238783	z3_phi	0.980161
			Section_4.Rho_c_max	NaN	z4_phi	1
			Section_5.M_max	337.2163148	z5_phi	1
			Section_5.M_pl_max	369.1604913	z6_phi	1
			Section_5.M_elas_corr	10000000000	z7_phi	0.961603
			Section_5.Phi_max	0.00240895	z_phi	0.961603
			Section_5.Phi_CD	-2.78E-17		
			Section_5.Rho_c_max	0.908511385	Zanchw	0.691608
			Section_6.M_max	309.0695602		
			Section_6.M_pl_max	10000000000	Zanc	0.512008
			Section_6.M_elas_corr	300.3537635		
			Section_6.Phi_max	0.00237936	Z_soil	1
			Section_6.Phi_CD	-0.12238783		
			Section_6.Rho_c_max	NaN	Zstruct	-0.02902
			Section_7.M_max	354.4931571		
			Section_7.M_pl_max	591.9666825		
			Section_7.M_elas_corr	10000000000		
			Section_7.Phi_max	0.001934744		
			Section_7.Phi_CD	0.050387294		
			Section_7.Rho_c_max	1		
			Phase_6.MStage	1		
			AnchorPlate.M2D	-113.147395		
			Anchor.Force	454.6512985		
			ZAncW	0.69160767		
			ZAnc	0.512007759		
			ZSoil	1		
			z_pl	0.086531948		
			z_el	-0.02901844		
			z_phi	0.961602548		
			ZStruct	-0.02901844		

Table H.10 Run H5, iteration 61, check on calculated LSF values. First 5 columns on the left show output values as shown in PTK including the results of the LSF functions. The two last columns on the right show the manually calculated LSF values based on the presented output values.

**H.5 Check on influence yield stress**

To be able to get more insight in the effect of the yield stress on the bending moment capacity we can make several cross sections in Figure H.8 parallel to the yield stress axis. The results have been presented in Figure H.9.

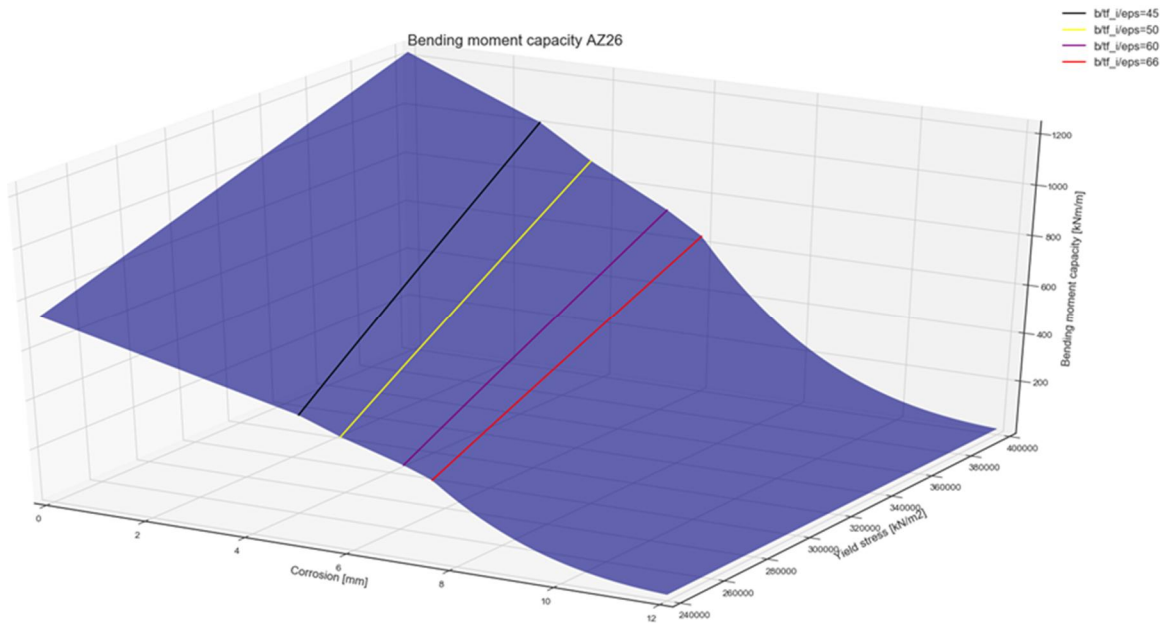


Figure H.8 3D figure indicating the relation between the maximum plastic bending moment capacity [kNm/m] (vertical axis) and the amount of corrosion [mm] and the yield stress [kN/m<sup>2</sup>]

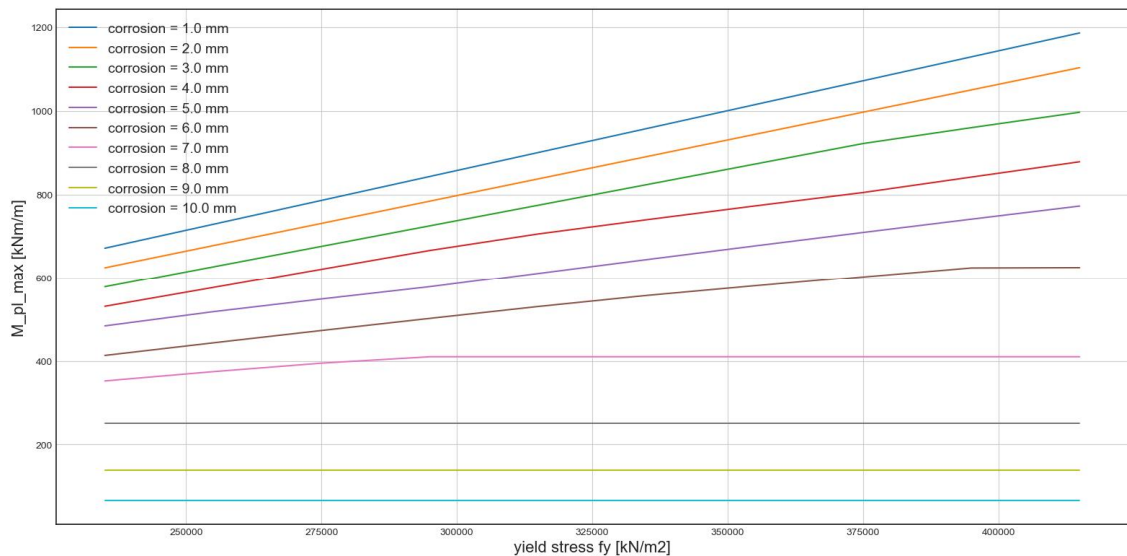


Figure H.9 Results of cross-sections made in Figure H.8 for different corrosion values

To further clarify some example calculations are presented.

<p>Assume</p> <ul style="list-style-type: none"> <li>• <math>b</math> = definition of width of AZ26 = 356 mm</li> <li>• <math>t_f</math> = initial thickness of flange = 13 mm</li> <li>• <math>f_y</math> = yield stress [kPa]</li> </ul> <p>by definition:</p> <ul style="list-style-type: none"> <li>• <math>\epsilon_p = \sqrt{235000 / f_y}</math></li> <li>• <math>t_{f_i} = t_f - dt</math></li> </ul> <p>suppose</p> <ul style="list-style-type: none"> <li>• <math>f_y = 240 \text{ N/mm}^2</math></li> <li>• <math>dt = 4.65 \text{ mm}</math></li> </ul> <p>then</p> <ul style="list-style-type: none"> <li>• <math>\epsilon_p = 0.99</math></li> <li>• <math>t_{f_i} = 13 - 4.65 = 8.35 \text{ mm}</math></li> <li>• <math>\text{ratio} = b/t_{f_i}/\epsilon_p = 356/8.35/0.99 = 43</math> (= Class 1&amp;2)</li> <li>• <math>\text{Rho}_{c\_max} = 1.0</math></li> <li>• <math>W_{pl\_max} = 2.13^E-3 \text{ m}^3/\text{m}</math></li> <li>• <math>M_{pl\_max} = f_y * W_{pl\_max} * \text{Rho} = 511 \text{ kNm/m}</math> (with a certain rotation capacity)</li> </ul> <p>Now suppose:</p> <ul style="list-style-type: none"> <li>• <math>f_y = 340 \text{ N/mm}^2</math></li> <li>• <math>dt = 4.65 \text{ mm}</math></li> </ul> <p>then</p> <ul style="list-style-type: none"> <li>• <math>\epsilon_p = 0.83</math></li> <li>• <math>t_{f_i} = 13 - 4.65 = 8.35 \text{ mm}</math></li> <li>• <math>\text{ratio} = b/t_{f_i}/\epsilon_p = 356/8.35/0.83 = 51.3</math> (= klasse 3)</li> <li>• <math>\text{Rho}_{c\_max} = 0.94</math></li> <li>• <math>W_{pl} = 2.13^E-3 \text{ m}^3/\text{m}</math></li> <li>• <math>M_{pl\_max} = f_y * W_{pl\_max} * \text{Rho} = 683 \text{ kNm/m}</math> (but with reduced rotation capacity)</li> </ul> <p>Conclusion:</p> <p>Expected increase based on increase in yield stress = <math>340 / 240 = 1.42</math></p> <p>Calculated increase = <math>683 / 511 = 1.34</math> (and less rotation capacity compared with lower yield stress)</p>
--

Table H.11 Example calculation for impact of yield stress as a stochastic variable for a corrosion = 4.65 mm (mean value)

<p>Assume</p> <ul style="list-style-type: none"> <li>• <math>b</math> = definition of width of AZ26 = 356 mm</li> <li>• <math>t_f</math> = initial thickness of flange = 13 mm</li> <li>• <math>f_y</math> = yield stress [kPa]</li> </ul> <p>by definition:</p> <ul style="list-style-type: none"> <li>• <math>\epsilon_p = \sqrt{235000 / f_y}</math></li> <li>• <math>t_{f_i} = t_f - dt</math></li> </ul> <p>suppose</p> <ul style="list-style-type: none"> <li>• <math>f_y = 240 \text{ N/mm}^2</math></li> <li>• <math>dt = 7 \text{ mm}</math></li> </ul> <p>then</p> <ul style="list-style-type: none"> <li>• <math>\epsilon_p = 0.99</math></li> <li>• <math>t_{f_i} = 13 - 7 = 6 \text{ mm}</math></li> <li>• <math>\text{ratio} = b/t_{f_i}/\epsilon_p = 356/6/1 = 60</math> (= klasse 1/2/3)</li> <li>• <math>Rho_{c\_max} = 0.9</math></li> <li>• <math>W_{pl};max =</math></li> <li>• <math>M_{pl};max = 358 \text{ kNm/m}</math> (but with softening capacity !)</li> </ul> <p>Now suppose:</p> <ul style="list-style-type: none"> <li>• <math>f_y = 340 \text{ N/mm}^2</math></li> <li>• <math>dt = 7 \text{ mm}</math></li> </ul> <p>then</p> <ul style="list-style-type: none"> <li>• <math>\epsilon_p = 0.83</math></li> <li>• <math>t_{f_i} = 13 - 7 = 6 \text{ mm}</math></li> <li>• <math>\text{ratio} = b/t_{f_i}/\epsilon_p = 356/6/0.83 = 71</math> (= Class 4)</li> <li>• <math>f_{y;red} = 235000/(b/t_{f_i}/\epsilon_p)^2 = 235000/(356/(13-7)/66)^2 = 291000 \text{ kN/m}^2</math></li> <li>• <math>W_{el} = 1.41 \cdot 10^{-3} \text{ m}^3/\text{m}</math></li> <li>• <math>M_{corr\_el} = W_{el} * f_{y;red} = 1.41 \cdot 10^{-3} * 291000 = 410 \text{ kNm/m}</math> (without softening capacity!)</li> </ul> <p>Conclusion</p> <p>Expected increase based on yield stress = <math>340 / 240 = 1.42</math></p> <p>Calculated increase = <math>410 / 358 = 1.15</math>, but results from run H3, 4 vs H8, 9 suggest that "this profit" is (at least partly) undone due to the loss of rotation capacity.</p>
---

Table H.12 Example calculation for impact of yield stress as a stochastic variable for a corrosion value of 7 mm

## I Improved Class 4 strength in 3<sup>rd</sup> series of calculations

In the first series of calculations as presented in [Deltares, 2018] corrosion was used as a deterministic value. As a result the sheet pile could not reach Class 4 by the end of the reference period of  $T = 75$  years and as such there was no need for a Class 4 strength formulation.

In the second series of calculations as presented in chapter 6 of this report corrosion was used as a stochastic variable and as such a Class 4 strength formulation was needed. For the 2<sup>nd</sup> series of calculations a simplified Class 4 strength model is used. In this simplified approach a reduced yield stress is used for the section such that the  $b/t_f/\varepsilon$  parameter is always equal to the Class 3 - 4 threshold. This is a conservative approach of the Class 4 strength.

To investigate the effect of using a more realistic (and less conservative) Class 4 strength the formulation is adjusted based on input by [ArcelorMittal, 2019] in the 3<sup>rd</sup> series of calculations. For a number of different yield stresses and different corrosion values AM provided the Class 4 strength for an AZ26 profile according to a critical stress calculation in line with EC3 guidelines. Deltares used the provided numerical values to fit a polynomial surface and generate a continuous representation of the Class 4 strength in the class 4 area. The previous is visualized in the figure below using the black dots (i.e. the provided numerical values by AM) and the polynomial surface fit represented as red see-through surface.

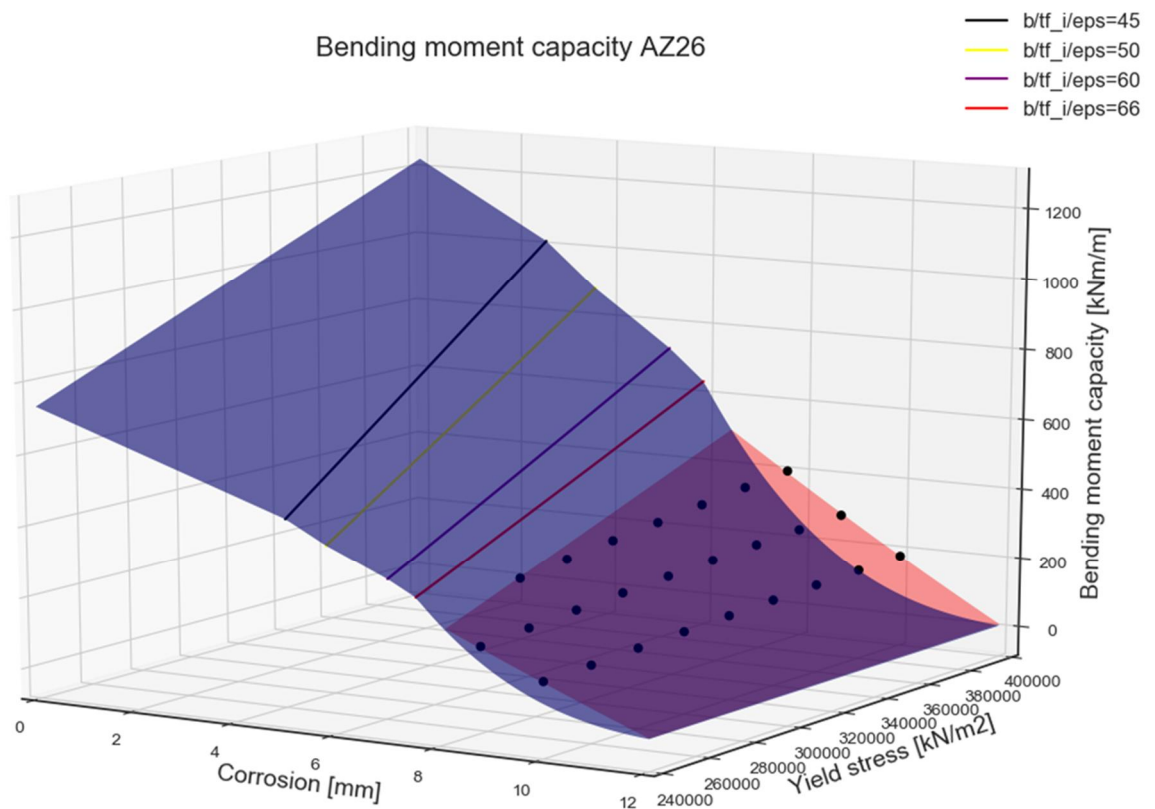


Figure I.1.. This figure is a copy of figure G.8 and shows a 3D figure indicating the relation between the maximum plastic bending moment capacity [kNm/m] (vertical axis) and the amount of corrosion [mm] and the yield



*stress [kN/m<sup>2</sup>]. In addition to figure G.8. here the improved Class 4 strength is represented as red see-through surface.*

Note to figure I.1.:

After performing the polynomial surface fit it was concluded that the fit does not intersect nicely with the Class 3 - 4 boundary as may be expected. The generated polynomial fit instead intersects with the surface representing the simplified Class 4 strength. This may suggest that the representation of the improved Class 4 strength is not ideal yet as it is expected that the more detailed calculations should provide less conservative strengths throughout the whole Class 4 area. Possibly non-linear effects play a stronger role closer to the Class 3 – 4 boundary. Additional calculations for the improved Class 4 strength closer to the Class 3 - 4 boundary may help to get a better insight and to improve the description of the improved Class 4 strength throughout the whole Class 4 area. Within this project it was not possible to further investigate the aforementioned behavior. In the 3<sup>rd</sup> series of calculations it was decided to use the maximum calculated value of the Class 4 strength coming from either:

- The reduced yield stress approach, or;
- the polynomial surface fitted on the numerical results of the critical stress calculation by AM.

## J Results of calculations (3<sup>rd</sup> series)

### Summary of calculation Input and Output

Run	Origin	Node	Model settings			Diff u per direction	Var. coeff. Failure	fy	Tc	Tref	Softening	AM line	model behaviour	Depth	Step size
			material model	corrosion	method										
H14		91	MC	stochast V = 0.5	DS	0.1	0.1	Yes	75	50	Yes	No	Varying	4	1
I1		92	MC	stochast V = 0.5	DS	0.1	0.1	Yes	75	50	Yes	Yes	Varying	4	1
I2		93	MC	stochast V = 0.5	DS	0.1	0.1	Yes	50	25	Yes	Yes	Varying	5	1
I3		94	MC	stochast V = 0.5	DS	0.1	0.1	Yes	26	1	Yes	Yes	Varying	8	1
I4	like I3	91	MC	stochast V = 0.3	DS	0.1	0.1	Yes	26	1	Yes	Yes	Varying	8	1
I5	like I3	92	MC	deterministic	DS	0.1	0.1	Yes	26	1	Yes	Yes	Varying	9	1
I6	like I3	31	MC	stochast V = 0.2	DS	0.1	0.1	Yes	26	1	Yes	Yes	Varying	8	1
I7	like I2	33/32	MC	stochast V = 0.3	DS	0.1	0.1	Yes	50	25	Yes	Yes	Varying	6	1
I8	like I1	93	MC	stochast V = 0.3	DS	0.1	0.1	Yes	75	50	Yes	Yes	Varying	4	1
I9	like I2	93	MC	deterministic	DS	0.1	0.1	Yes	50	25	Yes	Yes	Varying	7	1
I10	like I1	92	MC	deterministic	DS	0.1	0.1	Yes	75	50	Yes	Yes	Varying	6	1
I11	like I2	91	MC	stochast V = 0.2	DS	0.1	0.1	Yes	50	25	Yes	Yes	Varying	7	1
I12	like I1	31	MC	stochast V = 0.2	DS	0.1	0.1	Yes	75	50	Yes	Yes	Varying	5	1
I13	like I5	91	MC	deterministic	DS	0.1	0.1	Yes	75	1	Yes	Yes	Varying	8	1
I14	like I6	93	MC	stochast V = 0.2	DS	0.1	0.1	Yes	75	1	Yes	Yes	Varying	6	1
I15	like I4	94	MC	stochast V = 0.3	DS	0.1	0.1	Yes	75	1	Yes	Yes	Varying	5	1
I16	like I3	31	MC	stochast V = 0.5	DS	0.1	0.1	Yes	75	1	Yes	Yes	Varying	4	1
I17	like I13	32	MC	deterministic	DS	0.1	0.1	Yes	50	1	Yes	Yes	Varying	8	1
I18	like I16	31	MC	stochast V = 0.5	DS	0.1	0.1	Yes	50	1	Yes	Yes	Varying	6	1
I19	like I10	92	MC	deterministic	DS	0.1	0.1	Yes	75	50	Yes	Yes	Varying	8	1
I20	like I19	93	MC	stochast V = 0.2	DS	0.1	0.1	Yes	75	50	Yes	Yes	Varying	6	1
I21	like I19	94	MC	stochast V = 0.3	DS	0.1	0.1	Yes	75	50	Yes	Yes	Varying	5	1
I22	like I19	31	MC	stochast V = 0.5	DS	0.1	0.1	Yes	75	50	Yes	Yes	Varying	4	1

Run	Results		Calculation time				nr. iterations	nr. Runs	Versions used				Input Commands	comments
	Beta	var. coeff. Failure	start	stop	days	PLAXIS			PLX model	Python script	PTK			
H14	1.12	0.1	15-4-2020	19-4-2020	4	547	3148	2018.00	v1.0	v8.1	v1.9.23.1250	TimeList	for comparison	
I1	1.18	0.1	15-4-2020	20-4-2020	5	601	3445	2018.00	v1.0	v8.2	v1.9.23.1250	TimeList	label Hans, run 1A	
I2	2.71	0.127	15-4-2020	13-5-2020	28	5000	30675	2018.00	v1.0	v8.2	v1.9.23.1250	TimeList	label Hans, run 1B	
I3	5.34	0.405	15-4-2020	8-8-2020	115	10000	90684	2018.00	v1.0	v8.2	v1.9.23.1250	TimeList	label Hans, run 1C	
I4	5.42	0.458	22-4-2020	30-6-2020	69	7163	64729	2018.00	v1.0	v8.2	v1.9.23.1250	TimeList	label Hans, run 1D	
I5	5.45	0.291	22-4-2020	30-6-2020	69	4506	46104	2018.00	v1.0	v8.2	v1.9.23.1250	TimeList	label Hans, run 2A	
I6	5.45	0.567	22-4-2020	30-6-2020	69	6521	58978	2018.00	v1.0	v8.2	v1.9.23.1250	TimeList	label Hans, run 2B	
I7	4.54	0.44	26-4-2020	8-8-2020	104	10000	70050	2018.00	v1.0	v8.2	v1.9.23.1250	TimeList	label Hans, run 2C	
I8	1.93	0.1	15-5-2020	30-5-2020	15	2461	12905	2018.00	v1.0	v8.2	v1.9.23.1250	TimeList	label Hans, run 2D	
I9	4.65	0.266	10-6-2020	9-8-2020	60	5166	41781	2018.00	v1.0	v8.2	v1.9.23.1250	TimeList	label Hans, run 3A	
I10	3.99	0.381	8-7-2020	5-10-2020	89	3752	26331	2018.00	v1.0	v8.2	v1.9.23.1250	TimeList	label Hans, run 3B	
I11	4.59	0.285	3-7-2020	9-9-2020	68	4375	35254	2018.00	v1.0	v8.2	v1.9.23.1250	TimeList	label Hans, run 3C	
I12	2.63	0.151	3-7-2020	9-9-2020	68	2831	17445	2018.00	v1.0	v8.2	v1.9.23.1250	TimeList	label Hans, run 3D	
I13	4.78	0.38	9-9-2020	10-12-2020	92	3105	28222	2018.00	v1.0	v8.2	v1.9.23.1250	TimeList	label Hans, run 6A	
I14	2.84	0.198	9-9-2020	16-10-2020	37	2158	15800	2018.00	v1.0	v8.2	v1.9.23.1250	TimeList	label Hans, run 6B	
I15	2.05	0.117	9-9-2020	16-10-2020	37	1804	11500	2018.00	v1.0	v8.2	v1.9.23.1250	TimeList	label Hans, run 6C	
I16	1.38	0.1	9-9-2020	22-9-2020	13	870	4787	2018.00	v1.0	v8.2	v1.9.23.1250	TimeList	label Hans, run 6D	
I17	5.32	0.264	15-9-2020	10-12-2020	86	4613	41995	2018.00	v1.0	v8.2	v1.9.23.1250	TimeList	label Hans, run 7A	
I18	2.83	0.21	23-9-2020	16-10-2020	23	1939	14000	2018.00	v1.0	v8.2	v1.9.23.1250	TimeList	label Hans, run 7B	
I19	4.62	0.35	5-10-2020	10-12-2020	66	2782	25271	2018.00	v1.0	v8.2	v1.9.23.1250	TimeList	label Hans, run 8A	
I20	2.89	0.29	16-10-2020	1-12-2020	46	1271	9284	2018.00	v1.0	v8.2	v1.9.23.1250	TimeList	label Hans, run 8B	
I21	2.11	0.203	16-10-2020	23-10-2020	7	762	4824	2018.00	v1.0	v8.2	v1.9.23.1250	TimeList	label Hans, run 8C	
I22	1.38	0.11	16-10-2020	24-10-2020	8	718	3954	2018.00	v1.0	v8.2	v1.9.23.1250	TimeList	label Hans, run 8D	

Note on Run I3: after this calculation was performed an issue was found with the LSF formulation of the anchorwall in this run, resulting in an unrealistic high amount of anchorwall failures. In effect a too low Beta was calculated. The anchorwall failures were manually

removed from the data set and the Beta was manually recalculated. The influence factors for his run however could not be easily recalculated and as such are not reported here.

Input / Run	H14	I1	I2	I3	I4	I5	I6	I7	I8	I9	I10	I11	I12	I13	I14	I15	I16	I17	I18	I19	I20	I21	I22
Tc [year]	75	75	50	26	26	26	26	50	75	50	75	50	75	75	75	75	75	50	50	75	75	75	75
Tref [year]	50	50	25	1	1	1	1	25	50	25	50	25	50	1	1	1	1	1	1	50	50	50	50
Vcorrosion [-]	0.5	0.5	0.5	0.5	0.3	0	0.2	0.3	0.3	0	0	0.2	0.2	0	0.2	0.3	0.5	0	0.5	0	0.2	0.3	0.5
<b>Result</b>																							
Beta [-]	1.12	1.18	2.71	5.34	5.42	5.45	5.45	4.54	1.93	4.65	3.99	4.59	2.63	4.81	2.84	2.05	1.38	5.32	2.83	4.62	2.89	2.11	1.38
CoV [-]	0.10	0.10	0.13	0.41	0.46	0.29	0.57	0.44	0.10	0.27	0.38	0.29	0.15	0.42	0.20	0.12	0.10	0.26	0.21	0.35	0.29	0.20	0.11
<b>Influence factors [%]</b>																							
ZM.gammaunsat	1	1	1	N/A	5	2	1	0	1	4	2	1	1	1	1	1	0	2	1	1	2	1	1
ZM.phi	1	2	2	N/A	44	47	75	26	1	30	49	33	4	59	3	2	0	57	2	0	2	1	1
ZM.ERef	0	0	0	N/A	1	1	1	1	0	1	0	0	0	0	0	0	0	1	0	2	0	1	0
KM.phi	3	3	0	N/A	0	0	0	1	0	2	5	1	0	4	1	0	1	1	0	0	0	0	2
KM.ERef	0	1	2	N/A	0	0	1	2	2	3	4	4	2	3	1	2	1	3	2	0	1	2	1
KM.cref	2	2	1	N/A	13	4	5	5	1	3	2	5	2	7	2	0	0	4	0	1	0	0	0
ZD.phi	0	0	0	N/A	24	7	0	1	0	22	12	29	0	8	0	0	0	8	0	0	2	0	0
Bottom.ylevel	1	1	1	N/A	5	1	1	0	1	2	2	2	1	1	0	0	0	1	0	3	1	1	1
WL.waterlevel	1	0	0	N/A	5	34	9	1	0	29	11	11	0	4	0	1	0	21	1	88	0	1	0
LL1_1.OYStart	0	0	0	N/A	0	0	0	6	0	0	2	1	0	2	0	0	0	0	1	0	0	2	1
LL2_1.OYStart	2	1	1	N/A	0	1	2	0	0	1	4	1	2	0	4	0	0	1	1	2	2	0	0
LL3_1.OYStart	0	0	0	N/A	1	0	4	0	0	0	0	2	0	2	0	0	0	0	0	2	0	1	0
C1.dtD1	78	74	67	N/A	1		0	21	74			1	58		62	69	78		62		50	75	73
C2.dtD2	9	13	26	N/A	0		0	35	18			4	28		24	23	18		29		39	16	21
Steel.fy	2	1	0	N/A	0	2	0	0	0	2	6	5	0	7	0	1	0	3	1	0	0	0	0
<b>SUM</b>	<b>100</b>	<b>100</b>	<b>100</b>		<b>100</b>	<b>100</b>	<b>100</b>	<b>100</b>	<b>100</b>	<b>100</b>	<b>100</b>	<b>100</b>	<b>100</b>	<b>100</b>	<b>100</b>	<b>100</b>	<b>100</b>	<b>100</b>	<b>100</b>	<b>100</b>	<b>100</b>	<b>100</b>	<b>100</b>
<b>Nr of failures per LSF [#]</b>																							
z_anchw	0	0	0	0	0	0	0	0	0	0	0	0	0	0	0	0	0	0	0	0	0	0	0
z_anc	0	0	0	9	6	23	7	0	0	4	0	3	0	0	0	0	0	4	0	2	0	0	0
z_soil	0	0	0	48	40	123	36	0	0	30	6	15	0	19	0	0	0	33	0	59	1	0	0
z_pl	0	0	0	0	0	0	0	0	0	0	0	0	0	0	0	0	0	0	0	0	0	0	0
z_el	71	70	43	0	0	0	0	1	64	0	0	0	23	0	36	82	79	0	39	0	14	30	63
z_phi	20	23	51	26	11	45	9	7	42	31	14	23	42	45	49	35	18	30	28	15	27	12	17
<b>SUM</b>	<b>91</b>	<b>93</b>	<b>94</b>	<b>83</b>	<b>57</b>	<b>191</b>	<b>52</b>	<b>8</b>	<b>106</b>	<b>65</b>	<b>20</b>	<b>41</b>	<b>65</b>	<b>64</b>	<b>85</b>	<b>117</b>	<b>97</b>	<b>67</b>	<b>67</b>	<b>76</b>	<b>42</b>	<b>42</b>	<b>80</b>

